Università degli Studi di Padova
Dipartimento di Ingegneria Industriale
Corso di Laurea Magistrale in Ingegneria Energetica

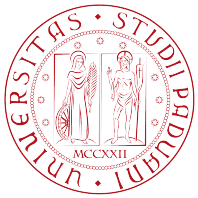

Master thesis

Analysis of data from existing buildings as a support for assessment of indoor environmental quality and prediction of energy use

Author:
Marco Tattoli

Supervisor:
Prof. Michele De Carli
Università degli Studi di Padova

Assistant Supervisor:
Prof. Jakub Kolarik
Danmarks Tekniske Universitet

Academic Year 2016-2017

Acknowledgements

First of all, I want to thank my supervisor Jakub Kolařík for being so kind and helpful despite his busy schedule. I want to thank him and all the people of the Building 118 at DTU for the great work environment I could experience.
A sincere thank you to my supervisor Michele De Carli, for giving me the great chance to spend a special chapter of my life in Copenhagen and for helping me with the thesis development.
Nevertheless, I want to thank Jan Široký and *Energocentrum Plus s.r.o* for providing me the data-base on which the whole work is based.
A huge thank you to the amazing friends that accompany my life since the first moment of high school: Marco, Andrea, Andrea, Andrea, Davide, Giovanni, Ilaria, Claudia, Nicolò.
Among the people I know since childhood, there is a group of friends I never stopped hanging out with in those years and despite the different lives we are still able to enjoy a pizza together at Civico2. Thank Marco, Pietro and Giacomo.
Moving to Padova meant diving into a totally new environment, knowing a lot of great people and living some of the craziest adventure of my life. Among the others, I want to thank Riccardo, Mattia, Francesco, Michele, Alessandro, Nicola, Davide, Angelo.
In Padova I had the chance to share the not-that-great-from-an-IAQ-point-of-view classrooms of DIM with an amazing crew of Lazzaroni, so thank Giulia, Luca, Nicola, Cecilia, Arianna e Giacomo.
The constant will to do more pushed me in another country to live the first great adventure of my life. In Portugal I had a crazy experience that I could share with a group of people that became my second family. A huge thank you to Vincenzo, Andrea, Simone, Letizia, Simona, Roberto, Michał, Francesca, Sara, Antonio. You will always have a place in my heart. You and the Pastéis de Nata. Aveiro è nosso!
Tired of good climate countries, in October 2016 I moved to Copenhagen, to my big dream. In the cool danish capital an hardcore crew of people kept me company with the essential help of Carbonara. So thank Lorenzo, Samuele, Stefano, Giovanni, Luigi, Mar, Léo. Special mention to Tuborg Classic, inevitable panacea to survive the danish darkness. Skål!
Some people dive through these groups of friends, nevertheless they are always there for me. Thanks to my awesome cousins Arianna and Denise and my lifelong friends Anna and Elvira.
Of course, none of these amazing experiences would have happen without the constant and unconditional support, trust and love of my family and especially my parents, who made me the person I am. The greatest thank you to Annalisa and Giuseppe.

Contents

Chapter 1

Introduction

Energy saving is a crucial topic of our time, for both environmental and economical reasons. It has been estimated that about 40% of primary energy used in Europe is due to the building sector [1], so there is room for substantial improvements. Of course, energy savings in buildings should not be reached at expense of indoor environmental quality (IEQ) and thermal comfort. For this purpose the first step is to optimize the systems present in buildings using the available measurements as an indicator.

The aim of this work is to give solid tools that could help the energy manager of the building in the regulation process of Heat, Ventilation and Air Conditioning (HVAC) systems. The available large amount of measurements are difficult to understand as they are, therefore the building data-base is used to come up with information everyone could understand and take advantage of.

Nowadays energy consumption problems are considered in the design process only and once the building is operating occupants care just about thermal comfort. The current scenario tells these two sides are equally important and since one is dependent on the other, they should be faced at the same time.

The foundation of the present thesis is the work of Tisov [2], who developed a method for buildings data analysis able to visualize both energy consumption and thermal comfort in a simple and useful way, through the use of a comprehensive figure. The method was developed using data coming from several building simulation scenarios and then it was applied to a real building. The aim of offering a clear information about thermal comfort and energy consumption was achieved.
The limitations of the method lie in the room to building data synthesis, since the available data-set featured a single temperature measure for the whole building, the work could not properly deal with the synthesis. Furthermore, the work was meant to review and compare past building indoor conditions, but it did not offer any guidelines for energy improvements.

The present thesis carries on this work with the following objectives:

- To improve room to building data synthesis and representative temperature determination by using a data-base featuring multi-room temperature measurements and studying several data synthesis methods
- To show on the comprehensive figure an optimal scenario for thermal comfort and energy use, alongside with the actual data-set, serving as guideline for the energy manager of the building

This thesis was carried on in collaboration with *Energocentrum Plus s.r.o*, that shared the building data-base on which this work is based.

Chapter 2

Literature review

2.1 Thermal comfort

Indoor Environmental Quality (IEQ) is defined as the ensemble of Indoor Air Quality (IAQ), acoustics, lighting and thermal comfort [3]. The degree of satisfaction of building occupants depends on IEQ, therefore it has a strong importance in people life quality. For the purposes of this thesis the focus will be principally on thermal comfort.

Defining thermal comfort needs both a physiologically and psychologically evaluation, since it could be defined as the degree of satisfaction with the thermal environment. Many parameters should be evaluated to define comfort conditions, among those the standard ASHRAE 55 [4] addresses six primary factors:

- Metabolic rate
- Clothing insulation
- Air temperature
- Radiant temperature
- Air speed
- Humidity

The standard considers a steady state thermal comfort using data of near sedentary physical activity, that is suitable for an office scenario. Of course forced air ventilated buildings follow different rules from natural ventilated buildings, where occupants have more control (for example by opening a window).

When the other variables are fixed a temperature range can be defined, within which the thermal environmental conditions are acceptable. Since there are personal and psychological factors, this range calls for a percentage of unsatisfied occupants. The acceptable percentage of dissatisfaction may be both general (whole body) and local (partial body).

Predicted Mean Vote (PMV) is developed to take in account this personal factor and it is defined as "*an index that predicts the mean value of the vote of a large group of people on the seven-point thermal scale*". Along with PMV the standard introduces the Predicted Percentage of Dissatisfied (PPD), defined as "*An index that establishes*

a quantitative prediction of the percentage of thermally dissatisfied people determined from PMV". The seven-point thermal scale, defined by ASHRAE to quantify thermal sensations of people, is the following:

- +3 hot
- +2 warm
- +1 slightly warm
- 0 neutral
- -1 slightly cool
- -2 cool
- -3 cold

The PMV model uses heat balance principles to relate the six key factors for thermal comfort to the average response of people on this scale, while the hypothesis with the PPD index is that people voting more than +1 or less than -1 are dissatisfied and it assumes PPD to be symmetric around a neutral PMV. Once the other key parameters are fixed, the thermal comfort temperature range is defined when PMV is within the comfort limits.

The standard EN ISO 7730 [5] suggested a categorization to define different comfort levels on the PMV/PPD basis. The criteria used to build the categories are explained in Table 2.1, while the recommended ranges are shown in Table 2.2. PMV/PPD index is defined over six different primary parameters, so once the category is chosen and the other key parameters are fixed, it is possible to define an operative temperature thermal comfort range. The standard EN15251 [6] proposes the temperature ranges shown in Table 2.3, where the following assumptions were made:

- Relative humidity equal to 50%
- Low air velocity
- Summer clo value equal to 0,5 clo
- Winter clo value equal to 1,0 clo
- Different activity levels depending on the chosen scenario, expressed in met

UNI EN 15251 [6] (Annex F) introduces three methods to evaluate a percentage of thermal comfort in buildings:

- Method A: Percentage outside the range
- Method B: Degree hours criteria
- Method C: PPD weighted criteria

Table 2.1: Criteria for the categories definition in EN15251 [6]

Category	Criteria
I	High level of expectation to be used for spaces occupied by sensitive and fragile people, like young children, sick or elderly people
II	Normal level of expectation to be used in new or renovated buildings
III	Moderate level of expectation to be used in existing buildings
IV	Inadequate thermal conditions, acceptable only for a limited part of the year

Table 2.2: Examples of recommended categories for design of mechanical heated and cooled buildings

Category	PPD [%]	PMV
I	< 6	$-0,2 < PMV < +0,2$
II	< 10	$-0,5 < PMV < +0,5$
III	< 15	$-0,7 < PMV < +0,7$
IV	> 15	$PMV < -0,7$; or $+0,7 < +0,7$

Method A was first introduced in ISO 7730 and revised in EN 15251 and it calculates the percentage of occupied hours when the operative temperature (or the PMV) is outside the comfort range defined over a chosen category. By deciding the category it is chosen the closeness with which the indoor conditions are controlled and the expectations on the indoor environmental quality (IEQ) of the building, where Category I stands for high expectations, and Category III stands for moderate expectations. To apply PMV limits to the temperature some assumptions about the other key parameters have to be done. Method A stands that "*the parameter in the rooms representing 95% of the occupied space is not more than as example 3% (or 5%) of occupied hours a day, a week, a month and a year outside the limits of the specified category*", fixing an acceptable threshold for thermal discomfort. The limit of this method is the absence of an indication of how bad the discomfort is.
Method B was introduced in ISO 7730 and revised in EN 15251 as well and it calculates the Degree Hours (DH), defined as the sum of occupied hours during which requirements are violated multiplied by weighting factor expressed as a difference (in °C) between actual and limit temperature. The hours with a temperature below the lower limit are expressed as heating degree hours (HDH), while the hours with a temperature above the higher limits are expressed as cooling degree hours (CDH). The discomfort is evaluated

Table 2.3: Examples of recommended categories for design of mechanical heated and cooled buildings

Type of building/space	Category	Operative Temperature [$°C$]	
		Minimum for heating season (1,0 clo)	Maximum for cooling season (0,5 clo)
Residential building (1,2 met)	I	21,0	25,5
	II	20,0	26,0
	III	18,0	27,0
Single office (1,2 met)	I	21,0	25,5
	II	20,0	26,0
	III	19,0	27,0
Kindergarten (1,4 met)	I	19,0	24,5
	II	17,5	25,5
	III	16,5	26,0
Department store (1,6 met)	I	17,5	24,0
	II	16,0	25,0
	III	15,0	26,0

on the basis of the width of the comfort range, which depends on the chosen category. Method C assumes the time during which the PMV exceeds the comfort boundaries to be weighted by a factor, that depends on the PPD. The PPD is a function of metabolic rate, clothing insulation, air temperature, mean radiant temperature, air velocity and air humidity. It is similar to Method B but it has a different weighting factor for the cooling and heating season.

2.2 Occupancy

Defining thermal comfort in a building and especially in an office building is feasible only by knowing when it is occupied, in order to obtain a trustworthy representation of the reality. For this purpose it is crucial to estimate the actual occupancy pattern of the building.

Knowing the occupancy pattern is beneficial when working on energy management, since people presence has a relevant effect on space heating, space cooling and ventilation demand. As said, the thermal comfort and IAQ are based on occupancy as well. Furthermore knowing the real time occupancy allows the energy manager to reduce energy waste by avoiding the use of HVAC systems when people are not present and the over-heating or over-cooling of zones where the number of occupants is different

from the peak one. This could lead to energy savings up to 20% [7]. The real time occupancy detection could be used in Building Management Systems (BMS) and in Building Automation Systems (BAS) to improve energy efficiency of the building.

The methods to detect or estimate occupancy can be categorized in direct or indirect approach. The former is based on motion and positioning technology as passive infrared (PIR) motion detector, video camera and radio-frequency indicator (RFID), while the latter consists in non-intrusive technologies by using energy consumptions and environmental sensor data mining.

Occupants of a building have a strong impact on several measures and so they could be used to evaluate the daily schedule. Among the options the carbon dioxide seems to be the most useful for an accurate estimation. Other options are the electricity consumptions of lighting systems and appliances, temperature, humidity and acoustics. Direct approach methods like motion sensors could lead to false negatives in many applications, in additions to their privacy issues.

The parameter mainly used to define occupancy profiles is the CO_2 concentration and its generation and decay. There are many methods developed for this purpose:

- Methods based on steady state CO_2 concentrations, reliable for a number of occupants in the order of hundreds [8]. It can estimate the real time occupancy by measuring the supply and return air CO_2 concentration and the supply airflow rate

- Methods based on a theoretical CO_2 mass balance equation [9], able to detect the presence of occupants in the order of tens, but which needs a lot of information like volume and air flow rate. It uses four differential equations, for total mass balance, single zones mass balance, total number of occupants estimation and number of occupants per room, based on the former two equations. Starting from these equations it is possible to calculate the single and total air flow rates

- Methods based on radial basis function (RBF) neural network [10], that require a preliminary learning phase through the use of actual occupancy profiles. The accuracy in the number of occupants detection is between 85% and 90%. It takes advantage of indoor temperature, humidity, CO_2 concentration, light sound and motion sensors to make the neural network estimate the real time number of occupants. It is a low cost and high resolution system able to provide instantly room level information of the number of occupants

- Methods based on machine learning techniques [11]. These are prediction models based on indoor environmental data and they use a decision tree algorithm. They are well suited for occupancy detection and prediction at the future state. Real-time data can be used for both training process and instantaneous control for HVAC systems

- Methods based on a dynamic model, called Feature Scaled Extreme Learning Machine (FS-ELM) [12], able to estimate the number of real-time occupants through a discrete-time state space model, estimated with a regression process. The differences with the standard ELM are an additional layer, which works like a preprocessing of the inputs, and the random hidden layer weight matrix that is scaled over the inputs

- Methods based on the CO_2 concentration measure [13], able to detect the sole presence or absence of occupants and the daily arrival and departure time. They use few sensors that are generally already present in the buildings, they don't need precise records of occupancy for the learning phase and they are reasonably precise (o precise enough) in the occupancy pattern evaluation. These methods may lead to both delayed evaluation due to overcrowded rooms and false negatives in case of open windows

The carbon dioxide concentration is not the only parameter used to estimate occupancy. There are methods with a direct approach:

- Video based method [14], detecting occupants in a video monitored space through the use of image-processing techniques. It may suffer of problems linked to line of sight, especially in partitioned spaces. It has also problems with the privacy of the occupants and with the huge amount of data to be stored and processed

- Methods based on magnetic reed switch door sensor and on a passive infrared sensor [15]. This approach works for single-occupancy offices and it needs to leave the door open when the occupants are in the office or nearby

- Methods based on a passive infrared motion sensor (PIR) [16] able to detect the presence or absence of occupants, but not their number. The accuracy of this method is 97,9% and it can be improved to 98,4% by combining multiple motion sensors, while the addition of other type of sensors (CO_2, sound, energy usage) leads to worse results. This may be due to over-fitting when different type of sensors are combined

- Methods based on the existing information technology infrastructures [17] to replace and/or help traditional sensors to detect occupancy by monitoring MAC and IP addresses in routers and wireless access points. The method, called *implicit occupancy sensing*, derives the occupancy from sources not directly intended for this purpose and for this reason the benefits are the absence of additional cost in terms of hardware and the capability to provide information not available from dedicated sensors

Limitations of the CO_2 concentration parameter as the only occupancy estimation input are the dependence on non anthropological causes, as passive ventilation. Furthermore it usually takes some time for the CO_2 concentration to build up, moving the time boundaries of occupancy, and because of that it can not be used alone in a real time estimation process.
Limitations of the use of passive infrared (PIR) and ultrasonic motion sensors are the high cost of installation, limited accuracy, incorrect installation and lack of networking capabilities. These sensors are generally not able to detect detailed location and movements, so they are mainly used to control only lighting system.

2.3 Clothing insulation prediction

Clothing works like thermal insulation so it has a strong influence on thermal comfort. It is considered through the use of the *clo* parameter, which is equal to 0,155 $\frac{m^2K}{W}$. The value of *clo* identifies the temperature range to be used for the thermal comfort evaluation. Clothing is also one of the six variables that affect the predicted mean vote (PMV) and predicted percentage of dissatisfied (PPD). The standard EN15251 [6] uses a seasonal fixed clo value, which is 1 clo for the heating season and 0,5 clo for the cooling season. This leads to the following thermal comfort temperature range (valid for Category II).

Table 2.4: Standard temperature ranges

	Winter season	Summer season
T min	20°C	22°C
T max	24°C	26°C

This approach leads to a significant loss of information and it is not representing the actual thermal situation. There are some attempts to find a correlation between environment parameters (for example indoor and outdoor temperature, relative humidity or air velocity) and clothing behaviour in order to predict the *clo* parameter and better fit the actual state. This achievement would lead to improve HVAC system operations and energy savings. In fact, people tend to adapt their clothing during the day by adding or removing layers (clothing adjustment). Furthermore, sometimes the type of clothing is prescribed by the workspace (dress code), limiting the adaptive actions of the individual. There may be gender and social differences in the clothing choice and adjustment. The developed methods are based on databases of people clothing behaviour by investigating both internal (indoor operative temperature, relative humidity, air speed) and external parameters (outdoor temperature, latitude). Different types of buildings are investigated, both air-conditioned systems (HVAC), natural ventilated (NV) and mixed systems (MIX).

De Dear and Brager [18] studied the relationship between clothing insulation and environmental parameters like indoor and outdoor temperature by using the average *clo* value per building to ensure homogeneous conditions, but the study lacks explicit verification of linear regression assumptions.

De Carli *et al.* [19] developed a linear regression to predict average clothing insulation as a function of outdoor temperature at 6 o'clock in the morning. Other options (mean daily temperature, mean temperature during the investigated period, weighted value on the temperature over the last four days) are considered but they are not reliable as the outdoor temperature since it comes out people tend not to have a "weather memory". The variation of the minimum and maximum average clo values is studied as well, to be used to define the optimal temperature range. The variation is negligible in NV buildings, where the indoor temperature may be considered equal to the external one due to the high rate of infiltration caused by natural ventilation. Gender differ-

ences are studied as well but they appear to be very limited and therefore considered negligible. The influence of latitude is negligible in HVAC buildings while it should be considered in NV buildings in latitude between 20° and 40°, and -20° and -40°. In HVAC buildings indoor air temperature plays no role in the clothing behaviour, so it does not influence substantially the clothing choice. In HVAC buildings the change of the *clo* value during the day is independent from the outside temperature and is about 0,2 clo. It corresponds to the insulation of a jacket or a sweater. The change is lower for NV buildings, especially at higher outside temperatures. A variation of 0,1 clo is enough to affect the comfort evaluation through the PMV-PDD model. This method found the following correlations for HVAC buildings:

$$clo_{mean} = -0,01x + 0.766 \tag{2.1}$$

$$clo_{min} = -0,008x + 0,684 \tag{2.2}$$

$$clo_{max} = -0,009x + 0,863 \tag{2.3}$$

Where x is the outdoor temperature at 6 AM.

Schiavon *et al.* [20] found some limitations in this model:

- No certainty about the correctness of the regression coefficients, due to the lack of homoscedasticity
- Absence of the variance introduced by the building
- Data was used regardless of the quality of the measurement
- By using single variable regression models it was lost the opportunity to check for interaction effect between different variables
- There is no information about the use of other variables such air velocity and relative humidity

Schiavon developed two multi-variable linear mixed models, the first one uses outdoor air temperature at 6 o'clock as the only variable affecting clothing behaviour, while the other one adds indoor operative temperature as a second variable. The predictive model is dynamic, changing daily or hourly in order to be applied in thermal comfort calculation as well as in HVAC sizing, building energy analysis and building operation. The results show a median clothing insulation of 0,59 clo in summer and 0,69 clo in winter, these values are quite different from the standard values of 0,5 clo in summer and 1 clo in winter. As reported by De Carli, the study reveals no significant gender difference in the clothing insulation behaviour and it seems to confirm outdoor temperature at 6 o'clock as the most influential environmental variable affecting clothing behaviour. The other variables are operative temperature, relative humidity and only partially air velocity and metabolic activity. The study reveals that where no dress code is in place (for example in shopping mall) the day-to-day variation in clothing levels is significant.

2.4 Energy use prediction

A reliable energy consumption prediction is useful both in the design and operative process of the building life-cycle.
While dealing renovations or construction of new buildings, this process is useful for assessing benefits of a renovation process and during the design process of Heating, Ventilation and Air Conditioning (HVAC) systems, whereas for the energy control strategies and the management of existing buildings it is used to optimize the energy use in the building, for example by setting the proper starting time of cooling/heating system and by deciding the amount of energy to be stored during off-peak hours in cool storage systems.

The methods aimed at predicting building load can be divided in three main categories:

- Physical models
- Black-box models
- Grey-box models

The physical models are the most detailed option and should be used in complex multiple zones buildings. They require a lot of parameters as input and a precise knowledge of the building envelope and systems. They are used in software like *EnergyPlus* [21], but this approach require a lot of time, making itself generally not cost-effective.

The black-box approaches are built solely on the inputs and outputs study, i.e. on the external operation of the system. Dhar *et al.* [22] developed a Generalized Fourier Series model (GFS), using weather independent loads (like internal loads) and weather dependent load (like HVAC energy use). In particular weather data are periodic so the use of the Fourier series is adequate for the study. This method is able to predict the hourly consumption in commercial buildings by using ambient temperature, ambient humidity and solar radiation as inputs. Dhar *et al.* [23] developed a Temperature based Fourier Series (TFS) to be applied in situations where only temperature data is available. This approach can model heating and cooling energy use accurately, using outdoor temperature as the only weather input. When humidity and solar data are available, the GPS approach has to be preferred because of its higher prediction power. Zhou *et al.* used a grey-box approach to develop an on-line weather prediction modules integrated with a building thermal load model for on-line cooling loading prediction. The weather variables inputs include global solar radiation, outdoor air dry-bulb temperature, and relative humidity. The prediction is used to properly set the Building Management System (BMS). The performance of the grey-box model is satisfactory while the prediction model could be affected by temporary weather changes. The methods is particularly suitable for the on-line prediction of building loads in the coming day and/or hours.

Simpler techniques are available when forecasting energy consumption on a daily basis and when a lower level of accuracy is required. The degree-day based techniques [24], mentioned in Section 2.1, is a commonly used method based on a weather normalized energy use data, performing reasonably well.

Besides weather dependent variables, the occupant behaviour could strongly influence the energy consumption of a building. The American Society of Heating, Refrigerating and Air-Conditioning Engineers (ASHRAE) [25] recommends a uniform occupancy schedule to evaluate occupants influence over the energy use. Yu *et al.* [26] used k-means clustering analysis to examine the effects of different behaviour patterns on energy consumption, identifying four behaviour clusters. Diao *et al.* [27] developed a method to use an unsupervised clustering algorithm to predict energy consumption using classified occupants behaviour. The method identifies 10 distinctive behaviour patterns able to offer a more accurate prediction than the ASHRAE standard schedule. By selecting the proper occupancy schedule, the user could reach energy and cost savings.

2.5 Energy management

Energy consumption coming from the building sector represents more than 40% of the European energy consumption [28]. This percentage has risen in the recent years mainly due to building HVAC systems use. The consumption could be strongly reduced by carrying out a proper energy management, which today is generally not continuous and only applied when achieving the energy certification. The technology needed to collect, analyze and exploit the data is available for its application in the building energy management to help practitioners solving problems they used to face. The benefit of a proper building management is the joined reduction of energy use, emissions and costs, while preserving or improving the thermal comfort in the building. Nowadays developing a solid building energy management process means dealing with a considerable amount of data. As reported by Molina-Solana *et al.* [29], the whole process can be improved through the use of Data Mining, which studies how to get non-trivial knowledge from collected data with an automated process, and Data Science, that includes a wide range of techniques for the analysis of complex data-sets. The latter is used to address the following problems:

- The prediction of energy demand
- The analysis and optimization of building operations and equipment
- The detection of energy consumption patterns
- The enabling of building retrofitting
- The analysis of economic impact of energy consumption

For these purposes classification and clustering methods are frequently used to help the building managers identifying the proper systems performance among the groups. The main steps of Data Science are:

- **Regression**: its main goal is to numerically estimate the relationship between the variables, understanding which ones are independent and which are not.
- **Clustering**: it is the separation of objects into groups based on their degree of similarity

- **Association rules**: they represent new information extracted from raw data and express them for decision-making in the form of implication rules.
- **Sequence discovery**: through different techniques it identifies statistically relevant patterns in data
- **Anomaly detection**: it identifies items, events or observations that deviate from expected patterns or usual behaviour of other data
- **Time series analysis**: it models data and it uses the model to predict or monitor future values of the time series.

Energy management is one if the key measures to reach more ambitious goal like net zero energy buildings (NZEBs) [30], to be used both in the design and the control processes of the buildings. To improve its usefulness an automated mathematical building performance optimization (BPO) paired with a building performance simulation (BPS) could be used in the process. The BPO is a process aiming to select the optimal solutions from a set of variables for a given control problem, according to a set of performance criteria, called objective functions, identifying the energy or cost or environmental impacts. Visualization techniques are essential to facilitate the extraction of relevant information.
In the control phase, the BPO could consider multiple objectives for the optimization process, like:

- HVAC system control parameters and/or strategy
- Thermal comfort
- Natural ventilation strategies
- Managing of energy storage
- Natural ventilation strategies

Privara *et al.* [31] presented the model predictive control (MPC), a different approach to the heating system control design. It predicts inside temperature trends according to the selected control strategy, using a weather forecast to have a continuous outdoor temperature prediction. It is able to track the desired temperature very accurately, to be preferred over a well tuned weather-compensated control. The drawbacks are the extra effort in the developing of the mathematical model of the building.

2.6 Building performance indicators

When developing performance indicators, we are focusing on three main categories:

- Energy performance indicators
- IEQ performance indicators
- Energy against IEQ performance indicators

The directive 2002/91/EC passed by the Council of the European Union in 2002 [28] expressed the need to establish a solid calculation methodology for building energy performance, in order to compare objectively different buildings, with the aim of making energy use more effective.
The energy performance indicator used for the building rating is usually defined as the fraction of annual energy use and the floor area inside the external walls $[\frac{kWh}{m^2}]$. The numerator is usually expressed with national energy weighting factors or with primary energy factors.
Catalina *et al.* [32] objected that this approach lacks of any considerations about the building morphology and thermal inertia, so another formulation is proposed, where the annual energy use is divided by the building envelope U-value, which is the comprehensive thermal transmittance that takes in account the insulation and consequently the energy loss through the envelope. This approach offers great design flexibility, allowing the engineering or the architect to choose which thermal element has to be improved to reduce the global energy use.
In a report by the Building EQ project [28] the energy signature is introduced, described as a visualization tool for weekly or monthly values, useful for internal benchmarking with the same building. It is able to show any faults with the building services systems, so it is significantly useful for commissioning and building management operations.

Some examples of IEQ measured indicators are air temperature, CO_2 concentration, relative humidity, illuminance level, air velocity, noise and polluting particles. In Section 2.1 the PMV/PPD indicators are introduced, they are used to elaborate measured data to build more effective indicators. Another thermal comfort indicator to be paired with PMV/PPD values is the thermal sensation vote (TSV), defined as the subjective human perception of the thermal environment on a 7 grade scale.
Wong *et al.* [33] presented the θ index, used to quantify the IEQ acceptance. It is defined as:

$$\theta = 1 - \frac{1}{1 + exp(\kappa_0 + \sum_{i=1}^{4} \kappa_i \phi_i(\zeta_i))} \tag{2.4}$$

The terms of Equation 2.4 are: θ_1 thermal environment acceptance, θ_2 IAQ acceptance, θ_3 aural environment acceptance, θ_4 visual environment acceptance, ζ_1 [%] PPD, ζ_2 $[ppm]$ CO_2 concentration, ζ_3 $[dBA]$ equivalent noise level, ζ_4 $[lux]$ illumination level, κ_i constants.

Wong *et al.* [33] presented also an index to correlate energy use with IEQ performance. The energy-to-acceptance ratio index α $[\frac{kWh}{m^2yr}]$ is defined as:

$$\alpha = \frac{E_c}{100 \times \theta} \tag{2.5}$$

The terms of Equation 2.5 are: E_c $[\frac{kWh}{m^2yr}]$ is the normalized annual thermal energy consumption and θ is the IEQ acceptance index defined in Equation 2.4.
Tisov [2] developed a "single number" indicator, to combine both types of performance indicators (energy and IEQ) in a single value. It is defined as:

$$OPR = \frac{CP}{PEC} \tag{2.6}$$

The terms of Equation 2.6 are: OPR overall performance ratio$[\frac{\%}{\frac{kWh}{m^2}}]$, CP calculated % of occupied hours when T_{oper} was inside the specified range (Category II, 20-26 °C) and PEC primary energy consumption $[\frac{kWh}{m^2}]$. It is possible to fix some limits for the OPR index by introducing the standard [6] requirements for IEQ performance.

Chapter 3

Methodology

3.1 Building information

This section reports the technical information available for the studied building, alongside with the data-base description.
To develop the method, the study is based on the IEQ data obtained from an office building located in Prostějov (Czech Republic). It is a bank built in 1996, with a floor area of 5042 m^2, posted on 5 different floors, that hosts 36 employers. The HVAC system consists of a gas boiler for heating (all floors) and a chiller for cooling (3rd floor). The fifth floor features mechanical ventilation, while the others present natural ventilation. Electricity for both cooling and ventilation is taken from the grid. The façade of the building is shown in Figure 3.1. The building envelope information are

Figure 3.1: Building façade

shown in Table 3.1.

There are 33 rooms with a temperature measurement, posted on 4 different floors. Among those, there are 16 rooms featuring also a reliable CO_2 measurement, that was used for the evaluation of human presence in the building, as described in Section 3.2. The measure of the outdoor temperature is available as well and it was used in Section 3.3 for the evaluation of clothing insulation, as described in Section 2.3.
It was possible to have access to this database thanks to *Energocentrum*. The database features measurements every 3 minutes, available since the beginning of September 2016 until January 2017, therefore only a heating season was studied. Despite the

Table 3.1: Building elements, area and heat transmittance

Building envelope element	Area $[m^2]$	Thermal transmittance $[\frac{W}{m^2K}]$	Primary energy factor $[-]$	Specific heat transfer loss $[\frac{W}{K}]$
External walls	3483,4	1,00	0,71	2473,2
Roof	1608,1	0,30	0,96	463,1
Floor	1608,1	0,72	0,46	532,6
Openings	748,4	2,01	1,00	1504,3
Total	7448,2	-	-	5619,1

limited data-base, the method is built in order to be applied to cooling season as well, therefore the drawn conclusions for thermal discomfort evaluation are relevant for the whole year.
The monthly energy consumption values are provided separately by *Energocentrum*, alongside with the energy audit of the building, featuring construction and equipment information.

3.2 Detection of occupancy pattern

In the thermal comfort evaluation it is crucial to have a reliable occupancy pattern, so that just the hours when people are present in a building are considered. This section describes the occupancy detection method used for this study.
Presented methods use environmental parameters as a presence indicator. The CO_2 concentration measurement is a common solution for this purpose. As mentioned in Section 2.2, there are different methods trying to estimate the presence from the CO_2 concentration measurement, but a lot of them use an Extreme Learning Machine (ELM) algorithm or neural networks [12, 11, 10]. These methods are too complex for the purpose of this work, so there is the need for something simpler.

As illustrated in the background study in Section 2.2, Guillaume Ansanay-Alex [13] suggested a simpler way to proceed.
The aim of the developed algorithm is to evaluate the sole presence or absence of any occupant, not counting how many occupants are present. The available data set for CO_2 concentration represents a measure every 3 minutes, that should be enough according to Guillaume Ansanay-Alex paper [13]. Figure 3.2a shows the CO_2 concentration measured data for a single day, where the fluctuation appears to be significant.
Firstly, the algorithm computes the CO_2 one hour moving average (Figure 3.2b), in order to smooth the CO_2 concentration data by filtering out the noise from random fluctuations.
Now looking at a single day data for a room, arrivals and departures will show up as buildups and decays in the CO_2 concentration curve. Instead of using the absolute value of the CO_2 concentration, the algorithm computes the variation of CO_2 concen-

tration, after cleaning it with the moving average technique, over each time step (one hour each), then the positive values of CO_2 variation, corresponding CO_2 concentration buildups, are separated from the negative ones, corresponding to CO_2 concentration decays.
Finally the algorithm creates two distribution plots, one for the positive variations of CO_2 (buildups) and one for the negative ones (decays). The plots feature on the *x-axis* the logarithm of the variation of CO_2 and on the *y-axis* the occurrences of each variation value. The logarithm is needed to make the peak variations easier to be visualized. The plots for a single day are shown in Figure 3.2c and Figure 3.2d.
The algorithm locates the growth and decrease rate peaks on the distribution plots, indicating the points of highest variation, and makes them the thresholds of the amplitude of buildups and decays, being able to evaluate the arrival and departure time, *i.e.* when the growth rate peak occurs for the first time within a day, the algorithm fixes in the relative hour the arrival time. The same process is used to evaluate the departure time. This process is based on the assumption that the highest variation of CO_2 concentration corresponds to significant occupancy variation.
If the difference between the maximum and the minimum CO_2 concentration within a day is lower than $150ppm$, the algorithm considers that day as unoccupied.

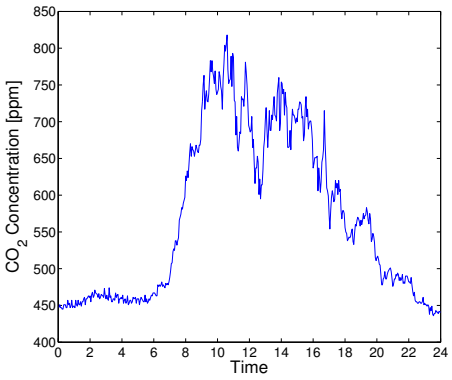

(a) CO_2 daily measure

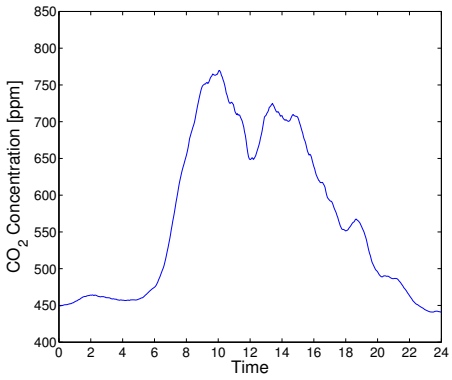

(b) CO_2 moving average

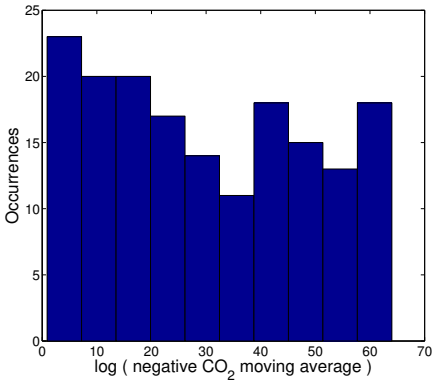

(c) Histogram of the build up of CO_2 within a day

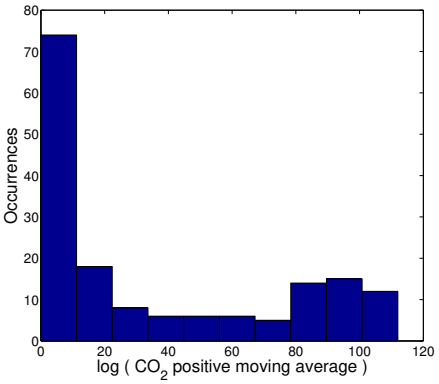

(d) Histogram of the decay of CO_2 within a day

Figure 3.2: Occupancy estimation from CO_2 measure

The results of the dynamic schedule evaluation are compared with the results obtained with a fixed occupancy pattern, corresponding to the actual opening hours of the office building, displayed in Table 3.2.
The results of the methods are discussed in Section 5.1.

Table 3.2: Fixed schedule (opening hours)

Day	Opening hour	Closing hour
Monday to Friday	7	16
Saturday and Sunday	Closed	

3.3 Comfort temperature range definition

In this section the aim is to identify the physical parameters affecting thermal comfort and to build a range of values able to identify satisfactory IEQ conditions.
When defining thermal comfort we are talking about an ensemble of IEQ parameters leading to the occupants satisfaction with the thermal environment. As mentioned in Section 2.1, the main parameters affecting thermal comfort are metabolic rate, clothing insulation, air temperature, radiant temperature, air speed and humidity. Dealing with an office building some assumptions could be made:

- Negligible air speed
- Constant relative humidity of 50%
- Constant metabolic rate of 1 met
- Mean radiant temperature equal to mean air temperature

With these hypothesis the thermal comfort depends upon indoor tempereature and clothing used, which is defined by the parameter *clo*, as explained in Section 2.3. Consequently by fixing the *clo* value the comfort temperature range is defined.
The first approach used for developing the method was the one suggested in the standard **EN 15251** [6], where it is suggested to use 1 clo for the winter (heating) season and 0,5 clo for the summer (cooling) season. This would lead to the temperature ranges of Table 3.3, where *Category II* is considered.
Since in fact the clothing transition through the seasons is not sharp, the winter and summer ranges were merged in order to obtain a simple temperature range, as shown in Table 3.3.

Table 3.3: Standard operative temperature ranges according to EN15251 (Category II)

	Winter season	Summer season	Simplified range
T min	20°C	22°C	20°C
T max	24°C	26°C	26°C

The second step is to implement a *clo* estimation algorithm using the method developed by De Carli *et al.* [19]. It uses experimental data to build an empirical correlation between the outdoor temperature at 6 AM and the expected *clo* value. The developed equations mentioned in Section 2.3 are reported here:

$$clo_{mean} = -0,01x + 0.766 \tag{3.1}$$

$$clo_{min} = -0,008x + 0,684 \tag{3.2}$$

$$clo_{max} = -0,009x + 0,863 \tag{3.3}$$

Where x is the outdoor temperature at 6 AM expressed in $°C$. The equations create a range of expected values of *clo* for each day. The results are shown in Figure 3.3, where the standard values are shown as well ($clo_{winter,std}$ and $clo_{summer,std}$).
In order to estimate a comfort temperature range from a *clo* value, the PMV absolute value was minimized having fixed all the parameters apart from the indoor temperature. An algorithm was developed to link the *clo* value to a temperature range, where T_{mean} stands for $PMV = 0$, T_{min} corresponds to $PMV = -0,5$ and T_{max} corresponds to $PMV = +0,5$. These are the recommended comfort limits according to ASHRAE 55 [4] and refer to *Category II*, as discussed in Section 2.1. Once a *clo* value is fixed the comfort temperature range is defined between T_{min} and T_{max}, with T_{mean} representing the optimal indoor temperature. Of course, higher values of *clo* would lead to lower acceptable temperatures, to account the larger thermal insulation. The results are shown in Figure 3.4, including the comfort temperature range for clo_{min} (3.4a), clo_{max} (3.4b) and clo_{mean} (3.4c).

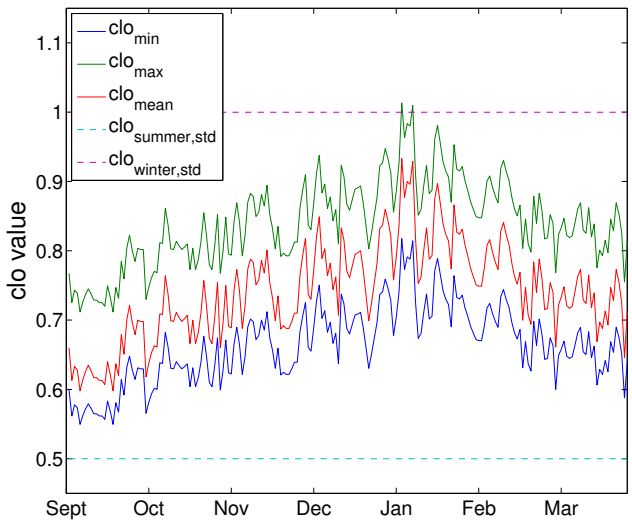

Figure 3.3: Estimated values of clo during the studied period

For a single day the *clo* estimation method produces a range of possible values of *clo*, to take in account the different thermal perception of occupants.

The thermal comfort temperature range is defined as follows:

- The lower acceptable temperature T_{min} corresponds to the lower extreme of the temperature range found using clo_{max}
- The optimal temperature T_{mean} corresponds to the central value of the temperature range found using clo_{mean}
- The higher acceptable temperature T_{max} corresponds to the higher extreme of the temperature range found using clo_{min}

This approach would generate the temperature range shown in Figure 3.4d able to guarantee thermal comfort for a wide range of people, by contemplating different behaviours.

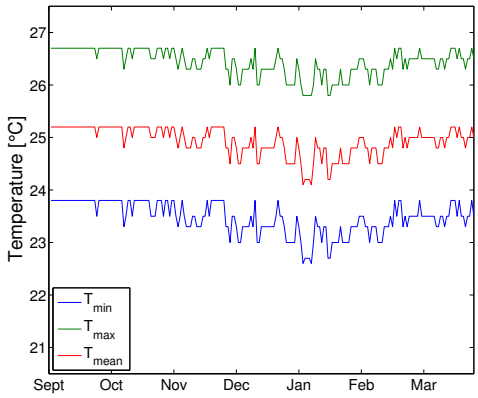

(a) Comfort temperature range (clo_{min})

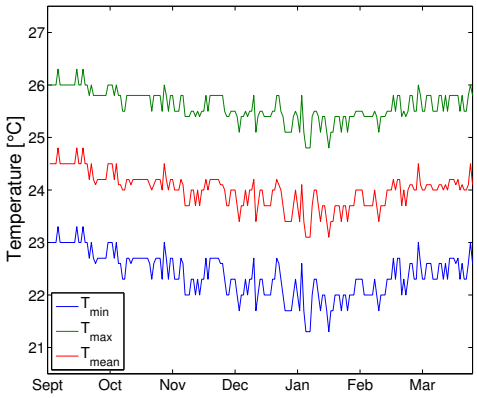

(b) Comfort temperature range (clo_{max})

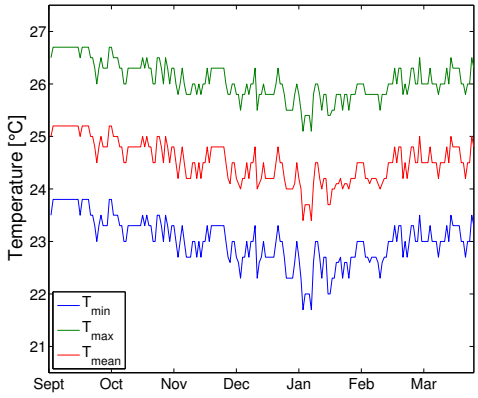

(c) Comfort temperature range (clo_{mean})

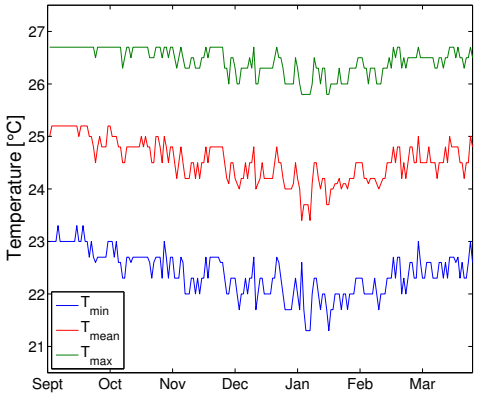

(d) Comprehensive comfort temperature range

Figure 3.4: Comfort temperature range from estimated clo values

3.4 Duration graph

The thermal comfort study is carried on using the assumptions stated in Section 3.3, for which the comfort depends only on indoor temperature: negligible air speed, constant relative humidity (50%), air temperature corresponding to radiant temperature, constant metabolic activity. Clothing insulation is studied using both fixed and estimated *clo* values, as discussed in Section 3.3. The comparison between the two methods is presented in Section 5.2.
In this section mathematical tools are used to get a clear representation of the indoor conditions in every room of the building, allowing comparison and synthesis on a monthly basis.
As illustrated in Section 3.1, there are 33 rooms in the building and with a measure taken every 3 minutes, there are 20 values per hour for each room. In order to have a simpler data-set the hourly mean temperature value for each room is calculated. The layout of the resulting table is shown in Figure 3.5.

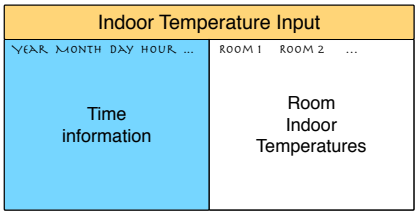

(a) Input data

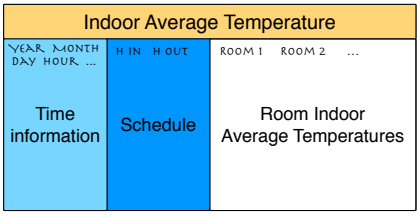

(b) Mean and schedule

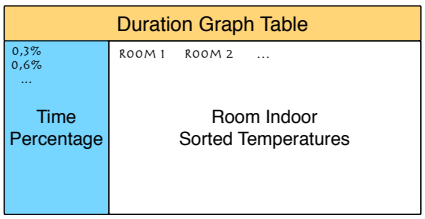

(c) Sorted data

Figure 3.5: Representation of tables composition

Since the thermal comfort evaluation requires to account only the occupied hours, the algorithm filters the hourly mean temperature values, to keep just the data referring to hours when occupants are present in the building. The daily pattern is deduced as explained in Section 3.2. The resulting table aspect is shown in Figure 3.5b.
Starting from the data-set created hereinbefore, the algorithm plots a duration graph

consisting of each room data for every month. This is a useful tool for visualizing data changing over time and it is done by sorting the data in ascending order and associating each value with a time percentage. The percentage tells how long the measured temperature is at least equal to the associated value in the considered month. The tables composition during the process is shown in Figure 3.5c.
The plot shows the measured temperature (in $°C$) on the *y-axis* and the percentage of time the indoor temperature is at least equal to that value on the *x-axis*. The algorithm creates a figure for every month, where a plot for each room is shown. An example of resulting duration graph is shown in Figure 3.6, where the simplified comfort temperature range according to the standard **EN15251** [6] is shown as well.
Once the limits are fixed, it is easy to evaluate the percentage time with thermal discomfort for each room, as the percentage of time outside the boundaries. Therefore the algorithm creates a data-set of monthly discomfort percentage time of each room by using the comfort temperature range developed in Section 3.3.

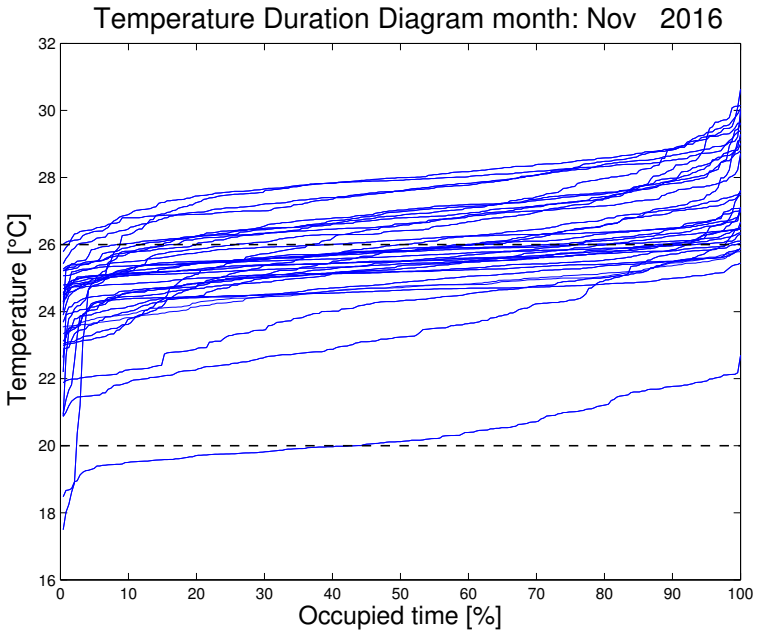

Figure 3.6: Temperature duration curve of every room (November 2016)

3.5 Rooms to building synthesis

Once the single rooms temperature data are available, they should be elaborated in order to create a simpler representation of the thermal conditions in the whole building. This is one of the main part of the whole work, aiming at the synthesis of measured data to develop a usable information of the building thermal conditions. In this section several statistical methods are used to develop this synthesis and to compute the average temperature data-set among the single room data-sets.
Starting from the data-set represented by the duration graph, with percentage of time in the first column and room temperature in the others, the algorithm creates two data-sets for each month, with the following content.
Table A:

- Mean temperature value
- Standard deviation (SD) of temperature data-set
- Mean temperature value − SD
- Mean temperature value + SD

Table B:

- Median temperature value
- 1st quartile of temperature data-set
- 3rd quartile of temperature data-set

Then the algorithm plots the results with two plots per figure, as shown in Figure 3.7. The plots include a curve for average values (mean and median) and the intervals to include the dispersion from the average value. It is crucial to include standard deviation and quartile curves in these figures, in order not to lose information about the building conditions on a room level. Using just the central value for the building conditions evaluation would mean losing information on the room level and would lead to overlooking thermal discomfort in the rooms with indoor conditions different from the average one.

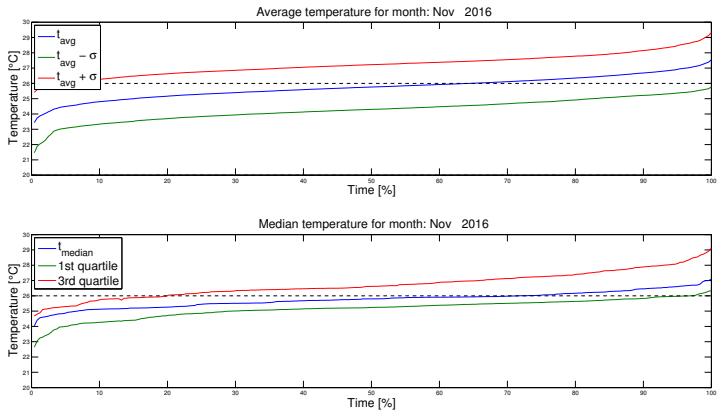

Figure 3.7: Mean and Median duration graph for November 2016

There are several ways to proceed for the average process, therefore two different methods are developed. The main problem lies in sorting the temperature values without losing the time information. To better understand this concept the methods are here explained:

A The initial data-set is shown in Figure 3.8a, it features the time information in the left part and the indoor temperature values for each room in the right part. Of course, the time information are ordered on a temporal basis, while the temperature values are not sorted yet. As shown in Figure 3.8b, the algorithm sorts the temperature values of every room, obtaining an ascending ordered data-set. This approach is the one used in Section 3.4 for the duration graph. Then the algorithm computes the mean, median, standard deviation and quartile values for the temperature averaging the sorted temperature data, as shown in Figure 3.8c. The resulting data-set aspect is shown in Figure 3.8d, while the average duration graphs for a single month are shown in Figure 3.9a

B Starting from the data-set shown in Figure 3.8a, the algorithm computes the mean, median, standard deviation and quartile values, averaging the temperature measured in each room at the same instant, as shown in Figure 3.8e. The resulting data-set features the temporal ordered time information in the left part and the unsorted average temperature values in the right part, as shown in Figure 3.8f. Then the mean and median temperature data-sets are sorted, obtaining the result shown in Figure 3.8g, where mean and median data-sets are ascending ordered, while standard deviation and quartile curves are not strictly ascending, since those values are temporally linked to the central data. The resulting duration graphs for a single month are shown in Figure 3.9b

Further comparisons and discussions are present in the next chapters.

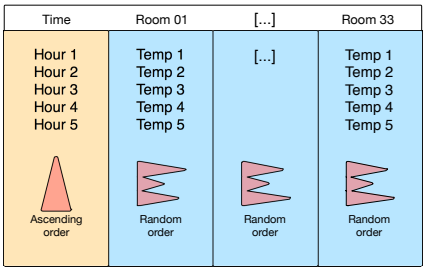

(a) Monthly temperature input data-set for every room

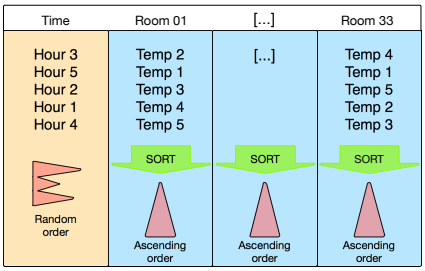

(b) Temperature data sorting for every room

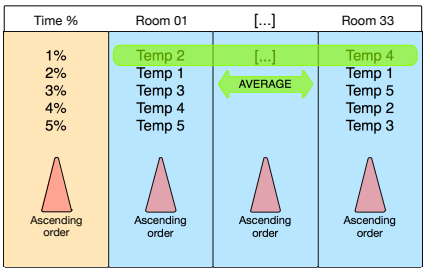

(c) Averaging process for sorted temperature data

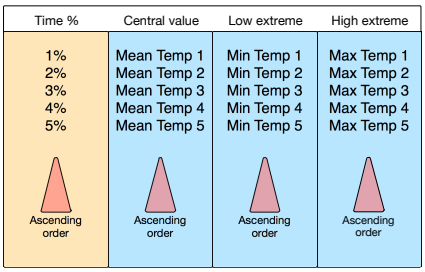

(d) Resulting average temperature data-set for Method A

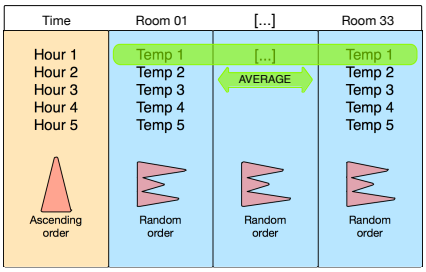

(e) Averaging temporally ordered temperature data

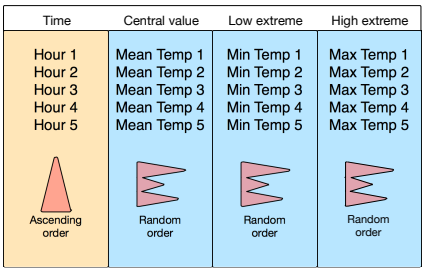

(f) Table look of unsorted average temperature data-set

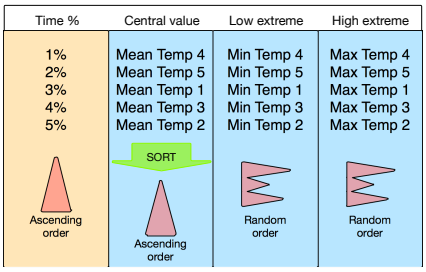

(g) Sorting process for average temperature data-set

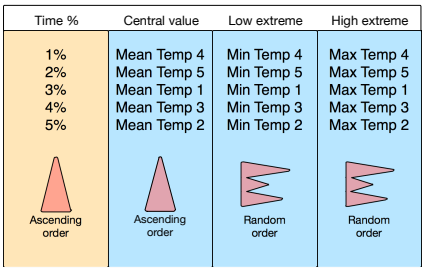

(h) Resulting average temperature data-set for Method B

Figure 3.8: Representation of averaging methods for temperature data-sets

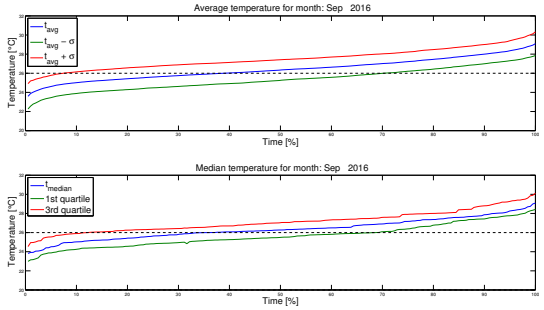

(a) Method A

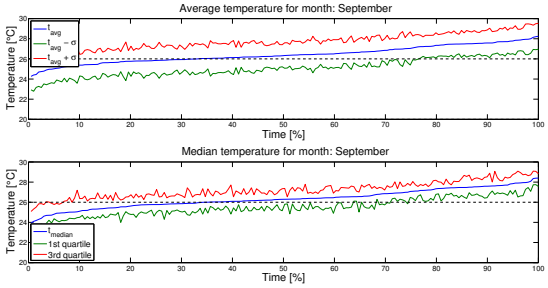

(b) Method B

Figure 3.9: Average duration curves for September 2016

Further attempts were made to get a building representation, in order to get different information to be compared with the central ones and to find the most appropriate way to picture the thermal conditions of the building. The first one considers just the problematic rooms in the mean and median evaluation. An algorithm creates a monthly data-set with data coming only from rooms that present a percentage of discomfort time higher than 5% of occupied time, which is the acceptable limit according to standard **EN 15251** [6].

The second studied attempt uses data filtering to consider just the main cluster of the data-set. The example of duration graph shown in Figure 3.6 shows that every month there are rooms with significantly different thermal conditions from the others, as can be seen in Figure 3.6, where three rooms are significantly colder. These rooms are not representative of the whole building and they influence the average value, undermining the thermal comfort information on the building level.
Two different approaches were adopted in order to get a more reliable data set for every month:

- Extreme data filtering
- Outlier data filtering

The former is a simple method developed for this purpose, while the latter is a more common way to proceed, as mentioned by Anderson *et al.* [34]. The results from both methods have to be compared in the next chapters.

The extreme values data filtering works with the monthly temperature data-set comprehensive of all rooms measures. The developed algorithm computes the hourly

mean temperature value and subtracts it from the actual hourly measure in every room, to display the dispersion from the central value. In order to show more clearly the dispersion and help the visualization, the algorithm computes the second power of every temperature difference, then it creates an array made up of the maximum hourly values of dispersion for the entire month, called extreme dispersion array. The use of the second power makes the algorithm to not consider if the difference is positive or negative, *i.e.* if the dispersion is above or below the central value. Considering the temperature duration graph of the previous example (Figure 3.6), the extreme dispersion array found by the algorithm is red marked in Figure 3.10. Once the array of the misleading temperature values is found, the algorithm filters the corresponding room data-sets for the whole month, in order to keep the main data cluster only. The resulting filtered data-set for the month of November 2016 is shown in Figure 3.11, in comparison with the complete data-set.

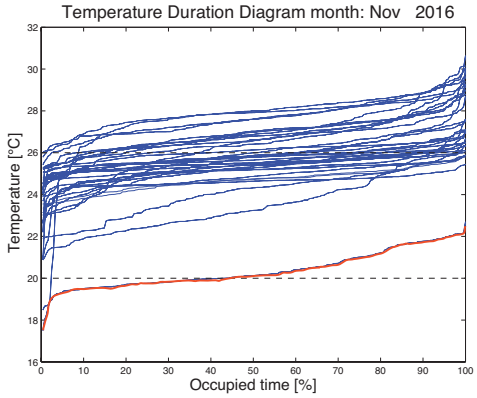

Figure 3.10: Graphic visualization of extreme dispersion array (marked in red) of data for extreme values data filtering

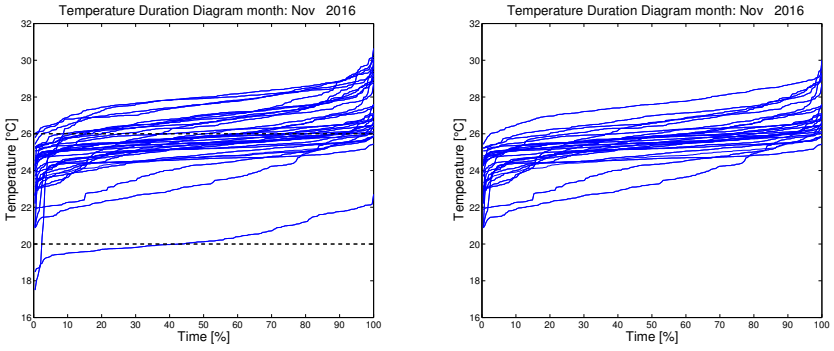

(a) Complete data-set (b) Extreme filtered data-set

Figure 3.11: Duration curves for complete and extreme filtered data-set for November 2016

As mentioned, the extreme data filtering method developed for this study should be compared with a more traditional data cleaning method through the use of outlier

detection.
The method [34] used to detect potentially wrong data considers as outliers the ones outside the range defined by:

$$[Q_1 - k * (Q_3 - Q_1), Q_3 + k * (Q_3 - Q_1)] \tag{3.4}$$

Where k defines the range extent ($k = 1$ in this study), while Q_1 and Q_3 are the first and third quartiles, respectively. For our case of study the range is found for every hourly observation. It becomes:

$$[2 * Q_1 - Q_3, 2 * Q_3 - Q_1] \tag{3.5}$$

The algorithm examines every room curve and creates a new data set without the rooms considered as outliers. The resulting duration graph is shown in Figure 3.12, where it is compared to the complete data set.

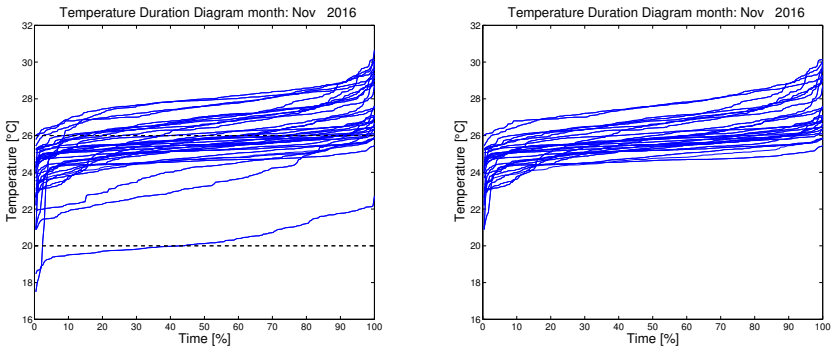

(a) Complete data-set (b) Outlier filtered data-set

Figure 3.12: Duration curves for complete and outlier filtered data-set for November 2016

Once the filtered data-sets are found, the algorithm computes mean, median, standard deviation and quartile values, for both extreme and outlier filtered data-sets, that could be used for thermal discomfort evaluation on building level.

The duration graphs resulting from extreme and outlier filtered data-sets are shown in Figure 4.2, while the methods are discussed in Section 5.3.

3.6 Thermal discomfort evaluation

In this section the temperature data-sets developed in the previous sections are used to quantify thermal discomfort on the building level. The study is based on the method A mentioned in the standard **EN 15251** [6] and reported in Section 2.1. The method defines thermal discomfort as the percentage time when indoor temperature exceeds the thermal comfort temperature range developed in Section 3.3. According to the standard, the thermal discomfort is acceptable if the monthly discomfort percentage time does not cross the 5% threshold, corresponding to the acceptable deviation to take in account thermal adjustment time, for example when opening windows. Several

approaches have been examined for the thermal discomfort evaluation, as reported hereinafter.

Firstly the algorithm computes the monthly thermal discomfort percentage time using mean (further called Method I in the report) and median (further called Method II in the report) values calculated using the methods explained in Section 3.5. Analogously to the evaluation of thermal discomfort done in Section 3.4 for every room data-set, the algorithm computes the monthly thermal discomfort percentage time as the sum of p_{low} and p_{high}, defined as the percentage of time below the lower comfort temperature limit and above the upper comfort temperature limit, respectively.
Then the algorithm makes use of standard deviation and quartiles to evaluate thermal discomfort. For the former, the hourly parameter to be studied are:

$$T_{min} = T_{mean} - SD \tag{3.6}$$

$$T_{max} = T_{mean} + SD \tag{3.7}$$

Where T_{mean} is the hourly mean temperature value and SD is the respective standard deviation.
The algorithm (further called Method III in the report) computes p_{low} as the percentage of time when T_{min} is below the lower comfort temperature limit and p_{high} as the percentage of time when T_{max} is above the upper comfort temperature limit.
Having called Q_1 the hourly 1st quartile value and Q_3 the hourly 3rd quartile value, the algorithm (further called Method IV in the report) computes p_{low} as the percentage of time when Q_1 is below the lower comfort temperature limit and p_{high} as the percentage of time when Q_3 is above the upper comfort temperature limit.

Moving forward, the hourly thermal discomfort is computed using the hourly mean temperature of the extreme filtered data-set (further called Method V in the report) and the outlier filtered data-set (further called Method VI in the report).

Since the methods just presented work with central values and dispersion range, they do not take in account the thermal discomfort of rooms with extreme conditions. Therefore further methods were developed in order to get a boundary information, to be compared with the results dealing central values.
Among these, the first solution (further called Method VII in the report) is to evaluate thermal discomfort by including only problematic rooms in the computing. According to the standard **EN 15251** [6] the monthly thermal conditions of a room are considered problematic if the thermal discomfort percentage time exceed the 5% threshold for that month, otherwise the room is considered suitable. The output data-set consists of problematic rooms only thermal discomfort percentage time, suitable rooms only thermal discomfort percentage time, all rooms thermal discomfort percentage time.
A further method (further called Method VIII in the report) to account extreme room conditions is to show monthly mean thermal discomfort percentage time alongside with worst room thermal discomfort percentage time. This approach helps showing both the average and extreme conditions to get a global idea of the overall thermal state.

The illustrated methods compute thermal discomfort percentage time using building synthesis data-sets as input, for example hourly mean temperature values. The forthcoming approach (further called Method IX in the report) computes overall thermal discomfort percentage time as the monthly mean of single rooms monthly discomfort percentage time.

3.7 Energy use forecasting

This part of the work deals with energy use prediction for energy management goals. In Section 2.4 several forecasting methods were presented, but they need detailed building information to be tuned and work. The aim of this work was to implement an energy forecasting algorithm using only indoor and outdoor temperature values and actual historical energy consumption data as input, in order to apply the method in a wide range of building studies. As a matter of fact, it is not that common to access detailed building information needed for precise energy simulations, whereas indoor and outdoor temperature measure are frequent and often available on a multi-zone basis.
The aim of the predicted energy consumption is to show an optimum energy use (for given thermal comfort respecting indoor conditions), alongside with the actual working point. The detection of the optimal working point is dealt in the next chapters and it is based on PMV minimization discussed in Section 3.3.
As discussed in Section 2.4, Girotto [35] developed a forecasting method able to forecast heating consumption using clustering method to gather the data and successively linear regression to interpolate the information. The available actual energy consumption data can be used to interpolate a function like this:

$$EC = f(T_{indoor}, T_{outdoor}) \tag{3.8}$$

Where EC are energy consumption data, depending on indoor and outdoor temperature only.
Each available energy consumption value forms an interpolation point together with the Δt parameter, defined as follows:

$$\Delta t = T_{indoor} - T_{outdoor} \tag{3.9}$$

Firstly a linear interpolation is studied in order to estimate the a and b parameters in the following equation:

$$EC = a * \Delta t + b \tag{3.10}$$

A 2nd grade polynomial interpolation is studied as well, where the parameters to be estimated are a, b and c of the following equation:

$$EC = a * \Delta t^2 + b * \Delta t + c \tag{3.11}$$

The parameters a, b and c used in Equation 3.10 and 3.11 are building characteristics. The fit process was done using *Curve fitting* app built in *Matlab*. The fit results are shown and discussed in Section 5.5. The current database does not feature an energy consumption measure, so the monthly data were provided externally. As mentioned in Section 3.1, the temperature measures in the database are available for 5 months only. As a result there are only 5 points to be interpolated for the forecasting formula development, corresponding to monthly energy consumption and monthly mean Δt values. The narrow data-set leaves room for future improvements, as discussed in Section 5.5.

3.8 Comprehensive figure

In this section the developing of the comprehensive figure is explained. It is the graphic approach developed by Tisov [2] for achieving a clear representation of the thermal indoor conditions of the building.
The figure represents the monthly IEQ conditions of a building alongside with the corresponding energy consumption. It is based on a scatter plot where each point corresponds to a single month conditions. Furthermore the dots are labeled to be identified and connected to better visualize the changes through time. The figure is composed as follow:

- On the *x-axis* the thermal discomfort percentage time [%] is shown, to account the monthly average IEQ conditions. The 5% limit is shown as well to help visualize whether the building has a thermal discomfort problem or not

- On the *y-axis* the monthly specific energy consumption $[\frac{kWh}{m^2}]$ is shown, to account the monthly thermal energy use.

The figure could be developed for every definition of thermal discomfort evaluation introduced in Section 3.6. The results and discussion are presented in the next chapters. In the comprehensive figure two data-sets are presented:

- Actual data-set, where thermal discomfort is evaluated using the methods illustrated in Section 3.6, while energy consumption values are the measured one

- Optimal data-set, where thermal discomfort is evaluated using the optimum indoor temperature and the energy consumption values are predicted to guarantee the optimal indoor temperature

The referred optimal indoor temperature in evaluated using the tools introduced in Section 3.3. As mentioned in Section 2.1, thermal comfort is quantified with the PMV parameter, where $PMV = 0$ represents the ideal absence of thermal discomfort and the complete satisfaction with the environmental conditions. The PMV values depends of air temperature, radiant temperature, relative humidity, air speed, metabolic activity and clothing insulation. For the study the assumptions presented in Section 3.3 are used. In Sections 2.3 and 3.3 the presented clothing prediction method achieves a range of reasonable *clo* values, identified by the extremes clo_{min} and clo_{max} and with the central value clo_{mean}. Then, every *clo* value identifies a range of acceptable temperature values, where the extremes are T_{min} ($PMV = -0.5$) and T_{max} ($PMV = +0.5$) and the central value is T_{mean} ($PMV = 0$). The daily optimal indoor temperature value corresponds to T_{mean} evaluated with clo_{mean}. The result is shown in Figure 3.13 as the central values plot, marked in red. The monthly optimal thermal discomfort is evaluated using the methods previously applied, by quantifying the percentage of time outside the comfort temperature range.

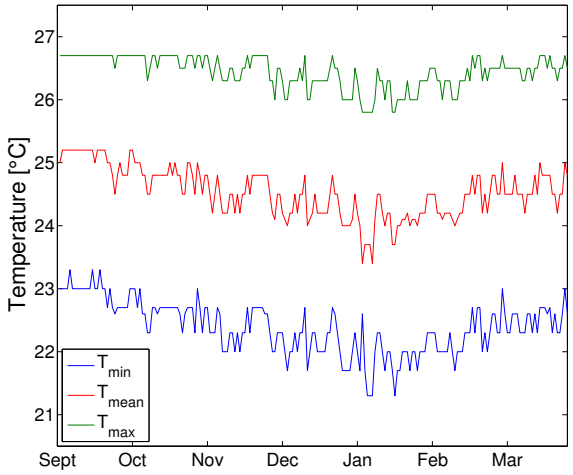

Figure 3.13: Optimal indoor temperature range

The optimal working points presented in the figure and especially the foreseen energy consumption could form two possible scenario, depending on what is causing the current discomfort:

- If the discomfort comes from an overheating (or overcooling) problem, the energy consumption would be reduced by setting a lower (or higher) operative temperature, resulting in both a comfort and consumption benefit
- If the discomfort comes form a subheating (or subcooling) problem, the energy consumption would be increased by setting an higher (or lower) operative temperature, resulting in an higher expense

The former option identifies the current building IEQ conditions studied in this work, where the indoor temperature is often too high causing thermal discomfort, even in the heating season. This scenario is reached with a senseless HVAC management. The latter option could be reached when the HVAC system is undersized or totally missing (for example in the cooling season). It could also be reached with inadequate energy management, meant to achieve economic saving. In both cases the indication follows the standard guidelines but since the thermal judgment is strongly personal, the information brought by the figure could also be used for a more aware choice about the energy management of the building. For example in the studied building the energy manager could choose to stick with an overheating approach and accepting higher energy consumption in order to better suit the occupants thermal perception.

In Figure 3.14 an example of comprehensive figure is shown, concerning thermal discomfort evaluated through the mean indoor temperature (Method I) and with standard fixed temperature range. The 5% boundary limit, defined in the standard **EN15251** [6] as the maximum acceptable discomfort percentage time, is shown as well.

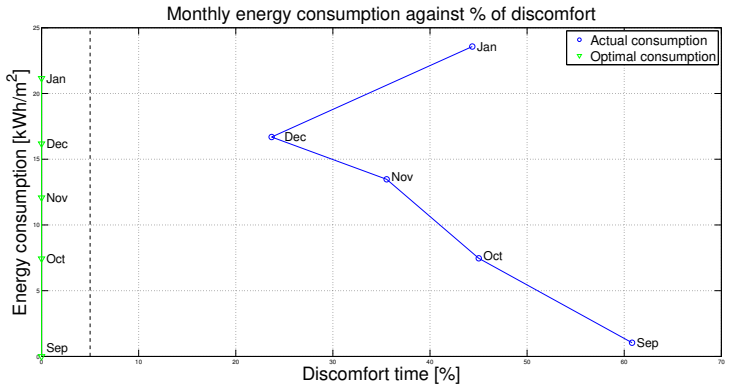

Figure 3.14: Comprehensive figure for mean temperature thermal discomfort (Method I)

Chapter 4

Results

4.1 Duration graphs

In this section, results for monthly duration graphs are presented. The figures are developed as discussed in Section 3.4 and show the plots for indoor temperature for every room of the building. The monthly data are sorted in ascending order and then plotted on a monthly figure.
The results are shown in Figure 4.1, where the dynamic comfort temperature range is shown as well, evaluated as discussed in Section 3.3.
In Section 3.5 extreme and outlier filtering methods are presented to be used for data synthesis. The duration graphs of filtered data-sets are shown and compared in Figure 4.2, while the results are discussed in Section 5.3.

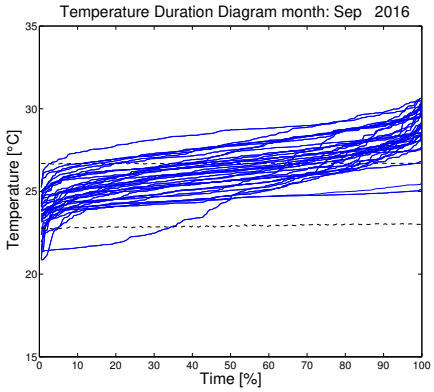

(a) Duration graph for September 2016

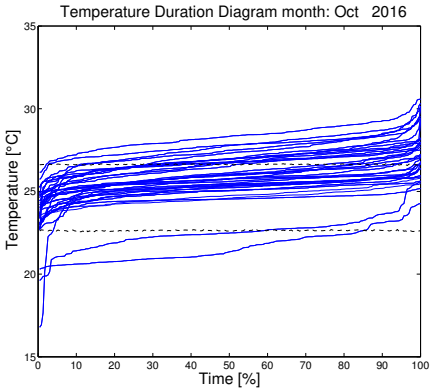

(b) Duration graph for October 2016

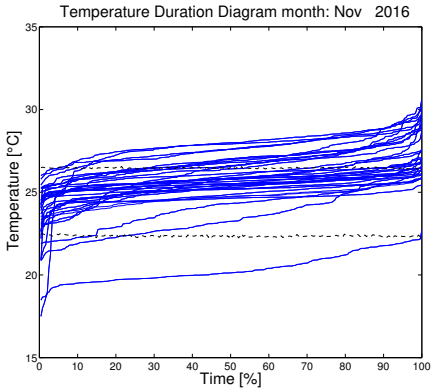

(c) Duration graph for November 2016

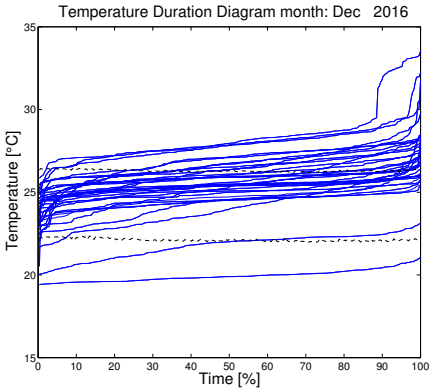

(d) Duration graph for December 2016

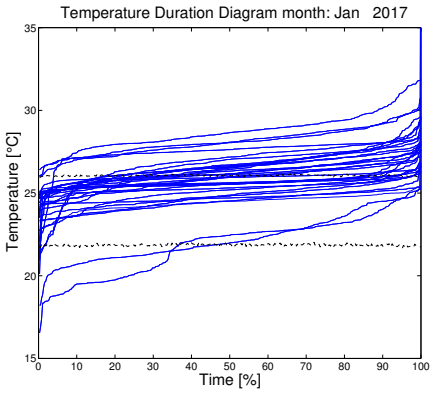

(e) Duration graph for January 2017

Figure 4.1: Monthly duration graphs for complete data-set

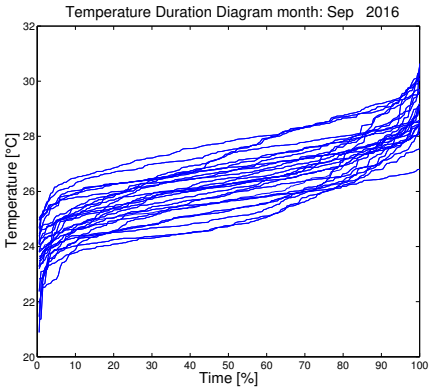

(a) Extreme filtered data-set (September 2016)

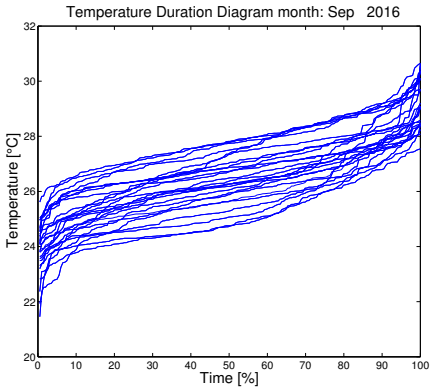

(b) Outlier filtered data-set (September 2016)

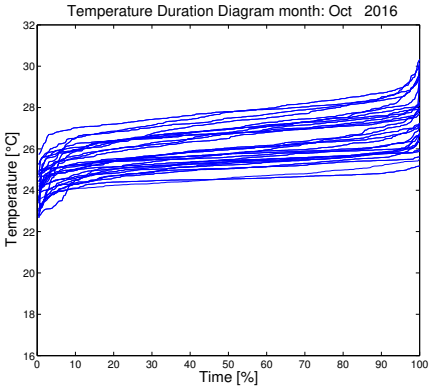

(c) Extreme filtered data-set (October 2016)

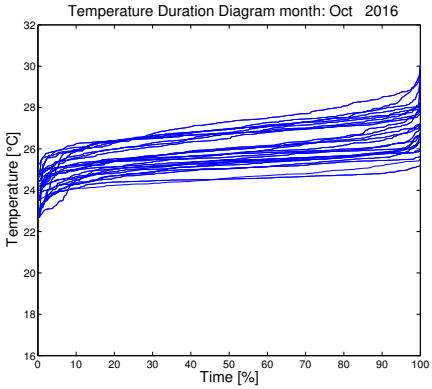

(d) Outlier filtered data-set (October 2016)

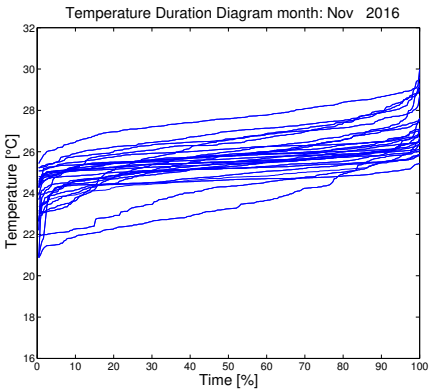

(e) Extreme filtered data-set (November 2016)

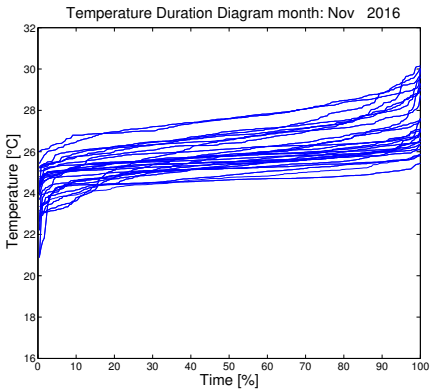

(f) Outlier filtered data-set (November 2016)

Figure 4.2: Monthly duration graphs for extreme and outlier filtered data-set

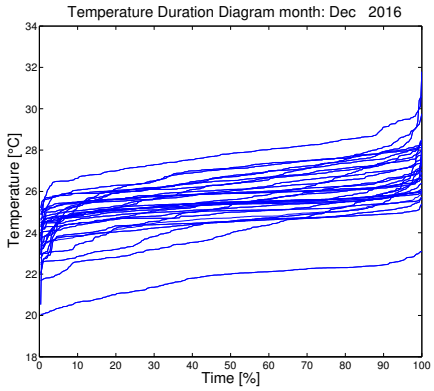

(g) Extreme filtered data-set (December 2016)

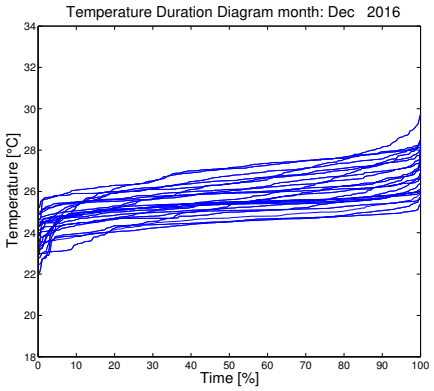

(h) Outlier filtered data-set (December 2016)

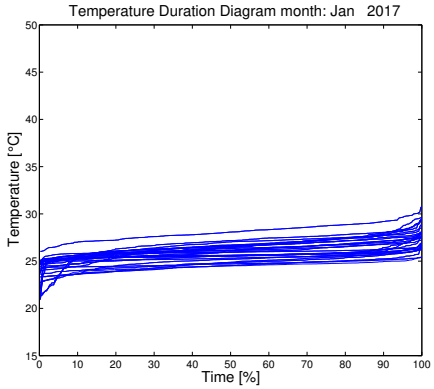

(i) Extreme filtered data-set (January 2017)

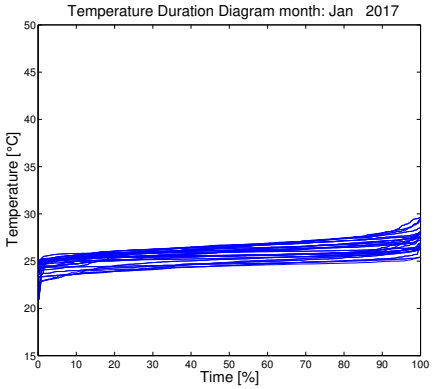

(j) Outlier filtered data-set (January 2017)

Figure 4.2: Monthly duration graphs for extreme and outlier filtered data-set (cont.)

4.2 Room to building synthesis

In this section results for room to building level data synthesis are presented, as discussed in Section 3.5. Each month features two figures, one for mean curve and the other for median curve. The dispersion range is shown in each figure, identified by standard deviation for the mean plot and 1st&3rd quartiles for the median curve. For the dispersion range Method B, presented in Section 3.5, is used, as discussed in Section 5.3.
The results are shown in Figure 4.3, where the standard fixed comfort temperature range is shown alongside, as presented in Section 3.3.

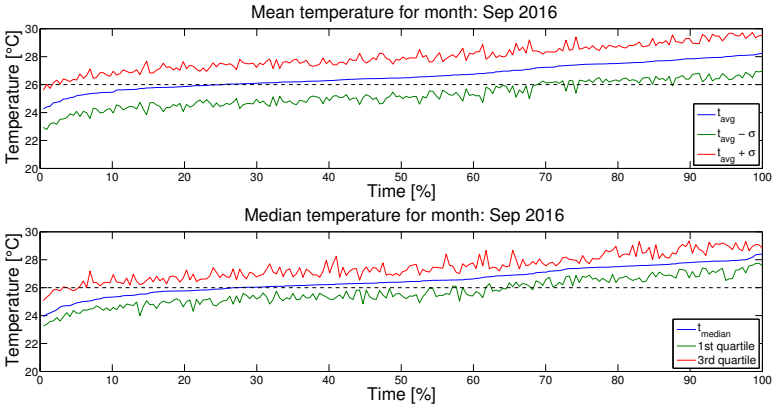

(a) Data synthesis for September 2016

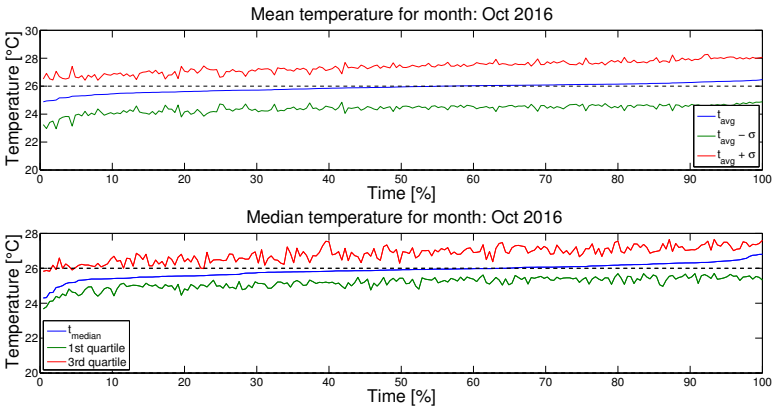

(b) Data synthesis for October 2016

Figure 4.3: Data synthesis for complete data-set

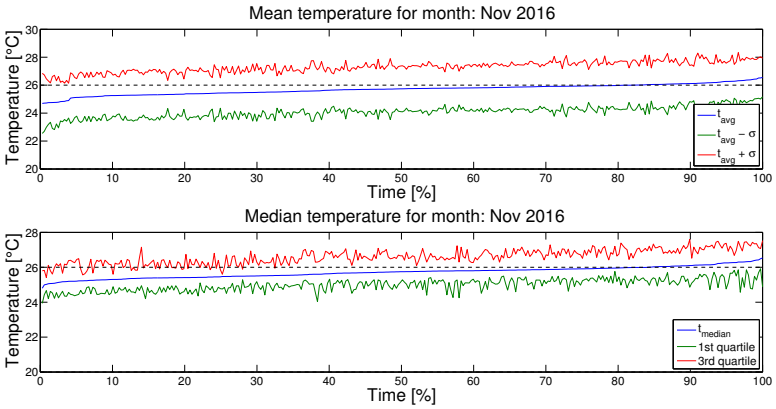

(c) Data synthesis for November 2016

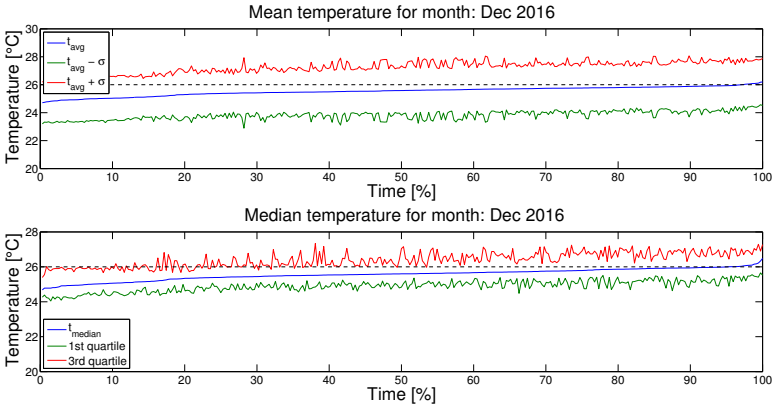

(d) Data synthesis for December 2016

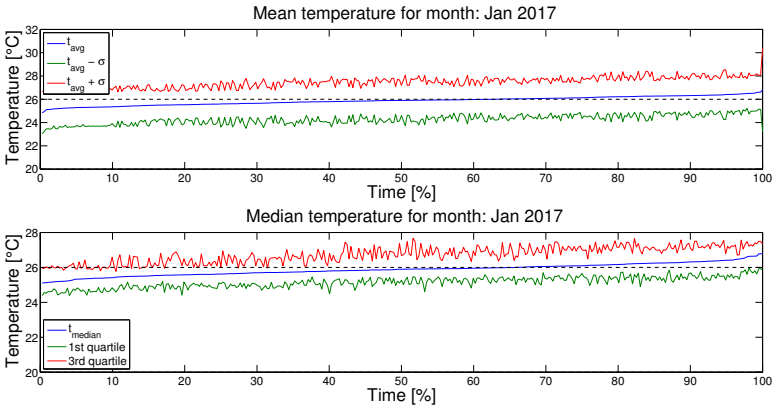

(e) Data synthesis for January 2017

Figure 4.3: Data synthesis for complete data-set (cont.)

4.3 Thermal discomfort evaluation

In this section, results for thermal discomfort percentage time are presented.
In Section 3.6 several methods for monthly thermal discomfort percentage time p_{tot} evaluation were presented. The same methods are reported in Table 4.1

Table 4.1: Thermal discomfort evaluation methods recap

Method	Indicator	Limit
I	T_{mean}	5%
II	T_{median}	5%
III	$T_{mean} \pm \sigma$	5%
IV	$1^{st}\&3^{rd}\ T_{quartile}$	5%
V	$T_{m,ext,filter}$	5%
VI	$T_{m,out,filter}$	5%
VII	$T_{m,problematic}$	5%
VIII	$p_{tot,worstroom}$	5%
IX	$p_{tot,mean}$	5%

Where the percentage time limit of 5% is the acceptable deviation as defined by the standard **EN 15251** [6] and described in Section 3.6.

These methods depends on the thermal comfort temperature range and occupancy patterns. Since for both of them different options were tried, as explained in Sections 3.2 and 3.3, the methods are applied in 4 studied scenarios:

- Fixed schedule, fixed temperature range (Table 4.2)
- Fixed schedule, dynamic temperature range (Table 4.3)
- Dynamic schedule, fixed temperature range (Table 4.4)
- Dynamic schedule, dynamic temperature range (Table 4.5)

Therefore all the methods have to be compared for a fixed scenario (see following tables) and each method has to be compared for the different scenarios (see Section 7.4). Figure 4.4 shows the graphical comparison for a fixed scenario, using the comprehensive figure, while Figure 4.5 shows a comprehensive figure for each discomfort evaluation method, comparing the different scenarios.
The scenarios comparison is developed in Sections 5.1 and 5.2, while the methods are compared in Section 5.4.

Table 4.2: Monthly discomfort evaluation with fixed occupancy and fixed temperature range

Year	Month	Method I	Method II	Method III	Method IV	Method V
2016	09	60,8%	63,3%	92,5%	87,4%	58,5%
2016	10	45,0%	45,9%	95,2%	87,9%	57,1%
2016	11	35,5%	28,1%	93,4%	79,8%	26,4%
2016	12	23,7%	27,5%	94,4%	74,6%	24,7%
2017	01	44,4%	50,3%	97,0%	74,2%	45,7%

Year	Month	Method VI	Method VII	Method VIII	Method IX
2016	09	65,3%	62,8%	99,0%	60,3%
2016	10	44,6%	81,8%	99,6%	44,9%
2016	11	43,4%	53,5%	99,6%	41,3%
2016	12	29,6%	45,3%	99,0%	37,5%
2017	01	33,3%	64,2%	99,7%	45,1%

Table 4.3: Monthly discomfort evaluation with fixed occupancy and dynamic temperature range

Year	Month	Method I	Method II	Method III	Method IV	Method V
2016	09	37,7%	35,2%	76,9%	61,8%	34,7%
2016	10	10,4%	12,6%	85,7%	63,6%	16,0%
2016	11	16,1%	10,7%	88,4%	61,6%	10,7%
2016	12	12,5%	9,8%	85,7%	56,4%	13,6%
2017	01	42,5%	48,7%	97,0%	72,8%	46,2%

Year	Month	Method VI	Method VII	Method VIII	Method IX
2016	09	40,7%	40,7%	96,5%	44,7%
2016	10	8,2%	34,6%	98,7%	38,0%
2016	11	18,2%	28,5%	99,6%	38,4%
2016	12	16,7%	40,8%	98,6%	36,2%
2017	01	29,8%	49,5%	99,7%	53,1%

Table 4.4: Monthly discomfort evaluation with dynamic occupancy and fixed temperature range

Year	Month	Method I	Method II	Method III	Method IV	Method V
2016	09	66,4%	67,7%	93,5%	86,2%	65,0%
2016	10	44,9%	45,8%	95,1%	88,0%	57,3%
2016	11	32,8%	24,6%	93,3%	79,6%	26,3%
2016	12	23,0%	26,7%	94,5%	73,3%	28,5%
2017	01	44,4%	50,3%	97,0%	74,2%	45,7%

Year	Month	Method VI	Method VII	Method VIII	Method IX
2016	09	69,6%	68,2%	99,1%	64,3%
2016	10	44,9%	81,8%	99,6%	45,0%
2016	11	41,5%	51,8%	99,4%	40,5%
2016	12	29,4%	44,8%	99,1%	36,9%
2017	01	33,3%	64,2%	99,7%	45,1%

Table 4.5: Monthly discomfort evaluation with dynamic occupancy and dynamic temperature range

Year	Month	Method I	Method II	Method III	Method IV	Method V
2016	09	45,2%	39,6%	80,6%	65,4%	41,0%
2016	10	11,1%	12,9%	85,8%	63,6%	16,4%
2016	11	14,0%	7,8%	86,0%	54,9%	10,9%
2016	12	14,5%	5,5%	85,5%	61,9%	14,5%
2017	01	42,5%	48,7%	97,0%	72,8%	46,2%

Year	Month	Method VI	Method VII	Method VIII	Method IX
2016	09	44,7%	47,9%	96,8%	49,0%
2016	10	8,4%	34,2%	98,7%	38,1%
2016	11	17,9%	24,1%	99,7%	38,0%
2016	12	14,5%	40,1%	98,8%	35,9%
2017	01	29,8%	49,5%	99,7%	53,1%

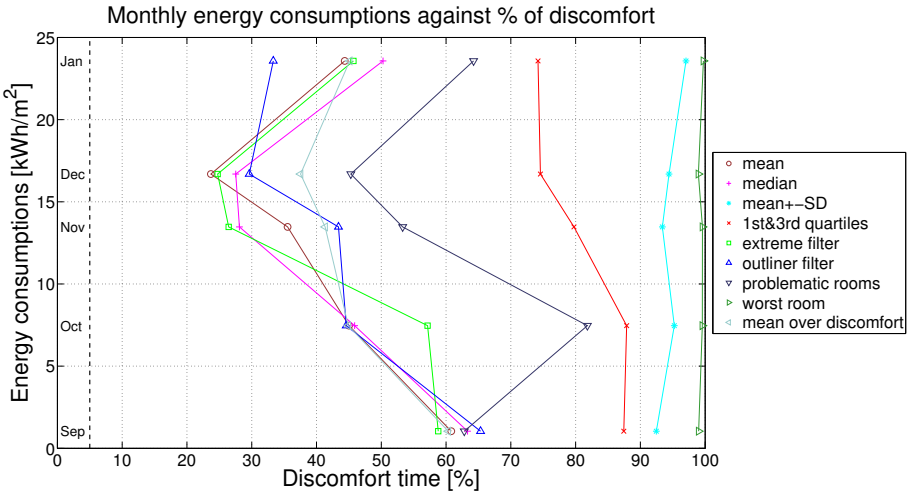

(a) Fixed schedule, fixed temperature range

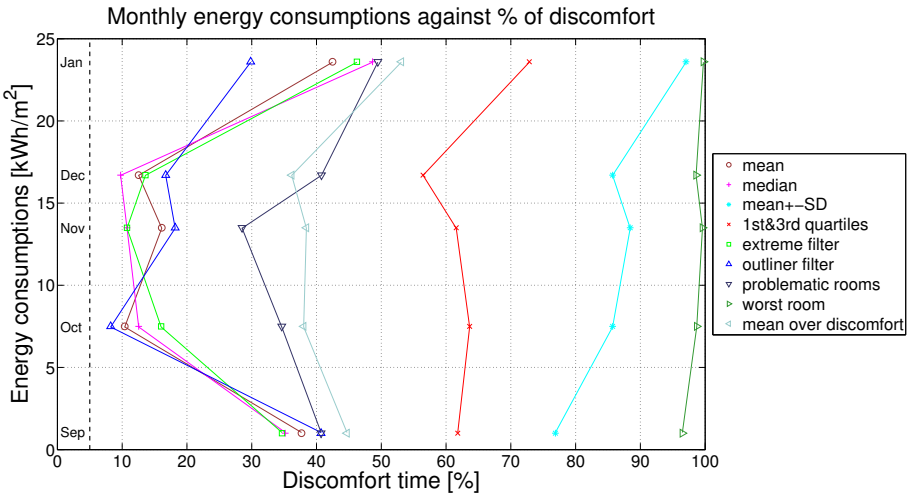

(b) Fixed schedule, dynamic temperature range

Figure 4.4: Discomfort evaluation methods comparison with fixed hypothesis for occupancy and comfort temperature range detection

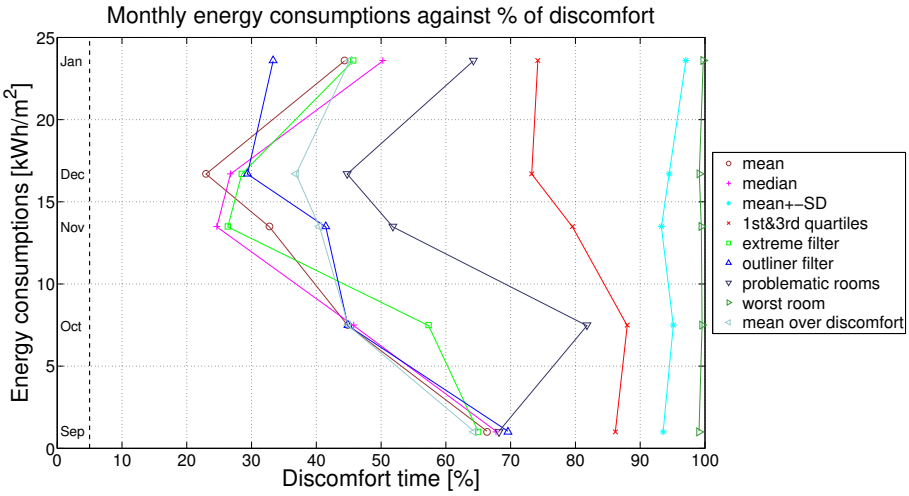

(c) Dynamic schedule, fixed temperature range

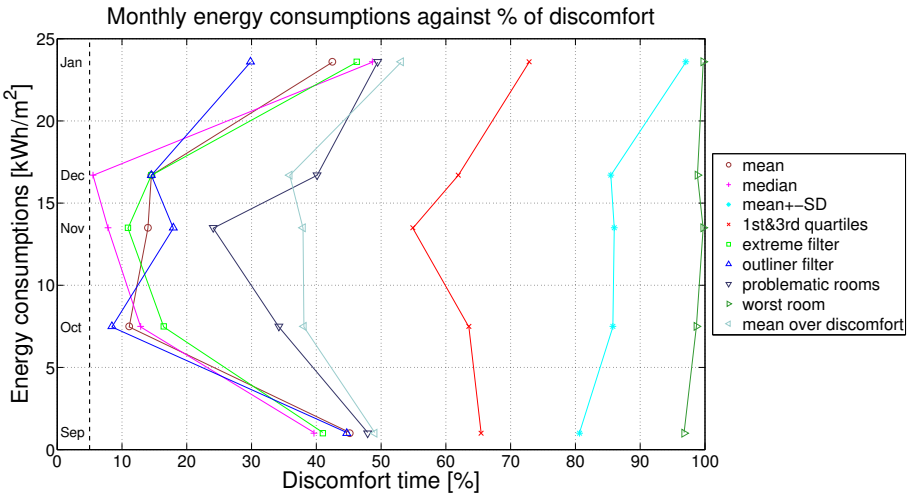

(d) Dynamic schedule, dynamic temperature range

Figure 4.4: Discomfort evaluation methods comparison with fixed hypothesis for occupancy and comfort temperature range detection (cont.)

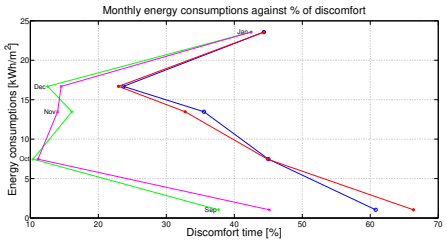

(a) Method I

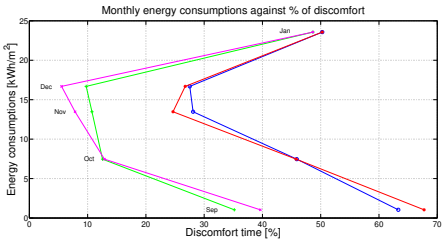

(b) Method II

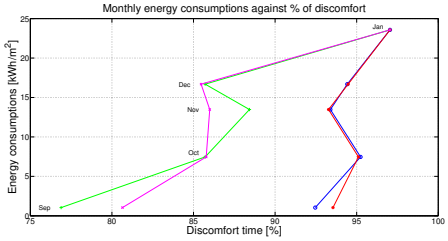

(c) Method III

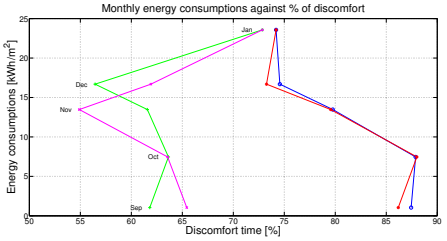

(d) Method IV

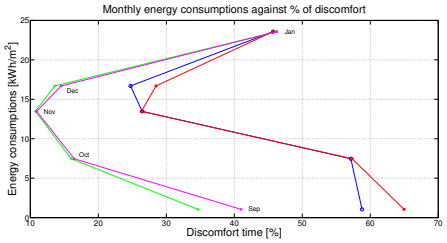

(e) Method V

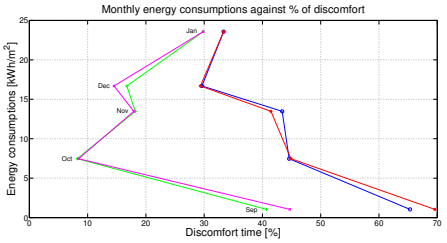

(f) Method VI

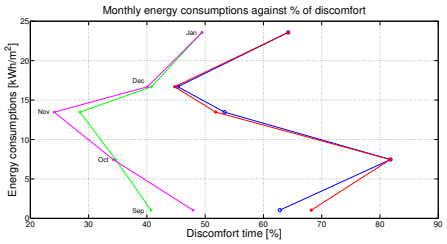

(g) Method VII

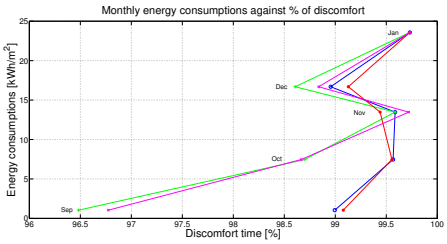

(h) Method VIII

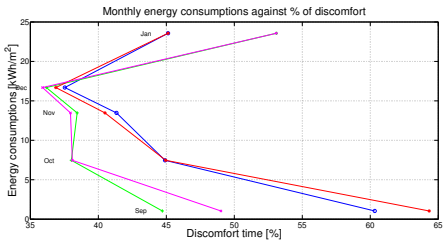

(i) Method IX

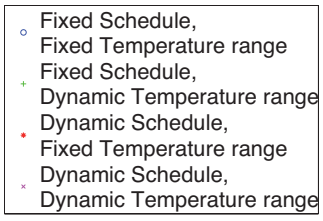

(j) Legend

Figure 4.5: Discomfort evaluation methods comparison with different hypothesis for occupancy and comfort temperature range detection

4.4 Energy use forecasting

In Section 3.7 energy forecasting method is developed, where both a 1st and 2nd grade polynomial fits were applied to the data-base. The comparison about the two methods and the goodness of the fit are discussed in Section 5.5.
Table 4.6 shows the monthly foreseen consumption values alongside with the actual consumption.

Table 4.6: Foreseen energy consumption for 1st and 2nd grade fits $[kWh/m^2]$

Year	Month	Actual data	1st grade polynomial fit	2nd grade polynomial fit
2016	09	1,0	0,0	0,0
2016	10	7,5	7,4	7,1
2016	11	13,5	12,1	11,6
2016	12	16,7	16,2	15,9
2017	01	23,6	21,2	21,4

4.5 Comprehensive figure

In this section results for comprehensive figure are presented. The figures are developed as discussed in Section 3.8 and show the scatter plots with monthly values for thermal discomfort percentage time on the *x-axis* and energy consumption on the *y-axis*. Each figure presents a different method for thermal discomfort evaluation, as presented in Section 4.3.
The figures refer to fixed schedule for occupancy (see Section 3.2) and dynamic temperature range for discomfort evaluation (see Section 3.3). This choice is discussed in Section 5.1 and 5.2.
The comprehensive figures for every scenario of occupancy detection and temperature range evaluation are shown in Section 7.5.

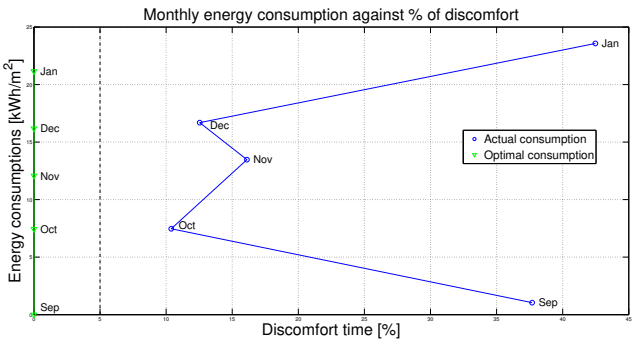

Figure 4.6: Comprehensive figure for Method I thermal discomfort evaluation

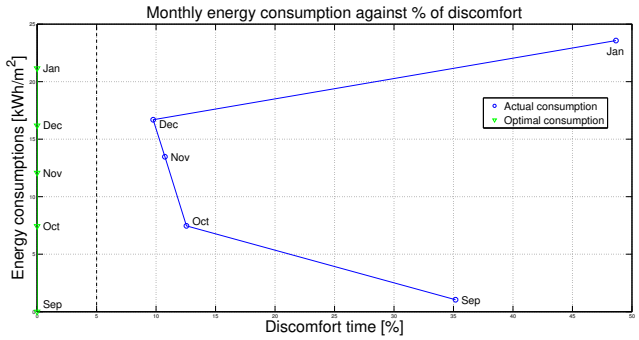

Figure 4.7: Comprehensive figure for Method II thermal discomfort evaluation

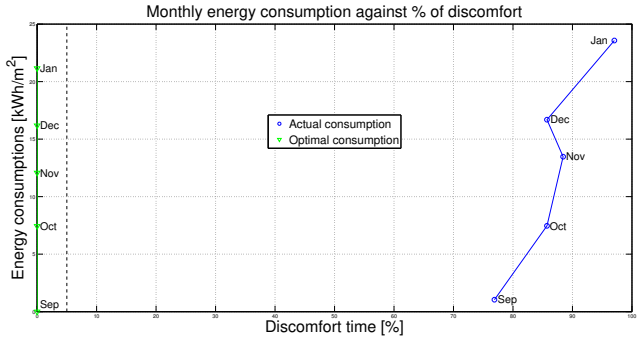

Figure 4.8: Comprehensive figure for Method III thermal discomfort evaluation

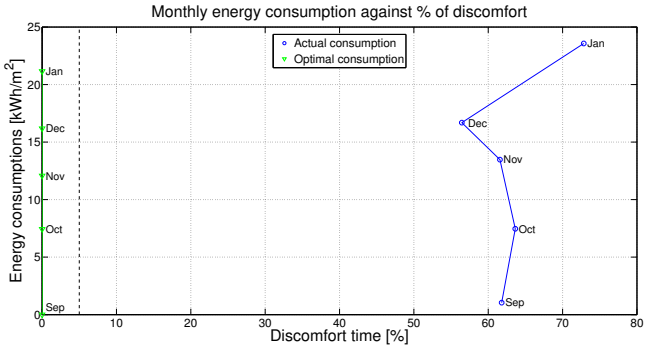

Figure 4.9: Comprehensive figure for Method IV thermal discomfort evaluation

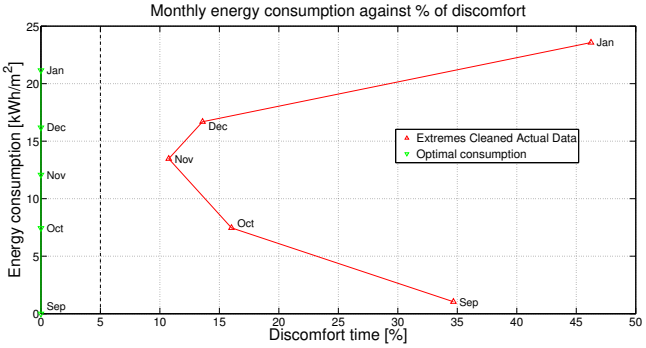

Figure 4.10: Comprehensive figure for Method V thermal discomfort evaluation

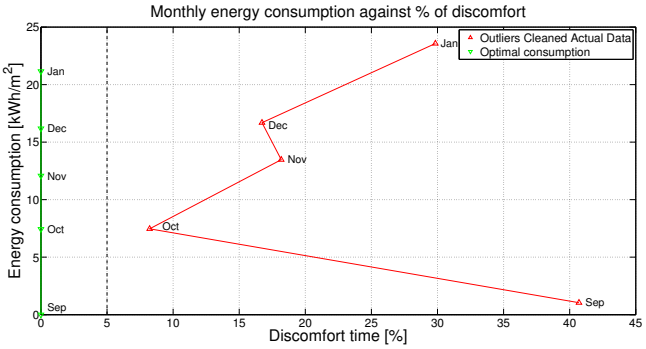

Figure 4.11: Comprehensive figure for Method VI thermal discomfort evaluation

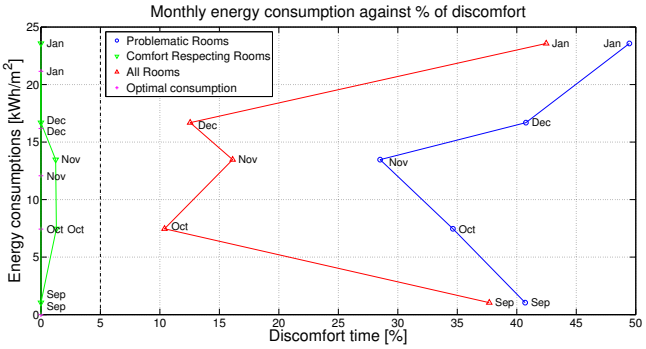

Figure 4.12: Comprehensive figure for Method VII thermal discomfort evaluation

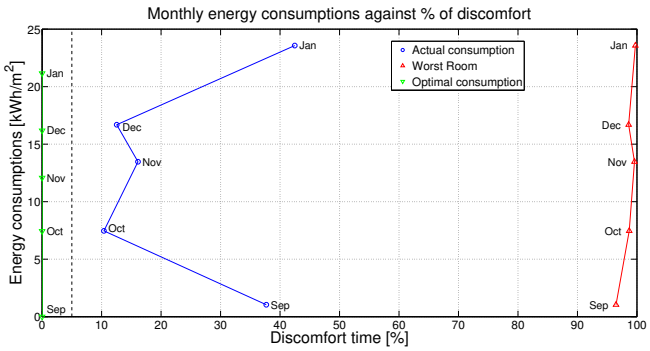

Figure 4.13: Comprehensive figure for Method VIII thermal discomfort evaluation

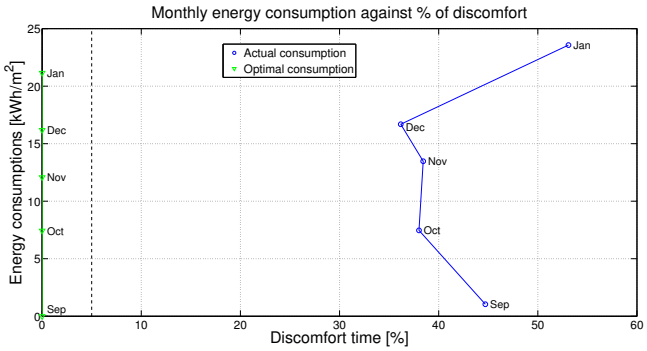

Figure 4.14: Comprehensive figure for Method IX thermal discomfort evaluation

Chapter 5

Discussion

5.1 Occupancy evaluation

As illustrated in Section 3.2, two approaches were studied for the occupancy detection, on which the thermal comfort evaluation is based:

- Fixed occupancy pattern, corresponding to the opening hours of the building reported in Table 5.1
- Dynamic occupancy pattern, evaluated from the indoor CO_2 concentration measurement

Table 5.1: Fixed schedule (opening hours)

Day	Opening hour	Closing hour
Monday to Friday	7	16
Saturday and Sunday	Closed	

Figure 5.1 shows the comparison between the two studied options, where the zero value corresponds to an unoccupied day. The results of the two methods appear to be quite close, both in the time prediction and the weekend detection. The problems lie in the peaks where the departure time reaches 10 PM, significantly later than the closing hour of the building. Some weekends are missed and appear to be occupied, that is equally suspicious, which leaves room for improvements and more accurate tuning.
As mentioned in Section 3.1, only half of the room feature a reliable CO_2 concentration measurement (some rooms have a fixed unconvincing measure), moreover the method appears difficult to be automated, especially in the CO_2 concentration peaks detection. For this reason, in the present study the occupancy pattern was evaluated for a single room measure and then it is applied to the whole building.

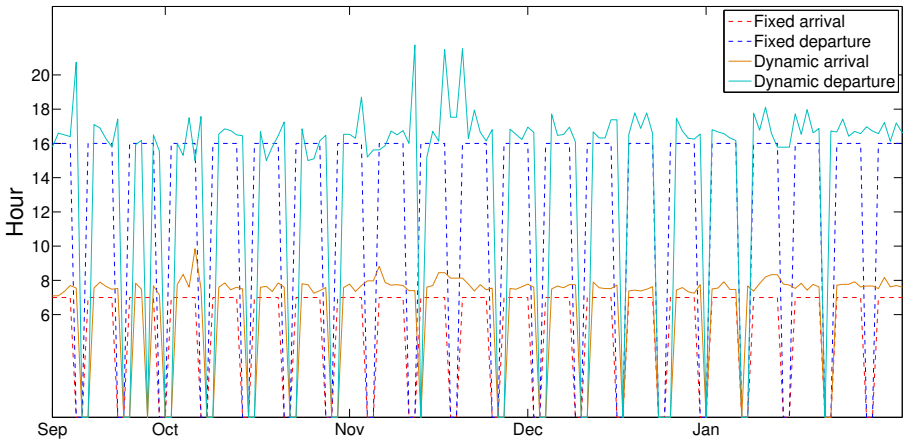

Figure 5.1: Arrival and departure time plot for both fixed and dynamic evaluation methods

A more detailed study would feature occupancy detection for every thermal zone, with individual comfort evaluation. This approach better fits the modern concept of office work, where each worker has its own schedule instead of a fixed one. A thermal comfort study must consider this behaviour to get a reliable information. Both methods studied are not capable of dealing this problem, a further study would feature a neural network or a machine learning algorithm for a better occupancy pattern detection.

Figure 5.2 shows the comprehensive figure displaying results for Method I, explained in Section 3.6, for a fixed comfort temperature range scenario, while Table 5.2 shows the numerical results.

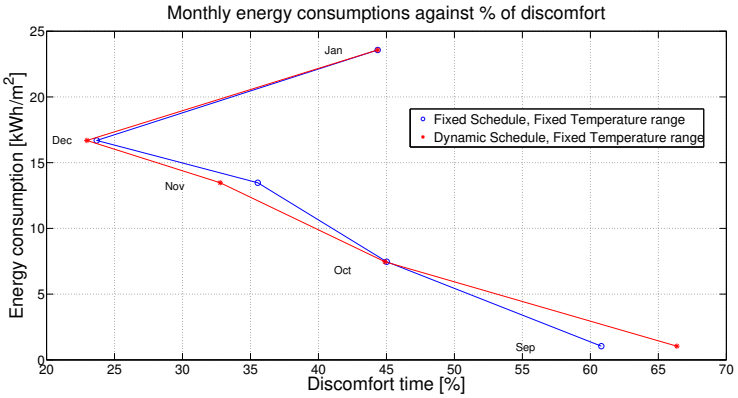

Figure 5.2: Comprehensive figure comparison for fixed and dynamic schedule (Method I)

Year	Month	Fixed limits	Dynamic limits
2016	09	60,8%	66,4%
2016	10	45,0%	44,9%
2016	11	35,5%	32,8%
2016	12	23,7%	23,0%
2017	01	44,4%	44,4%

Table 5.2: Table comparison for fixed and dynamic temperature range (Method I)

As predicted, the dynamic schedule results appear to be pretty close to the fixed one, since the predicted time table fits the opening hours of the building, as shown in Figure 5.1. In particular, the evaluated discomfort is nearly identical for October, December and January, while they move in September and November. Those months are characterized by the presence of the mentioned peaks, as shown in Figure 5.1.
The need is to understand if the deviation from the fixed schedule is due to a wrong evaluation or not. For this purpose, Figure 5.3 shows the CO_2 concentration level in every room during a week where a peak is located. The corresponding occupancy pattern evaluated by the algorithm is shown in Table 5.3. Figure 5.3 is pretty clear about the

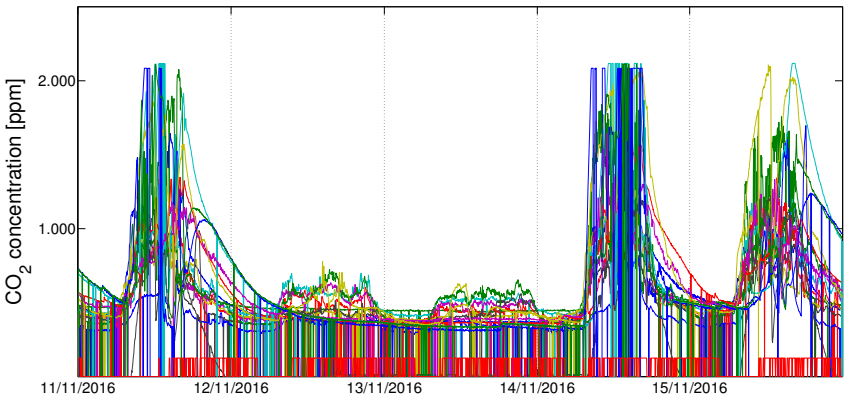

Figure 5.3: CO_2 concentration level [ppm] in every room for a problematic week

absence of occupants during the 12th of November 2016, while the algorithm detected a presence from 7:24 to 21:45. Furthermore the 12th of November is a Saturday, which justifies the previous impression.
This approach for occupancy pattern detection shows just minor benefits in comparison with the fixed schedule approach and the prevalent difference comes from fault detection of the algorithm. In conclusion the fixed schedule approach seems to work better for this study, while the dynamic occupancy pattern detection from CO_2 concentration presented in this work could be the starting point for further development.

Table 5.3: Detected occupancy pattern

Day	Arrival hour	Departure hour
11/11/2016	7:24	16:00
12/11/2016	7:24	21:45
13/11/2016	Unoccupied	
14/11/2016	7:36	15:12
15/11/2016	7:42	16:42

5.2 Temperature range definition

In Section 3.3 the comfort temperature range was dealt, using the hypothesis of negligible air speed, constant relative humidity of 50%, constant metabolic rate of 1 *met*, radiant temperature corresponding to air temperature. These simplified assumptions are needed to focus on the clothing insulation, which is the most time changing parameter. In particular, the metabolic rate assumption is relevant, since the standard **EN15251** [6] uses 1,2 *met* for an office scenario. A lower value leads to an higher temperature comfort limit, so it is a conservative choice with the available data-base characterized by an overheating problem. However, the elevated indoor temperature suggest that occupants have a different perception from what the standard fixed. This fact was considered by using a lower metabolic rate. With these assumptions two cases of study were compared:

- Fixed comfort temperature range defined over seasonal fixed *clo* values, 0,5 *clo* for summer (cooling) season and 1 *clo* for winter (heating) season, according to standard **EN 15251** [6]
- Dynamic comfort temperature range defined over daily estimated *clo* value, depending on the outdoor temperature at 6AM, described in Section 3.3

The data-base features only measurements from September to January, therefore the method was applied to the heating season only. Further studies could use the adaptive comfort model, described in standards **EN15251** [6] and ASHRAE 55 [4], to define a dynamic comfort temperature range for the cooling season. This model applies to natural ventilated building only and it considers human behaviour adjustments to better tolerate the warm weather, for example by opening windows and changing clothes. The dynamic temperature range is defined over outdoor mean temperature and results in a wider range compared to the standard fixed one.

Defining the thermal comfort temperature range just on the clothing insulation is clearly a simplification, but it works for an office building since it has generally standard indoor conditions (for example same activities and same schedule during the year).
The comparison between standard fixed and estimated *clo* value is shown in Figure 5.4. Looking at the figure, the estimated *clo* values appear to be significantly different from the standard fixed ones. The standard values appear to be a rough representation of

real clothing insulation, according to the database used to develop the *clo* evaluation method [19], since the fixed *clo* values are constantly outside the expected *clo* range. Furthermore a daily estimated value helps representing the gradual clothing changes through the season.

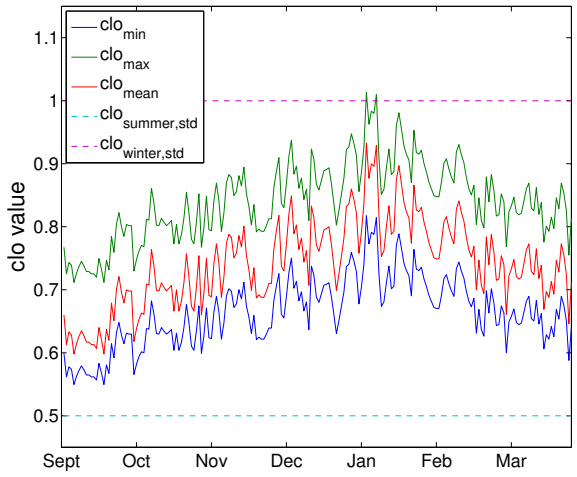

Figure 5.4: Estimated values of clo during the studied period compared to standard ones

Figure 5.5 shows the resulting thermal comfort temperature range from both methods.

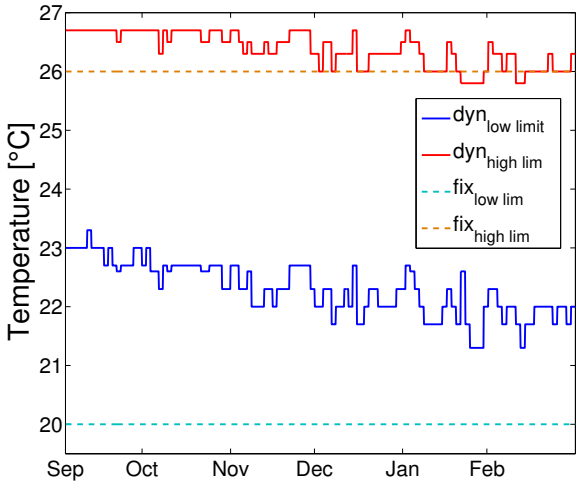

Figure 5.5: Estimated comfort temperature range compared to stadard fixed one

The dynamic temperature limits appear in the figure to be higher than the fixed ones. In particular the lower limit appears to be significantly different, while the higher

ones are close to each other, even if the standard limit is referring to the summer (cooling) season and the data-set refers to the winter (heating) season. Despite it depends on the assumption made at the beginning of the section, this fact reveals the unreliability of the standard hypothesis, that carries on a misleading information about thermal comfort. The superior temperature limit, by being higher, reveals a minor clothing insulation, in comparison to the fixed value of 1 *clo*. This accounts the behaviour of occupants, able to adapt their clothing to the environment, for example by taking off a jacket when they get into the building. The lower limit, being significantly higher than the standard one, reveals a minimum clothing insulation needed, for example for dressing code reasons.
The data-base shows a significant overheating problem in the building, as reported in the duration graph of Figure 3.6. By using the dynamic evaluated temperature limit, the computed discomfort percentage time would be lower, as shown in Figure 5.6, where Method I results are compared on the comprehensive figure for fixed and dynamic comfort temperature limits. The figure clearly shows that using fixed *clo* value leads to overestimation of discomfort. For both cases of study, fixed schedule is used. The table results are shown in Table 5.4.

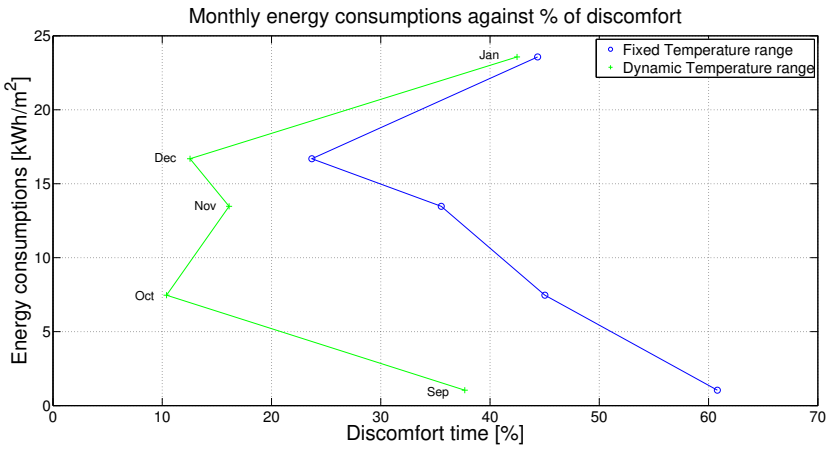

Figure 5.6: Comprehensive figure comparison for fixed and dynamic temperature range (Method I)

Year	Month	Fixed limits	Dynamic limits
2016	09	60,8%	37,7%
2016	10	45,0%	10,4%
2016	11	35,5%	16,1%
2016	12	23,7%	12,5%
2017	01	44,4%	42,5%

Table 5.4: Table comparison for fixed and dynamic temperature range (Method I)

5.3 Room to building synthesis

In Section 3.5 several hypothesis to achieve a reliable building synthesis were presented, aimed to obtain a thermal representation on the building level without sacrificing relevant information on the room level. The mathematical tool used to visualize the monthly data-base of the whole building is the duration graph, where the room temperature is plotted in ascending order. In this section temperature data synthesis is discussed, while thermal discomfort evaluation on the building level is discussed in Section 5.4.

Firstly a comparison between mean and median curves for complete data-set is developed. The curves were obtained averaging every room temperature measurements for a fixed instant, as discussed in Section 3.5. Figure 5.7 shows the comparison on the duration graph for a single month plot. It refers to November 2016, where the deviation is more visible. In order to better compare mean and median use for the data-

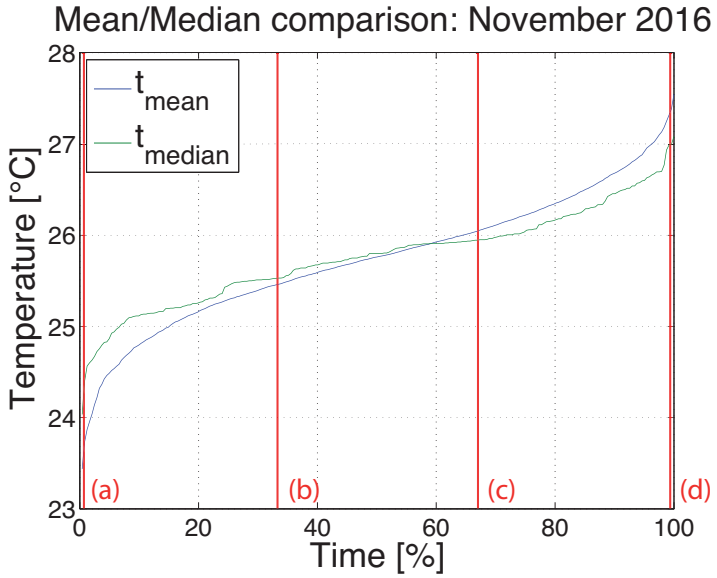

Figure 5.7: Mean and median temperature results comparison for November 2016

set synthesis, Figure 5.8 shows the temperature distribution over time for November 2016 in four points of the duration graph. They are marked in red in Figure 5.7 and correspond to 1% (a, Figure 5.8a), 33% (b, Figure 5.8b), 66% (c, Figure 5.8c) and 100% (d, Figure 5.8d) percentage time values on the *x-axis* of the duration graph. The other months distribution are shown in Appendix chapter (Section 7.3). The distribution has a slight negative skew in the left part of the duration graph (Figures 5.8a and 5.8b) and a slight positive skew in the right part (Figures 5.8c and 5.8d). The effect is observable in Figure 5.7, where the median is higher than the mean in the left part and lower in the right part. This tendency is observable in every month distribution, as shown in Section 7.3. However, the skew is not excessively large in any of the studied distribution, so the central tendency approach is considered reliable.

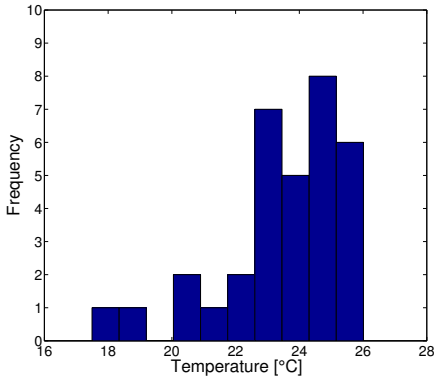

(a) Temperature distribution for a percentage time of 1%

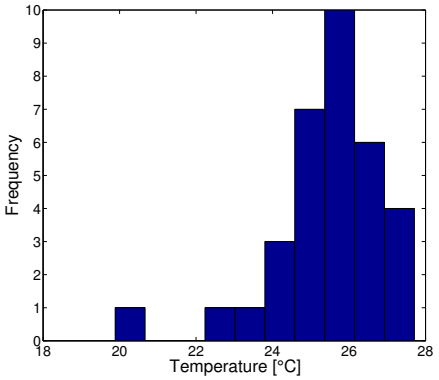

(b) Temperature distribution for a percentage time of 33%

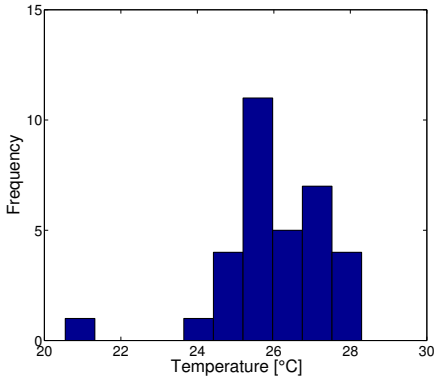

(c) Temperature distribution for a percentage time of 66%

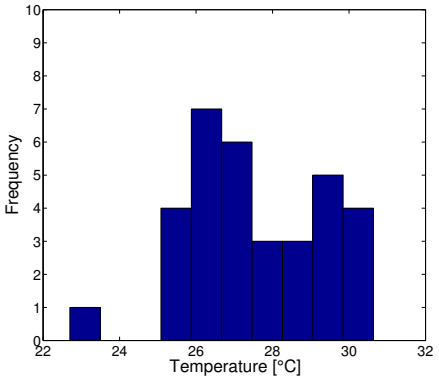

(d) Temperature distribution for a percentage time of 100%

Figure 5.8: Temperature distribution in November 2016

The presence of outliers is clear and it surely influences the mean value. The outliers tend to show up as temperature measures significantly lower than the others and they move the distribution to its left side. For example in Figure 5.8c the outlier makes the distribution to cancel skews present in the main cluster, while ignoring that value the result would be a positive skew.
However, these measurements still represent the thermal conditions of a single room, that could not be ignored, but in the meantime they downsize the overheating problem of the building. Further studies are needed to evaluate how much these measurements affect the global thermal information.
As explained in Section 3.5, two different methods were tried to filter the data-base from outlier values:

- Extreme values filtering
- Outlier values filtering

The results from the two methods are compared to evaluate if they improve the synthesis information or not. To fulfill the comparison, Figure 5.10 shows the duration graphs

featuring mean and median plots for complete data-set, alongside with mean plots for extreme and outlier data-set filtering methods, while Figure 5.11 shows the comparison between extreme and outlier filtered temperature distribution for the month of November 2016. The other months distribution comparisons are shown in Appendix chapter (Section 7.3). Monthly average duration graph comparison is developed hereafter:

- *September 2016* (Figure 5.10a): extreme filtered and outlier filtered plots are pretty close (maximum difference is $0,33°C$) and the complete data-set mean plot lies in between. The complete data-set median plot has a significant fluctuation but it follows the mean plot (maximum difference is $0,23°C$). For these data-sets there is no method to prefer over the others

- *October 2016* (Figure 5.10b): extreme filtered and outlier filtered plots are pretty close (maximum difference is $0,27°C$), but the former is superior, differently from Figure 5.10a. The complete data-set mean plot follows firmly the outlier filtered plot. The complete data-set median plot is still fluctuating but pretty close to the mean one. The extreme filtered plot is the only one giving a different information from the other methods

- *November 2016* (Figure 5.10c): extreme filtered and outlier filtered plots are more distant compared to previous cases (maximum difference is $0,38°C$), with the outlier filtered data-set mean higher than the extreme one. The mean curve is located among the extreme filtered mean curve and the outlier filtered mean curve, following the former on the left side (lower temperatures) and the latter on the right side (higher temperatures). Conversely, the median follows the outlier filtered mean curve on the left side (lower temperatures) and the extreme filtered data-set on the right side (higher temperatures)

- *December 2016* (Figure 5.10d): extreme filtered and outlier filtered plots are distant in the left side (maximum difference is $0,32°C$), while the distance shrinks to the right until they correspond. The complete data-set mean plot follows firmly the extreme filtered plot, while the complete data-set median plot is strongly fluctuating with values higher than the mean on the left side and lower on the right side. This tendency is visible in every month plot, but it is stronger in this case

- *January 2017* (Figure 5.10e): extreme filtered plot is higher than outlier filtered one, similarly to conditions of October 2016, with a maximum distance of $0,26°C$. Complete data-set mean plot starts lower than outlier filtered plot and ends just above the extreme filtered one. The complete data-set median plot is quite moved away from the other plots, being higher than the mean for almost the whole month, with a maximum distance of $0,66°C$

To better understand the values of complete data-set mean (CDMN), complete data-set median (CDMD), extreme filtered data-set mean (EFDM) and outlier filtered data-set mean (OFDM) a look at the monthly temperature distribution is needed. The distribution figures for each month could be found in Appendix chapter (Section 7.3), while Figure 5.11 shows the temperature distribution comparison for November 2016.

- *September 2016*: temperature distribution is nearly normal, so CDMN and CDMD values are close. On the right side the distribution shows a negative skew, resulting in CDMN to be higher than CDMD. Extreme and outlier data-set filtering work in the same temperature range, but the former cuts more on the right while the latter cuts more on the left side. Consequently OFDM is higher than EFDM

- *October 2016*: temperature distribution shows two outliers on the left side, corresponding to two rooms significantly colder than the others, and a positive skew in the main group of measures, for this reason CDMD is slightly superior than CDMN. Both extreme and outlier data-set filtering cut the two left outliers, but the latter cuts some measures on the right side too. The result is a value of EFDM higher than OFDM, which is closer to CDMN and CDMD

- *November 2016*: temperature distribution shows one outlier on the left side, while the main part of the data-set moves from a negative skew (left side of the duration graph) to a positive skew (right side of the duration graph), resulting in CDMD to be higher than CDMN in the left side of the data-set and lower in the right side. Both extreme and outlier data-set filtering cut the left outlier, but the latter method has a stronger effect. The result is a value of OFDM higher than EFDM

- *December 2016*: temperature distribution shows two outliers on the left side, corresponding to two rooms significantly colder than the others, while the main part of the distribution moves from a negative to a positive skew when the measured temperatures increase. The result is a value of CDMD higher than CMDN on the left side and lower on the right side. Extreme data-set filtering cuts only one left outlier, while outlier data-set filtering cuts both of them. Furthermore outlier data-set filtering cuts some measures on the right side, resulting in OFDM to be higher than EFDM due to the weight of the left outlier kept by extreme data-set filtering

- *January 2017*: temperature distribution shows an outlier on the left side, significantly different from the main part of the data-set, resulting in median value to be higher than mean value, especially for the left side of the duration graph, where the main part of the data-set has a positive skew, while in the right side of the duration graph the main part of the data-set has a negative skew, leading to CDMN to be alike CDMD. Both extreme and outlier data-set filtering cut the left outlier, with the latter cutting some measures on the right side too. The result is EDFM to be higher than ODFM, since the data-set is moved to the left

Globally, the data-base shows outliers on the left side, corresponding to rooms with a significantly lower indoor temperature compared to the others, leading to underrate the CDMN value. CDMD tends to be higher than CDMN of the left side on the duration graph and lower on the right, due to the temperature distribution moving from a negative to a positive skew in the main part of the data-set (ignoring outliers). This tendency is shown in Figure 5.9, where the skew is computed as follows:

$$s = \frac{3(T_{mean} - T_{median})}{\sigma} \tag{5.1}$$

Where σ is the standard deviation.
Except for September, which is not totally part of the heating season, the monthly curves show a skew moving from a negative to a positive value, especially in the main cluster, when moving from low to high temperatures (see changes from Figure 5.8a to 5.8d).
Extreme data-set filtering method tends to be more tolerant than the outlier data-set filtering method, which is cutting more measures, especially on the low temperature side.
Median curve for the complete data-set seems to better represent the whole building indoor conditions, since it is not cutting any temperature measures, but it is not distorted by the presence outliers as well.

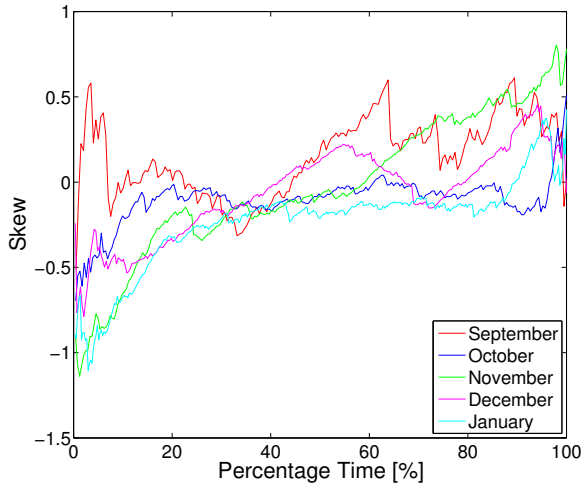

Figure 5.9: Monthly skew index plot

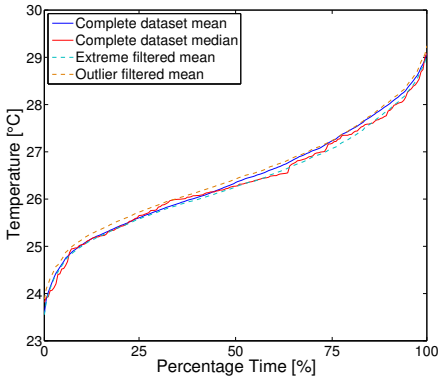

(a) Duration graph comparison for September 2016

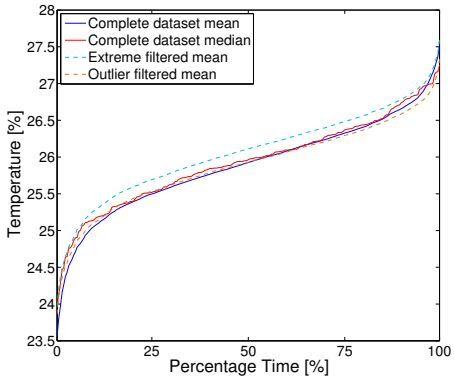

(b) Duration graph comparison for October 2016

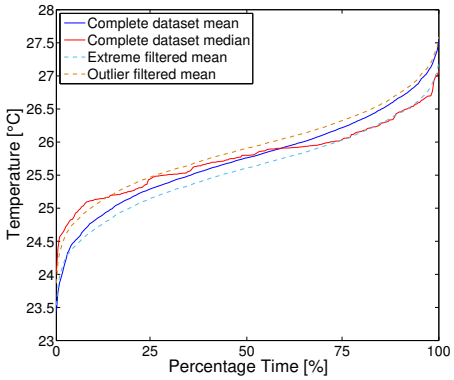

(c) Duration graph comparison for November 2016

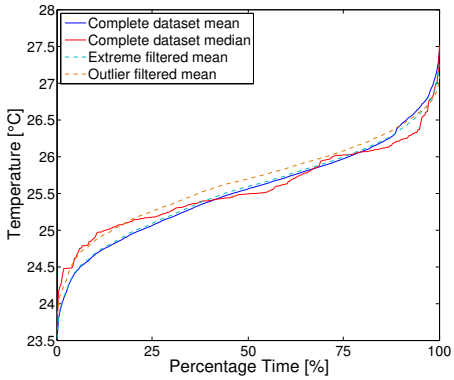

(d) Duration graph comparison for December 2016

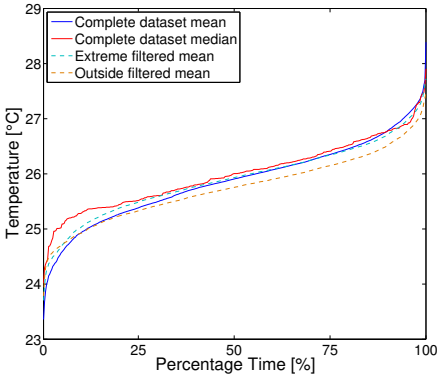

(e) Duration graph comparison for January 2017

Figure 5.10: Mean and median duration graph for complete and filtered data-set

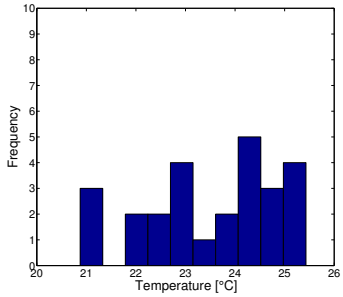

(a) Extreme filtered temperature distribution for a percentage time of 1%

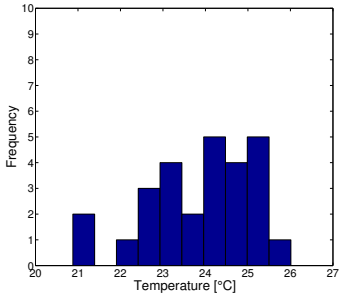

(b) Outlier filtered temperature distribution for a percentage time of 1%

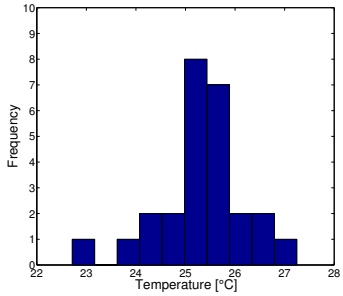

(c) Extreme filtered temperature distribution for a percentage time of 33%

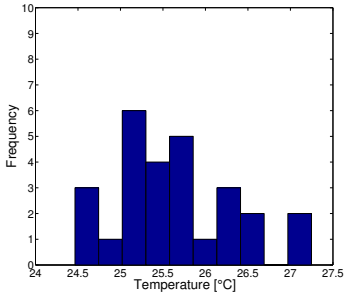

(d) Outlier filtered temperature distribution for a percentage time of 33%

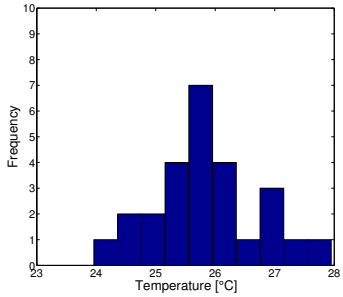

(e) Extreme filtered temperature distribution for a percentage time of 66%

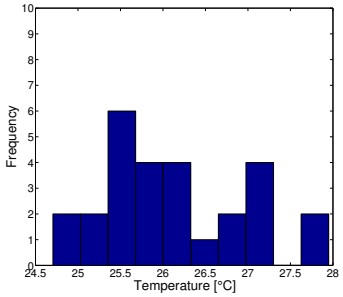

(f) Outlier filtered temperature distribution for a percentage time of 66%

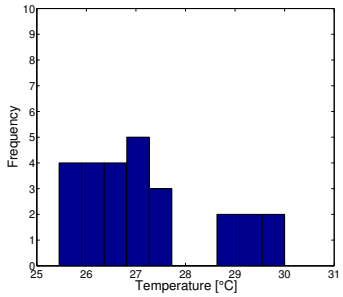

(g) Extreme filtered temperature distribution for a percentage time of 100%

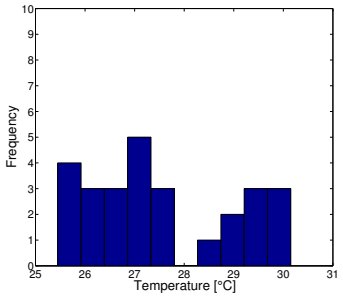

(h) Outlier filtered temperature distribution for a percentage time of 100%

Figure 5.11: Extreme and outlier filtered temperature distribution in November 2016

Lastly, the methods to compute average temperature data-set presented in Section 3.5 have to be discussed. The results for September 2016 are shown in Figure 3.9, the other months figures are shown in Section 7.3.
Figure 3.9a shows the results for Method A, where the room temperature values are sorted before computing the average. The result is losing the temporal link between the central value and the dispersion range, identified by standard deviation or quartiles.
Figure 3.9b shows the results for Method B, where the room temperature values are sorted after computing the average. The result is keeping the temporal link between the central value and the dispersion range, but through unsorted spread limits.
Method B has to be preferred, in order not to lose the temporal correlation among data. The central value has to be sorted for the purpose of duration graph, but once the average is defined, the energy manager should be able to know the actual dispersion for a specific temperature measure, instead of the spread of sorted values offered with Method A.

5.4 Thermal discomfort evaluation

In Section 3.6 several ways to define thermal discomfort on the building level are presented.
As a result of previous discussions, in this section the following assumptions were made:

- Fixed schedule is used for the occupancy pattern
- Dynamic comfort temperature range is used for thermal discomfort evaluation
- 1st grade polynomial fit is used for energy forecasting

The results for the other hypothesis are shown in Section 7.5.
The information resulting from the different methods used are significantly diverse, in particular three main groups are compared:

- Mean and median from complete data-set (Methods I,II,III,IV)
- Mean and median from filtered data-set (Methods V,VI)
- Other methods (Methods VII,VIII,IX)

Methods I and II define monthly thermal discomfort through evaluation of the hourly average temperature, using mean and median temperature, respectively. A comparison between the goodness of building conditions synthesis achieved by mean and median is developed in Section 5.3. As discussed, the monthly data-base do not follow a normal distribution, due to the presence of outliers that move the mean. In particular Figure 5.10 shows that the mean curve is higher than the median one for low temperatures (left side of the duration graph) and lower for high temperatures (right side of the duration graph). The result on thermal discomfort evaluation are shown in Table 5.5, Monthly discomfort comparison:

- *September 2016*: As shown in Section 5.3, the mean and median plots for September 2016 are quite close in the left side of the duration graph, while in the right side the median curve is slightly lower the mean, so the former crosses the thermal superior comfort boundary after the latter. The thermal discomfort evaluated by the median is lower than the one evaluated by the mean, but the difference in terms of discomfort percentage time is narrow (2,5%)
- *October 2016*: As shown in Section 5.3, the mean and medium plots for October 2016 are close, especially in the central area of the duration graph. The medium plot is slightly higher than the mean one, so the former crosses the superior comfort temperature limit before the latter. The thermal discomfort evaluated by the median is higher than the one evaluated by the mean, but the difference in terms of discomfort percentage time is narrow (2,2%)
- *November 2016*: As shown in Section 5.3, the mean and medium plots for November 2016 are more diverse compared to the previous months. The medium plot is higher than the mean plot in the left side of the duration graph and lower in the right side, so the former crosses the superior comfort temperature limit after the latter. The thermal discomfort evaluated by the median is lower than the one evaluated by the mean, with a significant difference in terms of discomfort percentage (5,4%)

- *December 2016*: As shown in Section 5.3, the mean and median plots for December 2016 follow a different trend, with the medium plot being higher than the mean plot in the left part of the duration graph and lower in the extreme right side, so the former crosses the superior thermal comfort boundary after the latter. The thermal discomfort evaluated by the median is lower than the one evaluated by the mean, but the difference in terms of discomfort percentage time is still narrow (2,7%)
- *January 2017*: As shown in Section 5.3, the mean and medium plots show a strong difference in the left side of the duration graph, that shrinks toward the right side. When they cross the superior comfort temperature limit, the medium plot is higher. The thermal discomfort evaluated by the median is higher than the one evaluated by the mean and the difference in terms of discomfort percentage time is relevant (6,2%)

Generally Method II presents a lower thermal discomfort percentage time with the use of predicted dynamic comfort temperature range, while using fixed comfort temperature range Method I presents a generally lower thermal discomfort percentage time, since the fixed temperature range is moved downward compared to the predicted one. Method II gives a proper building information, since the medium plot is less influenced by the presence of outliers and represents better the actual temperature distribution. Nevertheless, using Method I could give a more cautious information, since the mean is moved toward the extreme values. Methods III and IV are developed to evaluate thermal discomfort over the whole dispersion of the data-set, by using $T_{mean} - SD$ and 1st quartile to define lower thermal discomfort percentage time (p_{low}) and $T_{mean} + SD$ and 3rd quartile to define higher thermal discomfort percentage time (p_{high}). The concept is to show to the energy manager the information coming from a group of measures instead using the single central value. The problem lies in the complexity of the discomfort definition, thus the addressees (energy manager and practitioners) would get just a number, not being able to get a clear idea of what it represents. Of course this fact would not meet the building managers needs, making these methods not suitable for the purpose of this work.
Filtering methods were discussed in Section 5.3, with a proper look to their effect on the temperature distribution. The outlier filtering method revealed to cut more values compared to the extreme filtering method. This fact means not considering the thermal conditions of a relevant part of the building, developing an information of questionable reliability. As shown in Section 5.3, extreme and outlier filtered data-set plots are parallel on the duration graph, resulting in significantly diverse thermal discomfort information. Furthermore during some months (October and January) the discomfort percentage time computed by Method V is higher than the one computed by Method VI, while during other months (September, November and December) it is lower. Generally cutting measures out of the data-set restricts the benefits of the whole thermal discomfort detection method, furthermore the measures dispersion is taken into consideration by the median plot.
Among the other methods, Method VII considers just a narrowed data-set, computing thermal discomfort using only problematic rooms data. Therefore the information is not representing the actual thermal conditions of the whole building, but it could be used alongside with the average plot to monitor the boundary conditions and how much

they are diverse from the central value. However, Method VII needs another information about the percentage of problematic rooms to deliver a meaningful information, otherwise the energy manager could not know if the discomfort is restricted to few rooms or if it is spread in the whole building. Due to the extent of data needed to get a reliable information, Method VII appears not to be effective enough for the purpose of the work.
Method VIII presents the thermal discomfort percentage time of the room characterized by the worst thermal conditions. This approach could be used to get boundary conditions information and it is useful to avoid considering the central conditions only. Of course, the resulting discomfort is typically a very number, carrying few information if used alone. In particular, for the available data-base the worst room has always a thermal discomfort percentage time around 99%. Therefore this method could be used alongside with another one dealing with the average building conditions and it could be especially useful when the latter are good, to monitor if this information is true for the whole building. Compared to Method VII, Method VIII delivers a more extreme but clear information that could be preferred if the aim is to avoid thermal discomfort in the whole building.
Method IX computes mean thermal discomfort percentage time as the mean value of each room thermal discomfort percentage time, without using the average data-set obtained in the room to building data synthesis. It can be used as reference information to be compared with the central conditions coming from Methods I and II, but it could not be used by itself, since it is the average between the thermal problematic rooms and thermal good ones. As a result, a single room with bad thermal conditions could twist the thermal comfort information for the whole building. The main problem lies in avoiding the room to building data synthesis, which prevents data corrupting associated to the presence of outliers.

The values for thermal discomfort percentage time resulting from the described methods are compared to the acceptable deviation of 5% as defined by the standard **EN 15251** [6] and described in Section 3.6. It accounts transients for instantaneous thermal variations due to environmental adjustments (for example windows opening). Anyway, future improvements of the method should face this threshold and define a new one that could better fit the global discomfort definition and the actual thermal conditions.

Table 5.5: Monthly discomfort evaluation with fixed occupancy and dynamic temperature range

Year	Month	Method I	Method II	Method III	Method IV	Method V
2016	09	37,7%	35,2%	76,9%	61,8%	34,7%
2016	10	10,4%	12,6%	85,7%	63,6%	16,0%
2016	11	16,1%	10,7%	88,4%	61,6%	10,7%
2016	12	12,5%	9,8%	85,7%	56,4%	13,6%
2017	01	42,5%	48,7%	97,0%	72,8%	46,2%

Year	Month	Method VI	Method VII	Method VIII	Method IX
2016	09	40,7%	40,7%	96,5%	44,7%
2016	10	8,2%	34,6%	98,7%	38,0%
2016	11	18,2%	28,5%	99,6%	38,4%
2016	12	16,7%	40,8%	98,6%	36,2%
2017	01	29,8%	49,5%	99,7%	53,1%

5.5 Energy use forecasting

In Section 3.7 it was explained how the monthly energy consumption was predicted from the indoor and outdoor temperature measures. A fit was developed for both a 1st and 2nd grade polynomial interpolation, trying to define the coefficients of equations 5.2 and 5.3, respectively.

$$EC = a * \Delta t + b \tag{5.2}$$

$$EC = a * \Delta t^2 + b * \Delta t + c \tag{5.3}$$

The resulting coefficients are shown in Table 5.6, while the corresponding plots are shown in Figure 5.12. Table 5.7 shows foreseen energy consumption values, using optimal indoor temperatures, defined in Section 3.3, from both methods, in comparison with actual consumption.

Table 5.6: Curve fitting for energy forecasting

	1st grade polynomial fit	2nd grade polynomial fit
Model	$f(x) = p1 * x + p2$	$f(x) = p1 * x^2 + p2 * x + p3$
p1	1.032 (0.8684, 1.196)	0.009183 (-0.01783, 0.0362)
p2	-8.762 (-12.34, -5.182)	0.6712 (-0.4073, 1.75)
p3	ø	-5.732 (-15.55, 4.09)
R-square	0.9926	0.9964
RMSE	0.8573	0.7298

Table 5.7: Foreseen energy consumption for 1st and 2nd grade fits, in comparison with actual consumption [kWh/m^2]

Year	Month	Actual data	1st grade polynomial fit	2nd grade polynomial fit
2016	09	1,0	0,0	0,0
2016	10	7,5	7,4	7,1
2016	11	13,5	12,1	11,6
2016	12	16,7	16,2	15,9
2017	01	23,6	21,2	21,4

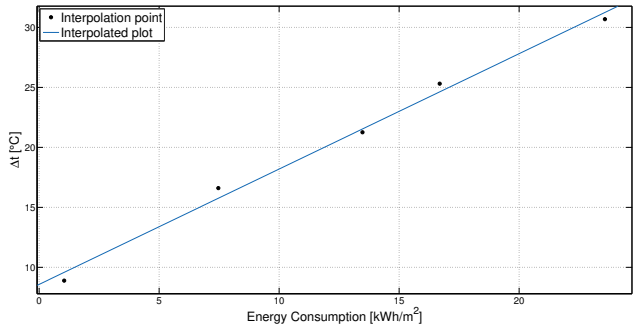

(a) 1st grade polynomial fit plot

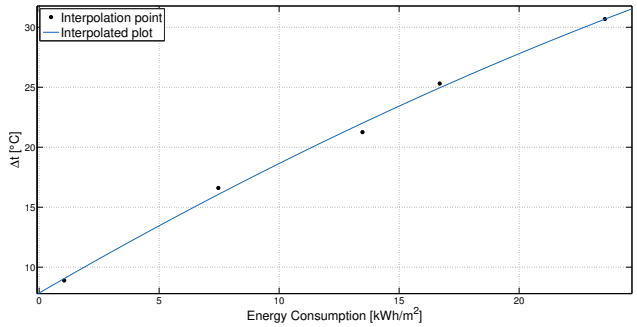

(b) 2nd grade polynomial fit plot

Figure 5.12: Polynomial interpolation plots

The results in terms of R-square value are nearly identical (see Table 5.6), so there is no need to embrace a more complex method for the energy forecasting purpose. Basing the judgment on the R-square and RMSE values, the fit seems accurate.
Table 5.7 shows how foreseen energy consumption values are pretty close among the two methods. This fact confirms that using the 1st grade polynomial fit would lead to reliable results.
The main problem lies in the available data-base, since the energy consumption measures are given on a monthly basis and they need to be coupled with monthly temperature data, available for 5 months only. The result is a data-base with 5 elements couple, as explained in Section 3.7, corresponding to monthly energy consumption and monthly mean Δt values. For a more reliable fit the data-base should cover several years of measures, in order to avoid wrong evaluations produced by oddity. For example, if a winter season is unusually warm the resulting energy consumption measures would not be the average ones.
However, for the purpose of the work, the presented forecasting method works well enough, since the goal is not an accurate thermal load prediction, but just a qualitative one, intended to offer an achievable optimal scenario to the energy manager of the building.

Table 5.7 shows the foreseen optimal energy use in comparison with the actual one. As discussed in Section 5.6, due to the overheating problem of the building, the optimal monthly energy consumption values are always lower than the actual ones, but the difference is not particularly significant.

Table 5.8: Actual and optimal energy use and resulting energy saving

Actual energy use	$313,8$ MWh
Optimal energy use	$286,6$ MWh
Energy saving	$27,3$ MWh

However, the values are presented in $\frac{kWh}{m^2}$, so considering the whole building floor area of $5042m^2$, the actual energy use reduction is significant, as shown in Table 5.8. The results show a significant energy savings value, especially because it comes from a smarter energy management and does not need expensive investments for structural or technology improvements.

5.6 Comprehensive figure

In Section 3.8 the developed comprehensive figure was presented, where both actual and optimal working points are presented, characterizing them by monthly thermal discomfort percentage time and monthly energy consumption.
The result is shown in Figure 5.13. The thermal discomfort percentage time of the ac-

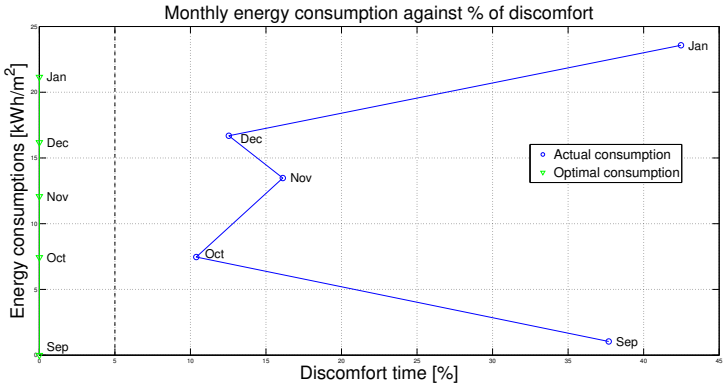

Figure 5.13: Comprehensive figure

tual conditions is defined as discussed in Section 5.4, using the mean temperature curve. The thermal discomfort percentage time of the optimal scenario is defined, as discussed in Section 3.7, using the central value of the comfort temperature range defined as discussed in Section 3.3. The resulting thermal discomfort is null, corresponding to the optimal scenario. Of course an energy manager could prefer an in-between scenario, for example trying to keep a thermal discomfort percentage time of 5%, corresponding to the standard boundary.

The actual monthly energy consumption data are part of the available data-base, as discussed in Section 3.1. The foreseen energy consumption value for optimal scenario are evaluated and discussed in Sections 3.7 and 5.5 and could present two scenario:

- If the discomfort comes from an excessively high use of heating (or cooling) system, the energy consumption would be reduced by setting a lower (or higher) operative temperature, resulting in both a comfort and consumption benefit
- If the discomfort comes form an excessively low use of heating (or cooling) system, the energy consumption would be increased by setting an higher (or lower) operative temperature, resulting in an higher expense

The available data lies in the first option and for this reason the foreseen energy consumption values result lower than the actual ones, even after the significant improvements in terms of thermal comfort. However, if the discomfort had been caused by excessively low use of heating, the information brought by the comprehensive figure would be equally meaningful, allowing the energy manager to visualize the actual thermal conditions and to have all the tools needed to decide how much getting close to the optimal scenario.
From this fact comes the main point of the work, whereas the energy manager of the studied building could get a simple information about indoor conditions, matching thermal comfort and energy consumption, that could be easy to read and understand, significant improvements could be achieved, even without technical and construction interventions. The method do not force a thermal indoor condition, instead it is meant to offer a clear picture of the actual conditions, letting the energy manager of the building choose consciously the strategy to adopt.

Chapter 6

Conclusions

6.1 Conclusions

This work developed a method to improve the energy management of buildings by an easy visualization of IEQ and energy consumption data on the comprehensive figure. Matching those information allows taking aware choices about HVAC systems regulation without neglecting neither thermal satisfaction of occupants nor energy performance.

Room to building synthesis was one of the key element of the developed method and several approaches were studied to come out with the most accurate building representation. Nevertheless single room information are elaborated and made available whereas a detailed analysis is needed.

Dealing with thermal satisfaction of building occupants can not avoid considering their behaviour, therefore a clothing insulation prediction were implemented in the method to evaluate thermal comfort as accurately as possible. The algorithm showed good results, improving the effectiveness of the discomfort evaluation compared to the conditions defined by the standard.

To enhance the decision process, an energy forecasting method was developed, in order to predict the consumption resulting from the energy manager choice. The algorithm is built using past energy consumption, indoor and outdoor temperature measurements only, in order to be adopted with the information of every data-base.

The developed comprehensive figure shows the monthly information concerning IEQ and energy use alongside with the optimal scenario based on recommended thermal conditions and resulting consumption. This tool should serve as a guideline for the energy manager of the building to allow judging the actual conditions in comparison to the optimal ones and knowing how far are these two scenarios.

The method was applied to an office building in Czech Republic to be tested and tuned. It revealed an overheating problem, resulting in significant thermal discomfort and high energy use. Overheating and overcooling are common problems everyone experiences and the developed method could help solving them. The study revealed that whereas the energy manager could get a simple information about indoor conditions, matching thermal comfort and energy consumption, that could be easy to read and understand, significant improvements could be achieved, even without technical and construction interventions.

The method offers a clear picture of the actual conditions, letting the energy manager of the building choose consciously the strategy to adopt.

6.2 Future work

As mentioned in Section 5.1, the method accuracy could be improved with a precise occupancy detection algorithm, by the use of an Extreme Learning Machine (ELM) or a neural network, able to detect the single room occupancy pattern from CO_2 measurement. Several parameters could be coupled to the CO_2 to improve the information, as mentioned in Section 2.2.

The figure could be used to compare different buildings from thermal conditions point of view. Every building information could be synthesized in a single value of thermal discomfort and consumption, for example a yearly indication, that could identify a single point on the comprehensive figure. The result would be a single figure where every dot represents a single building thermal conditions, leading to an easy comparison.

This work is dealing only the method describing how the monitoring system could work, but the actual look available for the users should be improved by a programmer and/or a designer. The first view should be the comprehensive figure, that can instantly give the first information about the building thermal conditions, then the user should be able to access more information. For example by clicking on a dot in the comprehensive figure, the system could show the actual discomfort percentage of every room or the discomfort temperature range. All these data are available in the algorithm but they should be displayed in a proper way.

Bibliography

[1] *Directive 2010/31/EU*. Directive. Off. J. Eur. Union: E. P. and Council, 2010.

[2] Ana Tisov. "A trade-off between indoor environmental quality and energy consumption in modern buildings – identification of performance indicators and evaluation of data collected in existing buildings". In: *DTU M.Sc. Thesis* (2016).

[3] *USGBC, A National Green Building Research Agenda*. Tech. rep. United States Green Building Council, 2007.

[4] *ANSI/ASHRAE Standard 55-2010. Thermal Environmental Conditions for Human Occupancy*. Standard. Atlanta, GA, USA: American Society of Heating, Refrigerating and Air-Conditioning Engineers, Inc., 2010.

[5] *EN ISO 7730. Indoor environmental input parameters for design and assessment of energy performance of buildings - addressing indoor air quality, thermal environment, lighting and acoustics*. Standard. 2006.

[6] *EN 15251:2007. Indoor environmental input parameters for design and assessment of energy performance of buildings - addressing indoor air quality, thermal environment, lighting and acoustics*. Standard. 2007.

[7] Varick L. Erickson and Alberto E. Cerpa. "Occupancy Based Demand Response HVAC Control Strategy". In: *2nd ACM Workshop on Embedded Sensing Systems for Energy-Efficiency in Buildings, BuildSys'10, November 2, 2010 - November 2, Association for Computing Machinery* (2010), pp. 7–12.

[8] Stanley A. Mumma. "Transient Occupancy Ventilation By Monitoring CO_2". In: *IAQ Application* (2004), pp. 21–23.

[9] Zhongwei Sun, Shengwei Wang, and Zhenjun Ma. "In-situ implementation and validation of a CO_2-based adaptive demand-controlled ventilation strategy in a multi-zone office building". In: *Building and Environment* 46 (2011), pp. 124–133.

[10] Zheng Yang et al. "A Multi-Sensor Based Occupancy Estimation Model for Supporting Demand Driven HVAC Operations". In: *Symposium on Simulation for Architecture and Urban Design* (2012), pp. 1–8.

[11] Seung Ho Ryu and Hyeun Jun Moon. "Development of an occupancy prediction model using indoor environmental data based on machine learning techniques". In: *Building and Environment* 107 (2016), pp. 1–9.

[12] Chaoyang Jiang et al. "Indoor occupancy estimation from carbon dioxide concentration". In: *Energy and Buildings* 131 (2016), pp. 132–141.

[13] Guillaume Ansanay-Alex. "Estimating Occupancy Using Indoor Carbon Dioxide Concentrations Only in an Office Building: a Method and Qualitative Assessment". In: *Conference: 11th REHVA World Congress "Energy efficient, smart and healthy buildings": Clima 2013, At Prague* (2013).

[14] Y. Benezeth et al. "Towards a sensor for detecting human presence and characterizing activity". In: *Energy and Buildings* 43(2-3) (2011), pp. 305–314.

[15] Yuvraj Agarwal et al. "Occupancy-Driven Energy Management for Smart Building Automation". In: *2nd ACM Workshop on Embedded Sensing Systems for Energy-Efficiency in Buildings, BuildSys'10, November 2, 2010 - November 2, Association for Computing Machinery* (2010), pp. 1–6.

[16] Ebenezer Hailemariam et al. "Real-Time Occupancy Detection using Decision Trees with Multiple Sensor Types". In: *Proceedings of the Symposium on Simulation for Architecture and Urban Design 2011, April 4-7* (2011).

[17] Ryan Melfi et al. "Measuring building occupancy using existing network infrastructure". In: *International Green Computing Conference, IGCC 2011, July 25, 2011 - July 28, IEEE Computer Society* (2011).

[18] Richard De Dear, Gail Brager, and Donna Cooper. "Developing an adaptive model of thermal comfort and preference". In: *Final report ASHRAE RP-884* (1997).

[19] Michele De Carli et al. "People's clothing behaviour according to external weather and indoor environment". In: *Building and Environment* 42 (2007), pp. 3965–3973.

[20] Stefano Schiavon and Kwang Ho Lee. "Dynamic predictive clothing insulation models based on outdoor air and indoor operative temperatures". In: *Building and Environment* 59 (2013), pp. 250–260.

[21] D. Crawley, L. Lawrie, and C. Pedersen. "EnergyPlus: energy simulation program". In: *ASHRAE Journal* 42(4) (2000), pp. 49–56.

[22] A. Dhar, T.A. Reddy, and D.E. Claridge. "Generalization of the Fourier series approach to model hourly energy use in commercial buildings". In: *Journal of Solar Energy Engineering* 121(1) (1999), pp. 54–62.

[23] A. Dhar, T.A. Reddy, and D.E. Claridge. "A Fourier series model to predict hourly heating and cooling energy use in commercial buildings with outdoor temperature as the only weather variable". In: *Journal of Solar Energy Engineering* 121 (1999), pp. 47–53.

[24] Joseph H. Eto. "On using degree-days to account for the effects of weather on annual energy use in office buildings". In: *Energy and Buildings* 12 (1988), pp. 113–127.

[25] *ANSI/ASHRAE Standard 62-2001. Ventilation for acceptable indoor air quality.* Standard. Atlanta, GA, USA: American Society of Heating, Refrigerating and Air-Conditioning Engineers, Inc., 2001.

[26] Z. Yu et al. "A systematic procedure to study the influence of occupant behaviour on building energy consumption". In: *Energy Build* 43 (2011), pp. 1409–1417.

[27] Longquan Diao et al. "Modeling energy consumption in residential buildings: A bottom-up analysis based on occupant behaviour pattern clustering and stochastic simulation". In: *Energy and Buildings* 147 (2017), pp. 47–66.

[28] Lennart Jagemar and Daniel Olsson. *The EPBD and Continuous Commissioning.* Tech. rep. Göteborg: CIT Energy Management AB, 2007.

[29] Miguel Molina-Solana et al. "Data science for building energy management: A review". In: *Renewable and Sustainable Energy Review* 70 (2017), pp. 598–609.

[30] Shady Attia et al. "Assessing gaps and needs for integrating building performance optimization tools in net zero energy buildings design". In: *Energy and Buildings* 60 (2013), pp. 110–124.

[31] Samuel Prívara et al. "On using degree-days to account for the effects of weather on annual energy use in office buildings". In: *Energy and Buildings* 43 (2011), pp. 564–572.

[32] Tiberiu Catalina, Joseph Virgone, and Eric Blanco. "Development and validation of regression models to predict monthly heating demand for residential buildings". In: *Energy and Buildings* 40 (2008), pp. 1825–1832.

[33] L.T. Wong and K.W. Mui. "An energy performance assessment for indoor environmental quality (IEQ) acceptance in air-conditioned offices". In: *Energy Conversion and Management* 50 (2009), pp. 1362–1367.

[34] David R. Anderson et al. *Essentials of statistics for business and economics 7e.* Cengage Learning, 2015. ISBN: 978-1-133-58779-8.

[35] Giacomo Girotto. "Development of a model for forecasting of Energy consumption and costs in buildings based on EnMS data". In: *DTU M.Sc. Thesis* (2015).

Chapter 7

Appendix

7.1 Appendix 1: Matlab script

```
A001_import_data
%
A010_occupancy_schedule
A011_label_creation
A012_daymean
A013_datacleaning
A014_templimit
A015_building_area
%%
A020_month_creation
roomtemperature=cell(mm,33);
discomfort=cell(mm,1);
clear i j k k_old mm m_0 a_0
%
% Room duration graph
A030_room_plots
%
A031_compl_tab_creation
%media
A040_average_plots
n_figura=mm+pd+1;
%ANA's Figure
A050_anas_1
%
A060_forecasting
A061_applied_formula
A062_saving_calculation
%final clean
A070_cleaning_values
```

7.2 Appendix 2: Script explanation

A summary of the main parts of the basic script:

- *A001_import_data*: it opens all the data needed from the *Excel* files downloaded from the *Mervis* database, for example temperature measures and energy consumption, as a matrix

- *A010_occupancy_schedule*: it opens the fixed schedule and it attach it to the indoor temperature database

- *A011_label_creation*: it creates the labels for every month

- *A012_daymean*: it calculates the hourly mean temperature for every room

- *A013_datacleaning*: it creates a new matrix with just the temperature data within the schedule time.

- *A014_templimit*: it fixes the standard temperature limits

- *A015_building_area*: it contains the floor area of the building to calculate the specific energy consumption

- *A020_month_creation*: it creates the line reference in the temperature table for each month

- *A030_room_plots*: it creates a figure for each month with a duration graph for each room and the temperature limits, then it calculates the monthly thermal discomfort for each room.

- *A031_compl_tab_creation*: it creates a cell array with the numeric values of each duration graph

- *A030_average_plots*: it calculates the mean and median hourly temperature, with standard deviation and quartiles, then it plots the mean and median duration graph for each month and it calculates the average monthly discomfort

- *A050_anas_1*: it creates the comprehensive figure with thermal discomfort in the x-axis and energy consumption in the y-axis.

- *A060_forecasting*: it fixes the outdoor temperature database and it calculates monthly average temperature for both indoor and outdoor temperature

- *A061_applied_formula*: it creates a matrix with the optimal points from the clo estimation method and it applies the fitting formula to these points, then it calculates the optimal thermal discomfort and it plots the optimal points on the comprehensive figure.

- *A062_saving_calculation*: it stores the new data in a new matrix

- *A070_cleaning_values*: it cleans the workspace from the unnecessary results.

7.3 Appendix 3: Temperature distribution figures

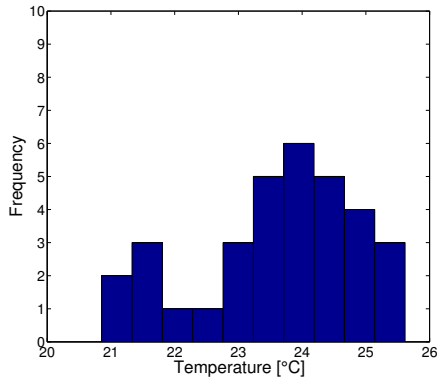

(a) Temperature distribution for a percentage time of 1%

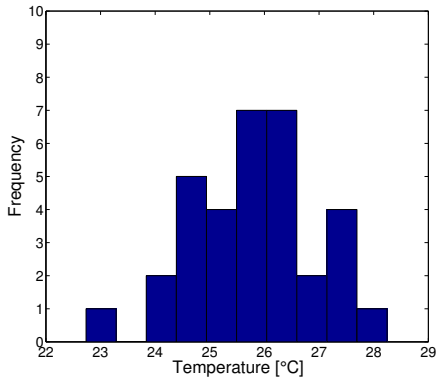

(b) Temperature distribution for a percentage time of 33%

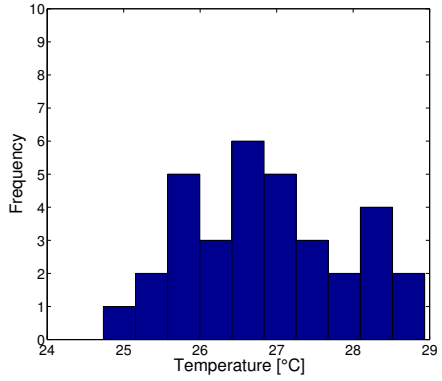

(c) Temperature distribution for a percentage time of 66%

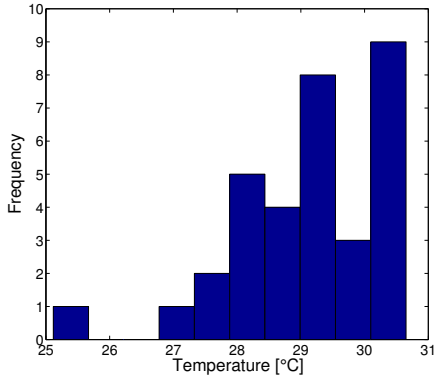

(d) Temperature distribution for a percentage time of 100%

Figure 7.1: Temperature distribution in September 2016

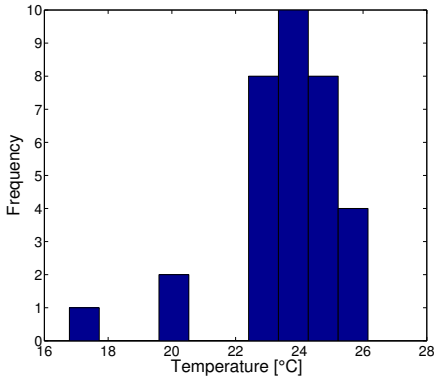

(a) Temperature distribution for a percentage time of 1%

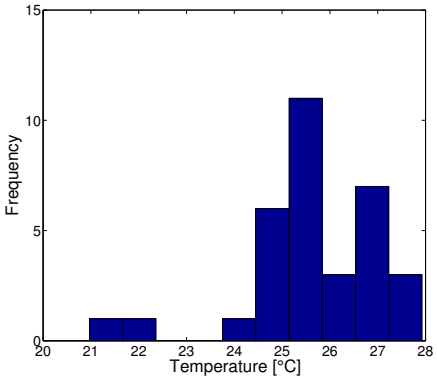

(b) Temperature distribution for a percentage time of 33%

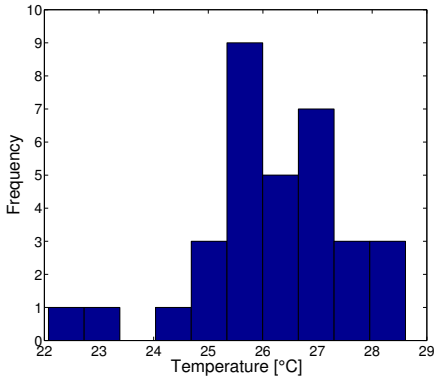

(c) Temperature distribution for a percentage time of 66%

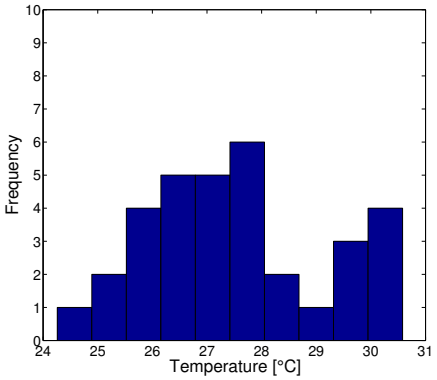

(d) Temperature distribution for a percentage time of 100%

Figure 7.2: Temperature distribution in October 2016

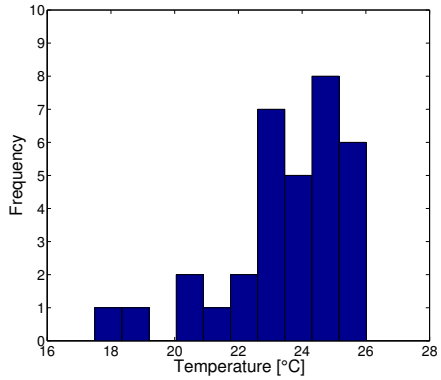

(a) Temperature distribution for a percentage time of 1%

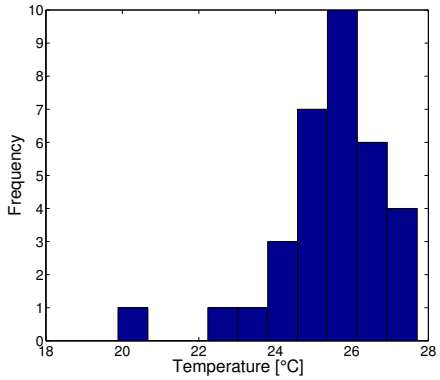

(b) Temperature distribution for a percentage time of 33%

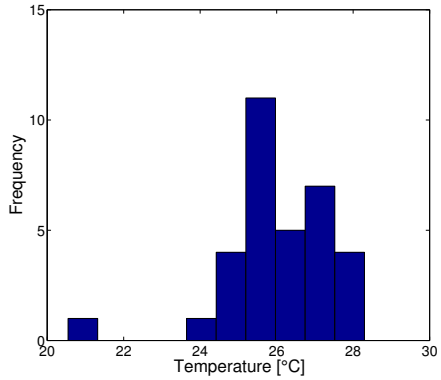

(c) Temperature distribution for a percentage time of 66%

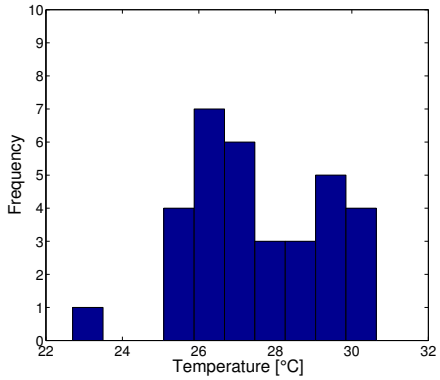

(d) Temperature distribution for a percentage time of 100%

Figure 7.3: Temperature distribution in November 2016

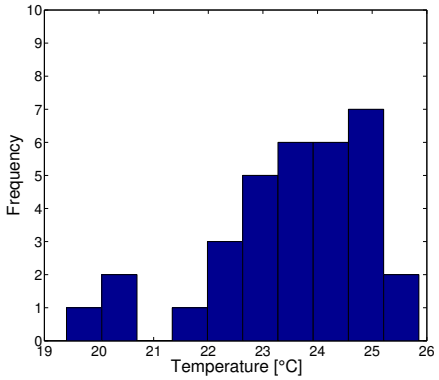

(a) Temperature distribution for a percentage time of 1%

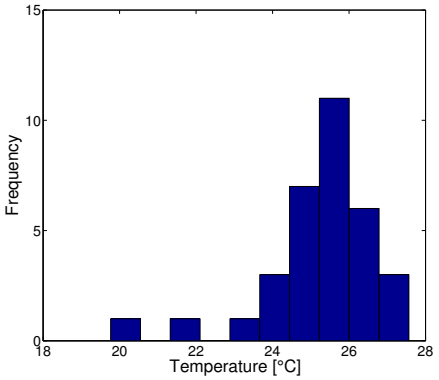

(b) Temperature distribution for a percentage time of 33%

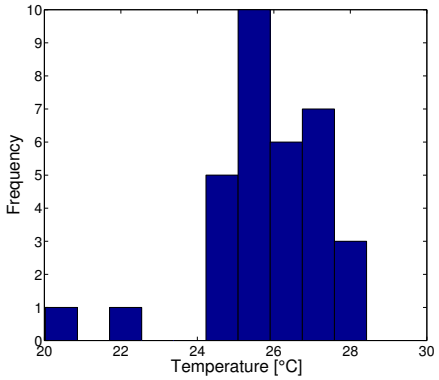

(c) Temperature distribution for a percentage time of 66%

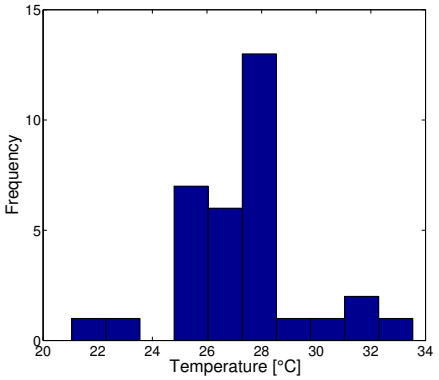

(d) Temperature distribution for a percentage time of 100%

Figure 7.4: Temperature distribution in December 2016

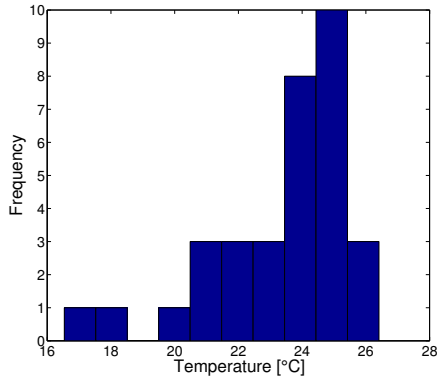

(a) Temperature distribution for a percentage time of 1%

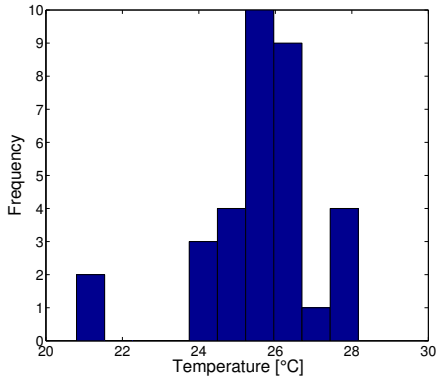

(b) Temperature distribution for a percentage time of 33%

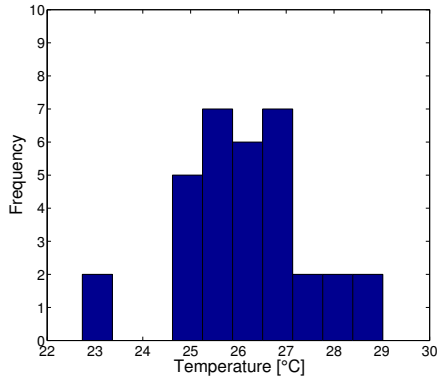

(c) Temperature distribution for a percentage time of 66%

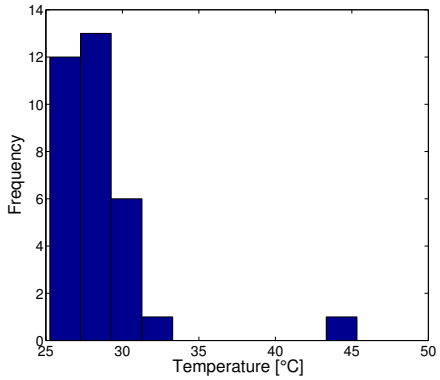

(d) Temperature distribution for a percentage time of 100%

Figure 7.5: Temperature distribution in January 2017

7.4 Appendix 4: Thermal discomfort comparison

This section features tables for thermal discomfort percentage time comparison. Each table refers to a different method and compare the results for the different scenarios, that are:

- Fixed occupancy, fixed comfort temperature range (labelled FF)
- Fixed occupancy, dynamic comfort temperature range (labelled FD)
- Dynamic occupancy, fixed comfort temperature range (labelled DF)
- Dynamic occupancy, dynamic comfort temperatre range (labelled DD)

Table 7.1: Thermal discomfort percentage time for Method I

Year	Month	FF	FD	DF	DD
2016	09	60,8%	37,7%	66,4%	45,2%
2016	10	45,0%	10,4%	44,9%	11,1%
2016	11	35,5%	16,1%	32,8%	14,0%
2016	12	23,7%	12,5%	23,0%	14,5%
2017	01	44,4%	42,5%	44,4%	42,5%

Table 7.2: Thermal discomfort percentage time for Method II

Year	Month	FF	FD	DF	DD
2016	09	63,3%	35,2%	67,7%	39,6%
2016	10	45,9%	12,6%	45,8%	12,9%
2016	11	28,1%	10,7%	24,6%	7,8%
2016	12	27,5%	9,8%	26,7%	5,5%
2017	01	50,3%	48,7%	50,3%	48,7%

Table 7.3: Thermal discomfort percentage time for Method III

Year	Month	FF	FD	DF	DD
2016	09	92,5%	76,9%	93,5%	80,6%
2016	10	95,2%	85,7%	95,1%	85,8%
2016	11	93,4%	88,4%	93,3%	86,0%
2016	12	94,4%	85,7%	94,5%	85,5%
2017	01	97,0%	97,0%	97,0%	97,0%

Table 7.4: Thermal discomfort percentage time for Method IV

Year	Month	FF	FD	DF	DD
2016	09	87,4%	61,8%	86,2%	65,4%
2016	10	87,9%	63,6%	88,0%	63,6%
2016	11	79,8%	61,6%	79,6%	54,9%
2016	12	74,6%	56,4%	73,3%	61,9%
2017	01	74,2%	72,8%	74,2%	72,8%

Table 7.5: Thermal discomfort percentage time for Method V

Year	Month	FF	FD	DF	DD
2016	09	58,5%	34,7%	65,0%	41,0%
2016	10	57,1%	16,0%	57,3%	16,4%
2016	11	26,4%	10,7%	26,3%	10,9%
2016	12	24,7%	13,6%	28,5%	14,5%
2017	01	45,7%	46,2%	45,7%	46,2%

Table 7.6: Thermal discomfort percentage time for Method VI

Year	Month	FF	FD	DF	DD
2016	09	65,3%	40,7%	69,6%	44,7%
2016	10	44,6%	8,2%	44,9%	8,4%
2016	11	43,4%	18,2%	41,5%	17,9%
2016	12	29,6%	16,7%	29,4%	14,5%
2017	01	33,3%	29,8%	33,3%	29,8%

Table 7.7: Thermal discomfort percentage time for Method VII

Year	Month	FF	FD	DF	DD
2016	09	62,8%	40,7%	68,2%	47,9%
2016	10	81,8%	34,6%	81,8%	34,2%
2016	11	53,5%	28,5%	51,8%	24,1%
2016	12	45,3%	40,8%	44,8%	40,1%
2017	01	64,2%	49,5%	64,2%	49,5%

Table 7.8: Thermal discomfort percentage time for Method VIII

Year	Month	FF	FD	DF	DD
2016	09	99,0%	96,5%	99,1%	96,8%
2016	10	99,6%	98,7%	99,6%	98,7%
2016	11	99,6%	99,6%	99,4%	99,7%
2016	12	99.0%	98,6%	99,1%	98,8%
2017	01	99.7%	99,7%	99,7%	99,7%

Table 7.9: Thermal discomfort percentage time for Method IX

Year	Month	FF	FD	DF	DD
2016	09	60,3%	44,7%	64,3%	49,0%
2016	10	44,9%	38,0%	45,0%	38,1%
2016	11	41,3%	38,4%	40,5%	38,0%
2016	12	37,5%	36,2%	36,9%	35,9%
2017	01	45,1%	53,1%	45,1%	53,1%

7.5 Appendix 5: Comprehensive figures for every scenario

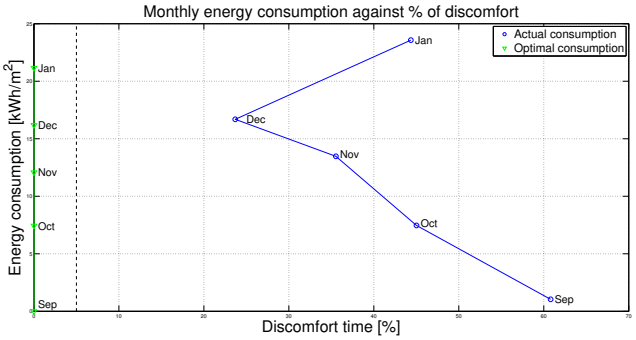

Figure 7.6: Comprehensive figure for Method I thermal discomfort evaluation for fixed occupancy and fixed comfort temperature range

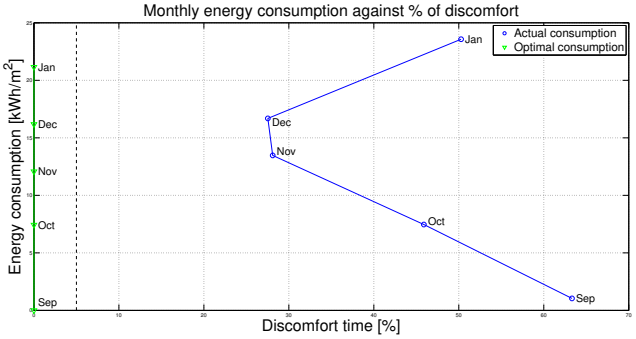

Figure 7.7: Comprehensive figure for Method II thermal discomfort evaluation for fixed occupancy and fixed comfort temperature range

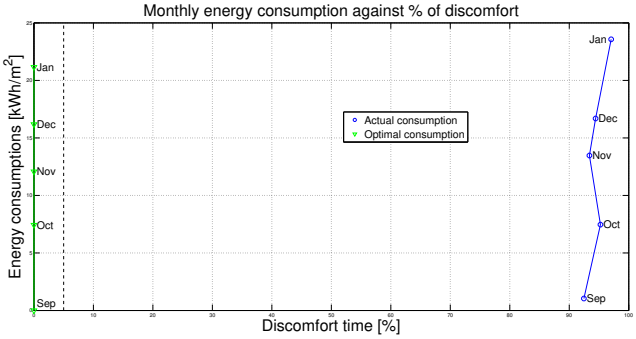

Figure 7.8: Comprehensive figure for Method III thermal discomfort evaluation for fixed occupancy and fixed comfort temperature range

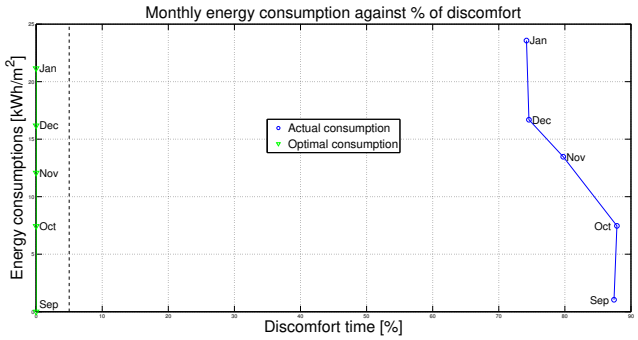

Figure 7.9: Comprehensive figure for Method IV thermal discomfort evaluation for fixed occupancy and fixed comfort temperature range

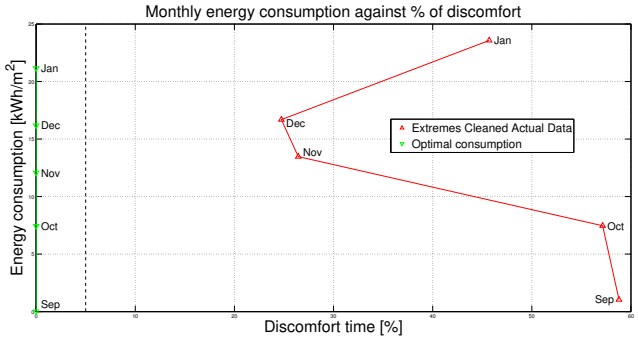

Figure 7.10: Comprehensive figure for Method V thermal discomfort evaluation for fixed occupancy and fixed comfort temperature range

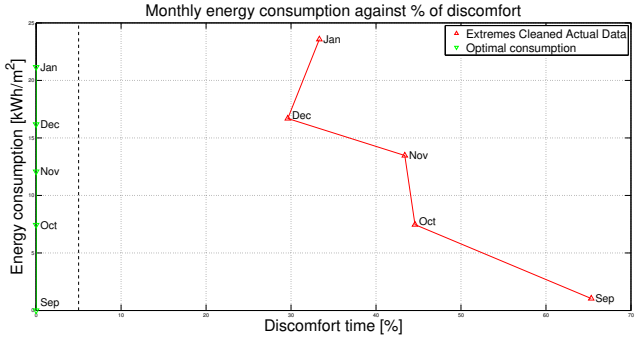

Figure 7.11: Comprehensive figure for Method VI thermal discomfort evaluation for fixed occupancy and fixed comfort temperature range

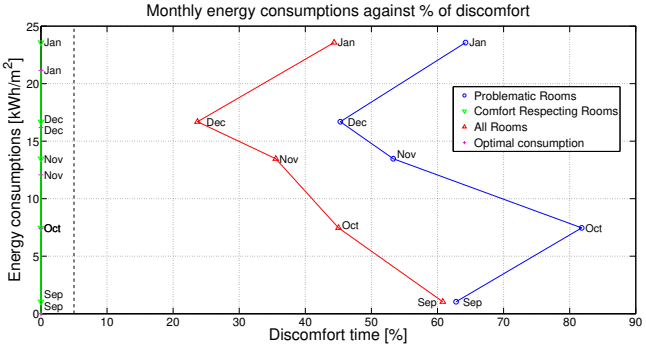

Figure 7.12: Comprehensive figure for Method VII thermal discomfort evaluation for fixed occupancy and fixed comfort temperature range

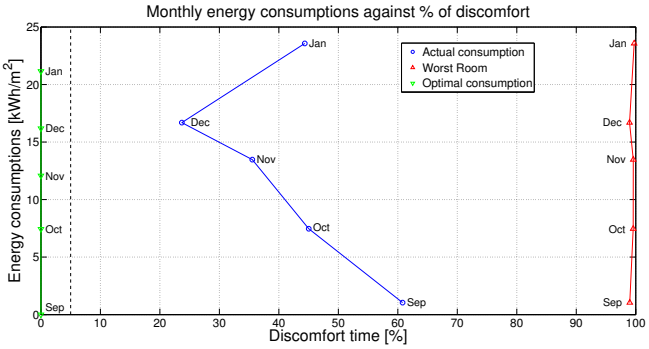

Figure 7.13: Comprehensive figure for Method VIII thermal discomfort evaluation for fixed occupancy and fixed comfort temperature range

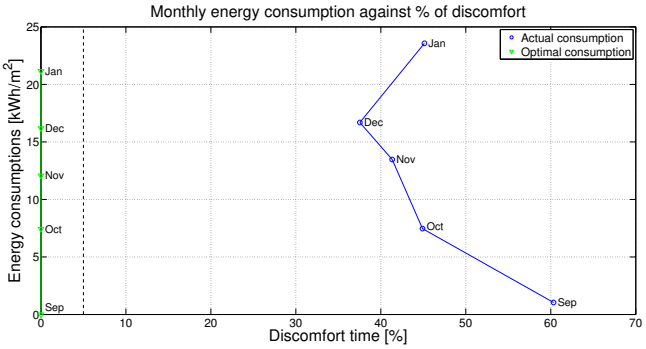

Figure 7.14: Comprehensive figure for Method IX thermal discomfort evaluation for fixed occupancy and fixed comfort temperature range

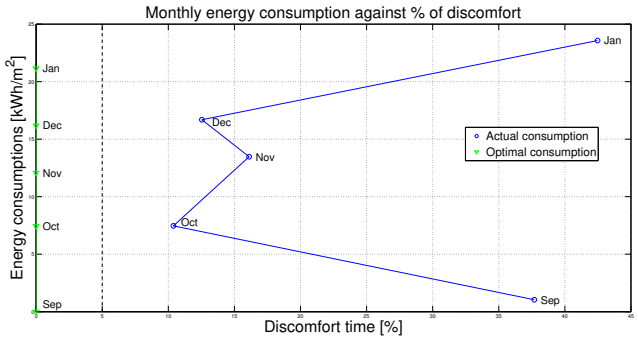

Figure 7.15: Comprehensive figure for Method I thermal discomfort evaluation for fixed occupancy and dynamic comfort temperature range

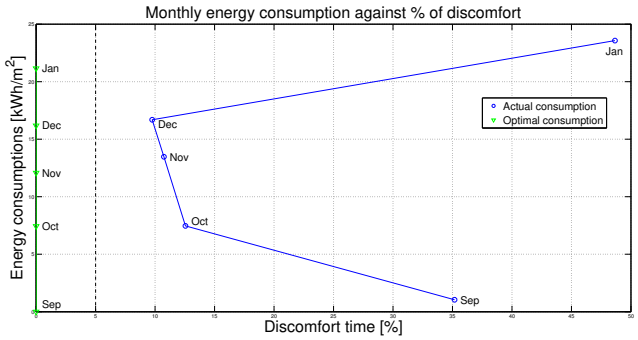

Figure 7.16: Comprehensive figure for Method II thermal discomfort evaluation

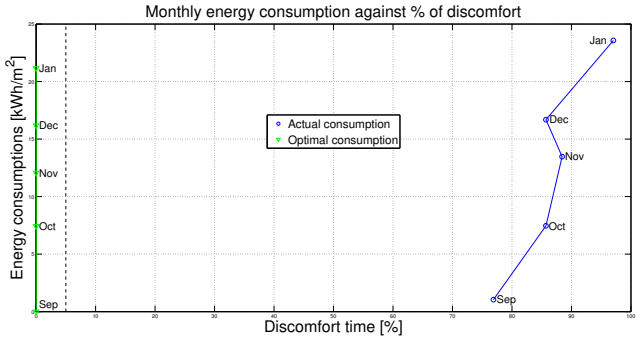

Figure 7.17: Comprehensive figure for Method III thermal discomfort evaluation

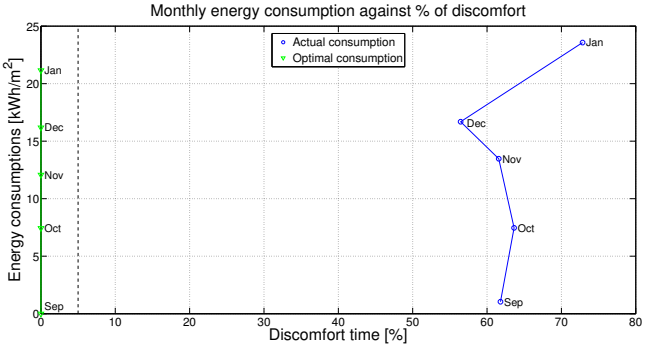

Figure 7.18: Comprehensive figure for Method IV thermal discomfort evaluation

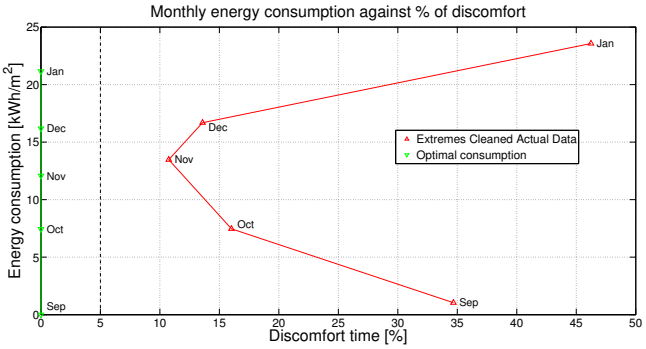

Figure 7.19: Comprehensive figure for Method V thermal discomfort evaluation

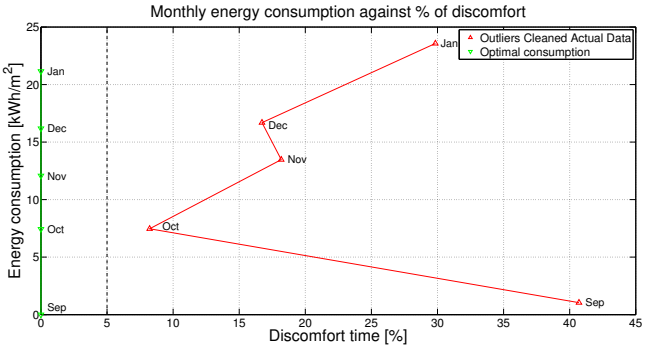

Figure 7.20: Comprehensive figure for Method VI thermal discomfort evaluation

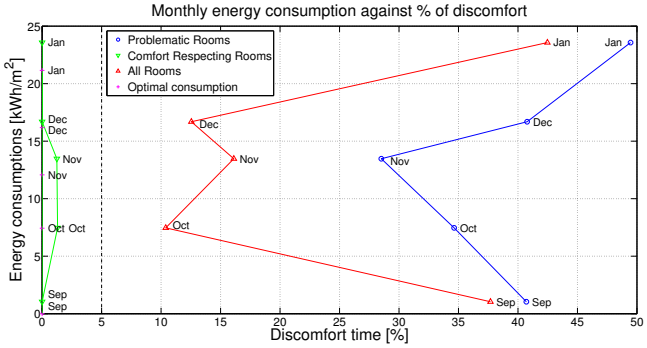

Figure 7.21: Comprehensive figure for Method VII thermal discomfort evaluation

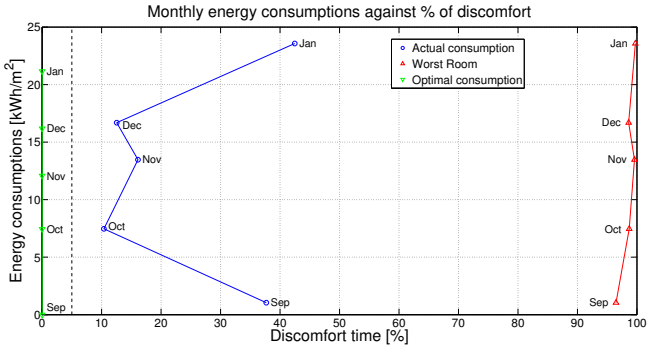

Figure 7.22: Comprehensive figure for Method VIII thermal discomfort evaluation

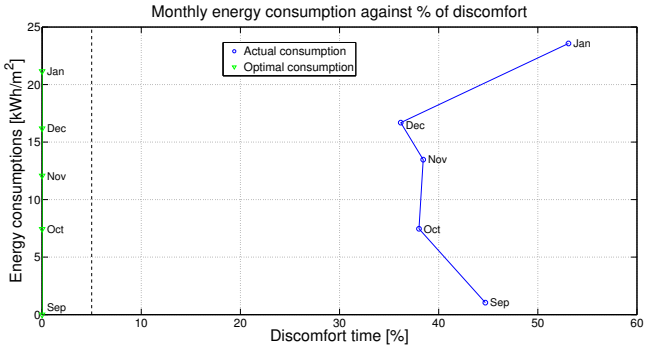

Figure 7.23: Comprehensive figure for Method IX thermal discomfort evaluation

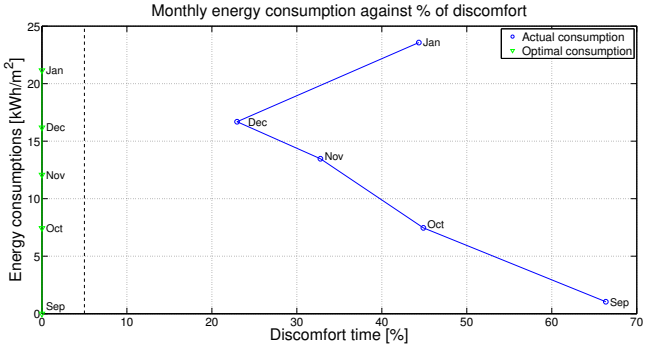

Figure 7.24: Comprehensive figure for Method I thermal discomfort evaluation for dynamic occupancy and fixed comfort temperature range

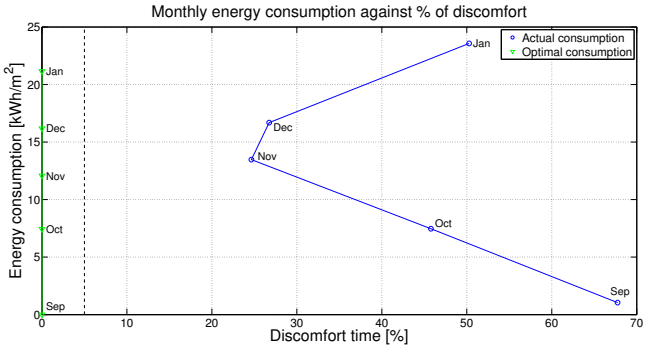

Figure 7.25: Comprehensive figure for Method II thermal discomfort evaluation for dynamic occupancy and fixed comfort temperature range

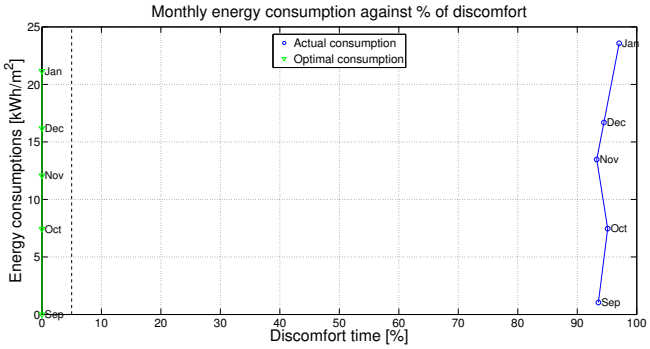

Figure 7.26: Comprehensive figure for Method III thermal discomfort evaluation for dynamic occupancy and fixed comfort temperature range

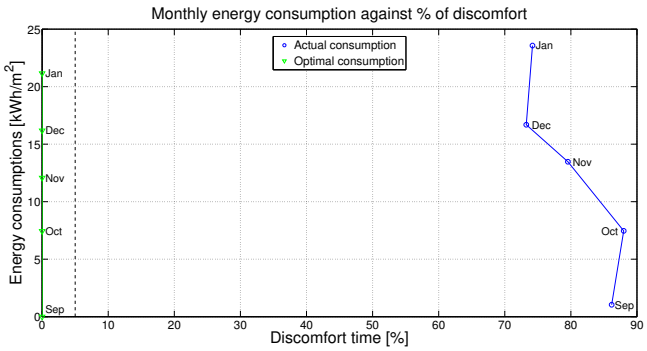

Figure 7.27: Comprehensive figure for Method IV thermal discomfort evaluation for dynamic occupancy and fixed comfort temperature range

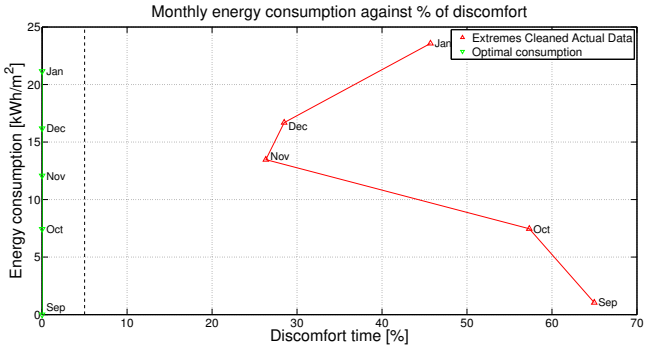

Figure 7.28: Comprehensive figure for Method V thermal discomfort evaluation for dynamic occupancy and fixed comfort temperature range

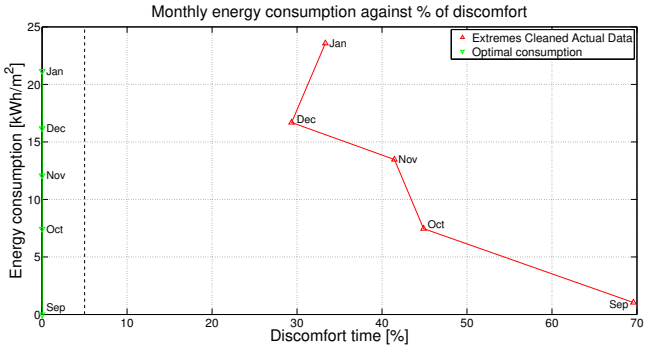

Figure 7.29: Comprehensive figure for Method VI thermal discomfort evaluation for dynamic occupancy and fixed comfort temperature range

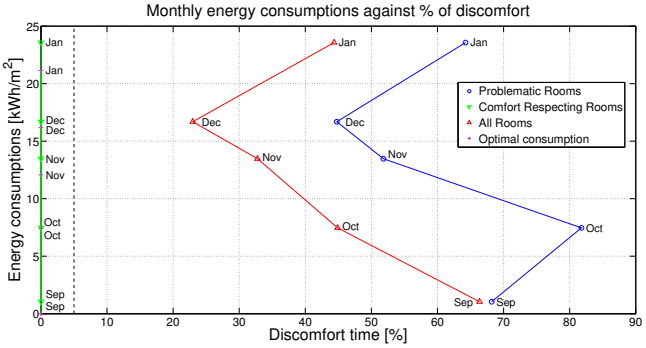

Figure 7.30: Comprehensive figure for Method VII thermal discomfort evaluation for dynamic occupancy and fixed comfort temperature range

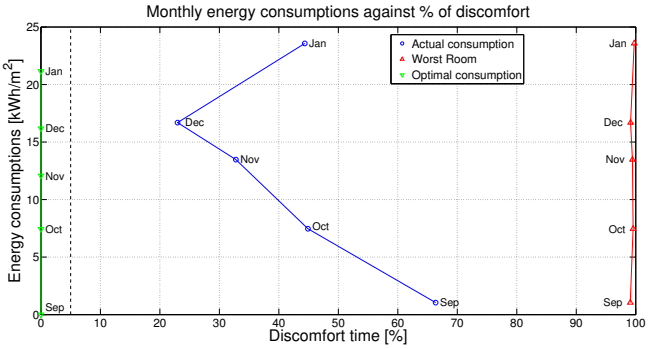

Figure 7.31: Comprehensive figure for Method VIII thermal discomfort evaluation for dynamic occupancy and fixed comfort temperature range

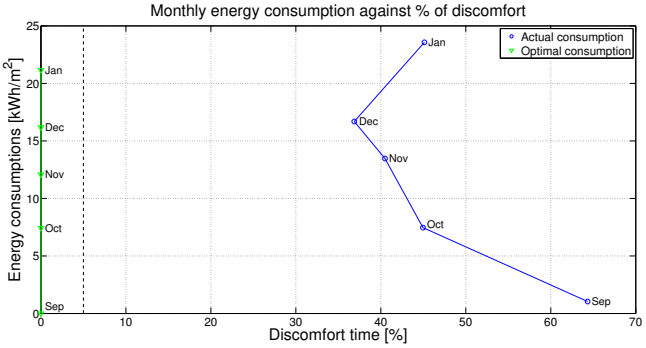

Figure 7.32: Comprehensive figure for Method IX thermal discomfort evaluation for dynamic occupancy and fixed comfort temperature range

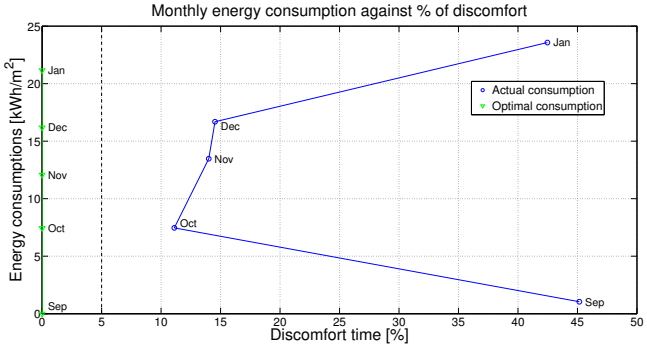

Figure 7.33: Comprehensive figure for Method I thermal discomfort evaluation for dynamic occupancy and dynamic comfort temperature range

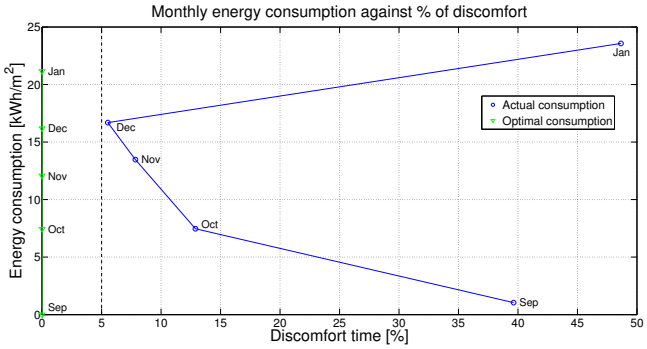

Figure 7.34: Comprehensive figure for Method II thermal discomfort evaluation for dynamic occupancy and dynamic comfort temperature range

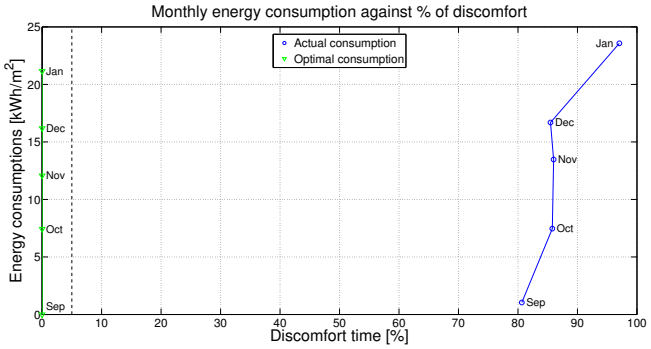

Figure 7.35: Comprehensive figure for Method III thermal discomfort evaluation for dynamic occupancy and dynamic comfort temperature range

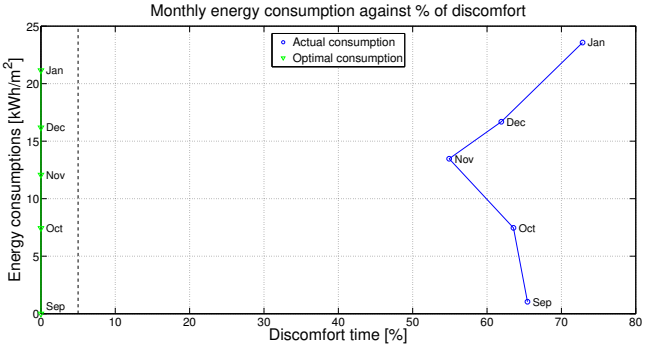

Figure 7.36: Comprehensive figure for Method IV thermal discomfort evaluation for dynamic occupancy and dynamic comfort temperature range

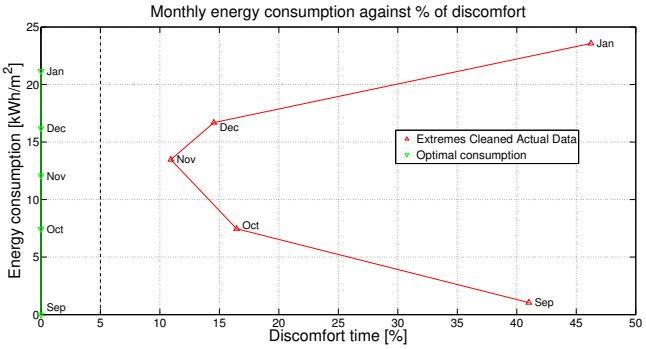

Figure 7.37: Comprehensive figure for Method V thermal discomfort evaluation for dynamic occupancy and dynamic comfort temperature range

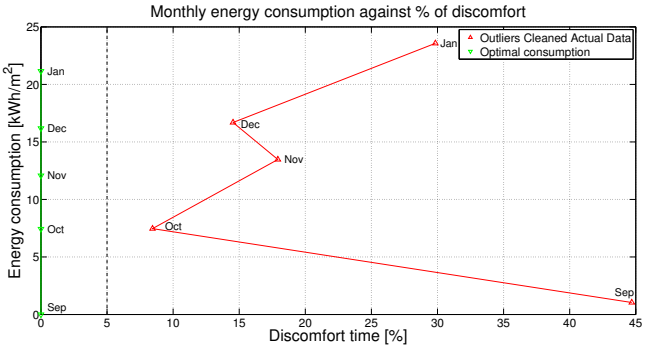

Figure 7.38: Comprehensive figure for Method VI thermal discomfort evaluation for dynamic occupancy and dynamic comfort temperature range

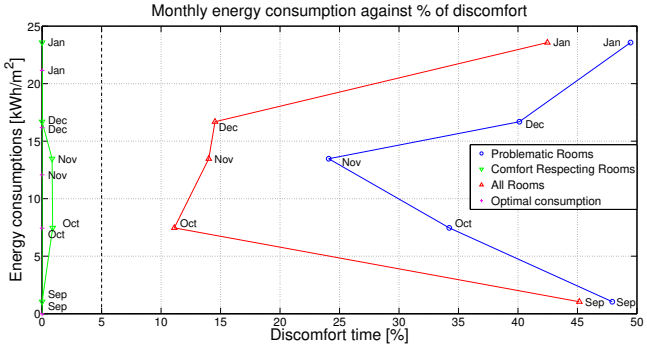

Figure 7.39: Comprehensive figure for Method VII thermal discomfort evaluation for dynamic occupancy and dynamic comfort temperature range

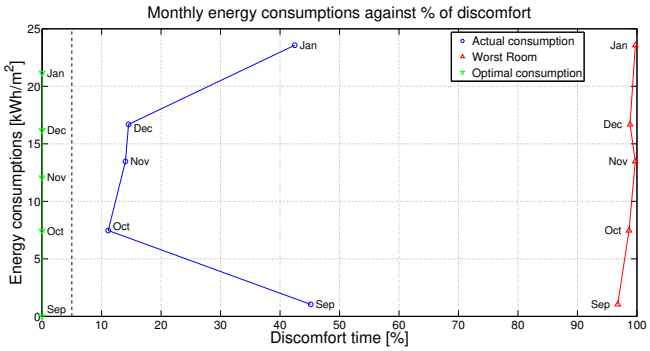

Figure 7.40: Comprehensive figure for Method VIII thermal discomfort evaluation for dynamic occupancy and dynamic comfort temperature range

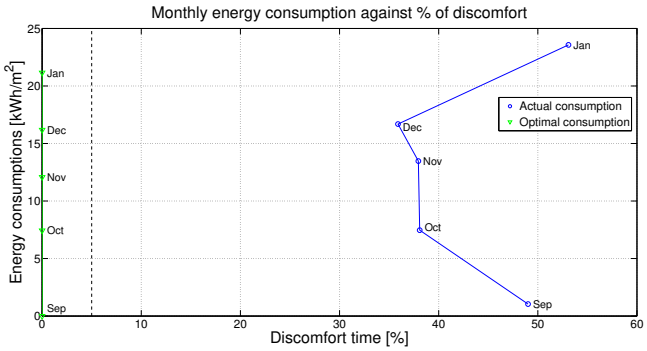

Figure 7.41: Comprehensive figure for Method IX thermal discomfort evaluation for dynamic occupancy and dynamic comfort temperature range